

การเตรียมซิลิกาที่เคลือบด้วยพอลิเอทิลีนโดยพอลิเมอร์ไรเซชันแบบอินซิทูด้วยตัวเร่งปฏิกิริยาเมทัลโลซีน



บทคัดย่อและแฟ้มข้อมูลฉบับเต็มของวิทยานิพนธ์ตั้งแต่ปีการศึกษา 2554 ที่ให้บริการในคลังปัญญาจุฬาฯ (CUIR)  
เป็นแฟ้มข้อมูลของนิสิตเจ้าของวิทยานิพนธ์ ที่ส่งผ่านทางบัณฑิตวิทยาลัย

The abstract and full text of theses from the academic year 2011 in Chulalongkorn University Intellectual Repository (CUIR)  
are the thesis authors' files submitted through the University Graduate School.

วิทยานิพนธ์นี้เป็นส่วนหนึ่งของการศึกษาตามหลักสูตรปริญญาวิศวกรรมศาสตรมหาบัณฑิต  
สาขาวิชาวิศวกรรมเคมี ภาควิชาวิศวกรรมเคมี  
คณะวิศวกรรมศาสตร์ จุฬาลงกรณ์มหาวิทยาลัย  
ปีการศึกษา 2559  
ลิขสิทธิ์ของจุฬาลงกรณ์มหาวิทยาลัย

Preparation of silica coated with polyethylene by *in situ* polymerization with  
metallocene catalyst

Miss Sineenart Jamnongphol



A Thesis Submitted in Partial Fulfillment of the Requirements  
for the Degree of Master of Engineering Program in Chemical Engineering

Department of Chemical Engineering

Faculty of Engineering

Chulalongkorn University

Academic Year 2016

Copyright of Chulalongkorn University

Thesis Title	Preparation of silica coated with polyethylene by <i>in situ</i> polymerization with metallocene catalyst
By	Miss Sineenart Jamnongphol
Field of Study	Chemical Engineering
Thesis Advisor	Professor Bunjerd Jongsomjit, Ph.D.

---

Accepted by the Faculty of Engineering, Chulalongkorn University in Partial Fulfillment of the Requirements for the Master's Degree

..... Dean of the Faculty of Engineering  
(Associate Professor Supot Teachavorasinskun, D.Eng.)

THESIS COMMITTEE

..... Chairman  
(Assistant Professor Suphot Phatanasri, D.Eng.)

..... Thesis Advisor  
(Professor Bunjerd Jongsomjit, Ph.D.)

..... Examiner  
(Chutimon Satirapipathkul, D.Eng.)

..... External Examiner  
(Ekrachan Chaichana, D.Eng.)

สินีนานู จำนวนองค์ผล : การเตรียมซิลิกาที่เคลือบด้วยพอลิเอทิลีนโดยพอลิเมอร์โรเซชันแบบอินซิทูด้วยตัวเร่งปฏิกิริยาเมทัลโลซีน (Preparation of silica coated with polyethylene by *in situ* polymerization with metallocene catalyst) อ.ที่ปรึกษาวิทยานิพนธ์หลัก: ศ. ดร. บรรเจิด จงสมจิตร, 91 หน้า.

ปัจจุบันยางธรรมชาติเป็นวัตถุดิบในการผลิตผลิตภัณฑ์มากมายเนื่องจากมีความแข็งแรงจำเพาะสูงและสามารถหาได้จากแหล่งธรรมชาติ แต่เนื่องจากมีข้อจำกัดคือมีสมบัติเชิงกลต่ำ ดังนั้นจึงควรปรับปรุงสมบัติโดยการใช้สารเติมแต่ง (filler) งานวิจัยนี้ให้ความสนใจซิลิกาจากแกลบเนื่องจากราคาไม่แพงและหาได้จากขยะเกษตรกรรม อย่างไรก็ตามข้อเสียของซิลิกาที่เป็นสารที่มีขี้ซึ่งผสมเข้ากันได้ไม่ดีกับยางธรรมชาติที่มีสมบัติไม่มีขี้ ดังนั้นจึงควรปรับปรุงผิวของซิลิกาโดยการเคลือบด้วยสารที่ไม่มีขี้เป็นพอลิเอทิลีนก่อนนำไปผสมยางธรรมชาติโดยวิธีอินซิทูพอลิเมอร์โรเซชันซึ่งใช้ซิลิกาทั้ง 3 ชนิดได้แก่ ซิลิกาจากแกลบ ซิลิกาทางการค้าและซิลิกาสังเคราะห์ และใช้ MMAO เป็นตัวเร่งปฏิกิริยาร่วม งานวิจัยนี้ศึกษาทั้งหมด 3 ส่วน ส่วนแรกเป็นการพิสูจน์เอกลักษณ์ซิลิกาก่อนและหลังการเคลือบฝัง MMAO ด้วยเทคนิคต่างๆเช่น เอกซเรย์ฟลูออเรสเซนซ์ (XRF), N<sub>2</sub>- physisorption, กล้องจุลทรรศน์อิเล็กตรอนแบบส่องกราด-วิเคราะห์ธาตุเชิงปริมาณ (SEM/EDX), เอกซ์เรย์ดิฟแฟรกชัน (XRD), สเปกโตรสโคปีของอนุภาคอิเล็กตรอนที่ถูกปลดปล่อยด้วยรังสีเอกซ์ (XPS) และวิเคราะห์สมบัติทางความร้อนด้วยเครื่องที่จีเอและเครื่องดิฟเฟอเรนเทียลสแกนนิ่งแคลอริมิเตอร์ (TGA-DSC) ส่วนที่ 2 เป็นการศึกษาความสามารถในการเกิดปฏิกิริยาเคมี (activity) ที่ 60°C และ 70°C พบว่าความสามารถในการเกิดปฏิกิริยาเคมีที่เคลือบฝังด้วยอินซิทูมีค่ามากกว่าเอ็กซิทู ซิลิกาทางการค้าที่ทำการเคลือบฝังด้วยเอ็กซิทูและพอลิเมอร์โรเซชันที่อุณหภูมิ 70 °C มีค่าความสามารถในการเกิดปฏิกิริยาเคมีมากที่สุด แต่สัณฐานพอลิเมอร์จากวิธีการเคลือบฝังด้วยเอ็กซิทูให้รูปร่างคล้ายทรงกลมซึ่งดีกว่าวิธีอินซิทูที่ให้รูปร่างไม่แน่นอน ส่วนที่ 3 เป็นการพิสูจน์เอกลักษณ์พอลิเมอร์ที่ได้จากกระบวนการพอลิเมอร์โรเซชันด้วยเทคนิคกล้องจุลทรรศน์อิเล็กตรอนแบบส่องกราด-วิเคราะห์ธาตุเชิงปริมาณ (SEM/EDX), เอกซ์เรย์ดิฟแฟรกชัน (XRD), และวิเคราะห์สมบัติทางความร้อนด้วยเครื่องที่จีเอและเครื่องดิฟเฟอเรนเทียลสแกนนิ่งแคลอริมิเตอร์ (TGA-DSC) พบว่าพอลิเมอร์ที่ใช้ซิลิกาทางการค้าเป็นตัวรองรับและเคลือบฝังด้วยวิธีเอ็กซิทูจะให้ค่าความสามารถในการเกิดปฏิกิริยาเคมีที่อุณหภูมิ 70°C มากที่สุด ในขณะที่พอลิเมอร์ที่ใช้ซิลิกาแกลบเป็นตัวรองรับและเคลือบฝังด้วยวิธีเอ็กซิทูให้ค่าความสามารถในการเกิดปฏิกิริยาเคมีที่อุณหภูมิ 70°C ต่ำที่สุด

ภาควิชา วิศวกรรมเคมี ลายมือชื่อนิสิต .....

สาขาวิชา วิศวกรรมเคมี ลายมือชื่อ อ.ที่ปรึกษาหลัก .....

ปีการศึกษา 2559

# # 5870253021 : MAJOR CHEMICAL ENGINEERING

KEYWORDS: POLYMERIZATION, POLYETHYLENE, METALLOCENE, SILICA

SINEENART JAMNONGPHOL: Preparation of silica coated with polyethylene by *in situ* polymerization with metallocene catalyst. ADVISOR: PROF. BUNJERD JONGSOMJIT, Ph.D., 91 pp.

Nowadays, natural rubber is used as a raw material to produce several products due to its high strength. However, it has a limit to be used because of low mechanical property. So, it needs to be improved by adding some filler, which is silica. Nevertheless, silica needs altering to be more hydrophobic as the rubber matrix. Thus it could be used to improve the silica surface by *in situ* polymerization. In this study, the *in situ* polymerization of ethylene over metallocene catalyst with three types of silica obtained from rice husk, commercial and synthesized silica. The modified methylaluminoxane (MMAO) is used as cocatalyst. There were three parts of this study. The first part was studied the characteristics of silica before and after immobilization with MMAO, prepared by *ex situ* immobilization method by XRF,  $N_2$  physisorption, SEM-EDX, XRD, XPS, and TGA-DSC. The second part studied the catalytic activities of silica at different temperatures ( $60^\circ\text{C}$  and  $70^\circ\text{C}$ ) and immobilization method (*ex situ* and *in situ*). The *in situ* immobilization expressed higher catalytic activity than the *ex situ* method. The activity of polymerization via *ex situ* immobilization of  $\text{SiO}_2\text{-Com}$  was the highest at  $70^\circ\text{C}$  and  $\text{SiO}_2\text{-Syn}$  was the highest catalytic activity at  $60^\circ\text{C}$ . However, the morphologies of polymer with *ex situ* immobilization, which were spheroidal, were better than *in situ* immobilization which was irregular shape. All obtained polymers were characterized in the third part by SEM-EDX, XRD, and TGA-DSC. It can be concluded that the  $\text{SiO}_2\text{-Com}$  coated with polyethylene by *in situ* polymerization with metallocene catalyst at  $70^\circ\text{C}$  via *ex situ* immobilization expressed the highest catalytic activity.  $\text{SiO}_2\text{-RH}$  coated with polyethylene by *in situ* polymerization with metallocene catalyst at  $70^\circ\text{C}$  via *ex situ* immobilization expressed the lowest catalytic activity.

## ACKNOWLEDGEMENTS

The author would like to express her special gratitude to Professor.Dr. Bunjerd Jongsomjit, my advisor, for his generosity in providing encouragement and useful suggestions. She would not have accomplished this far and this research would not have been completed without all supports from him.

In addition, she wish to thank Assistance Professor Suphot Patthanasri , Dr. Chutimon Satirapipathkul, and Dr.Ekrachan Chaichana as the members of the thesis committee for their invaluable information as the guidance of this research and all their help.

This dissertation would not be possible without of her family for their tremendous support, overwhelming encouragement, and endless love all the times. The achievement of graduation is dedicated to her family.

She would like to take this opportunity to thank Department of Chemical Engineering, Faculty of Engineering Chulalongkorn University , Faculty of Pharmaceutical Sciences Chulalongkorn University, and Department of Chemistry, Faculty of Science, Nakhon Pathom Rajabhat University.

Finally, she would like to thank to Miss Thanarat Souwapanon, Miss Thanyathorn Niyomthai, Mr. Aniroot Ratchadaphet, Mr.Rajneesh Saini, Mr.Pasucha Thongyoo, Ms. Thanyaporn Pongchan, and all her friends and members in the Center of Excellence on Catalysis and Catalytic Reaction Engineering, Department of Chemical Engineering, Chulalongkorn University for all their support and encouragement.

## CONTENTS

	Page
THAI ABSTRACT .....	iv
ENGLISH ABSTRACT .....	v
ACKNOWLEDGEMENTS .....	vi
CONTENTS .....	vii
LIST OF FIGURE.....	13
LIST OF TABLE .....	17
Chapter I .....	1
INTRODUCTION.....	1
1.1 General Introduction.....	1
1.2 Research objectives .....	3
1.3 Research scopes .....	3
1.4 Research methodology .....	4
Chapter II .....	5
THEORIES AND LITERATURE REVIEWS .....	5
2.1 Metallocene catalyst.....	5
2.2 Polymerization reaction .....	6
2.3 Polyethylene.....	7
2.3.1 High-Density Polyethylene (HDPE) .....	8
2.3.2 Low-Density Polyethylene (LDPE) and Linear Low-Density Polyethylene (LLDPE) .....	8
2.4 Modified methylaluminoxanes , MMAO .....	9
2.5 Mechanism of Polymerization with single site catalysts.....	10
2.6 Silica .....	12

	Page
2.6.1 Silica synthesis.....	13
2.6.2 Silica with MAO .....	13
2.6.3 Silica from Husk.....	14
2.6.4 Silica for rubber composite.....	15
Chapter III .....	17
EXPERIMENTAL .....	17
3.1 Equipment .....	17
3.1.1 Schlenk line .....	17
3.1.2 Gas supply.....	18
3.1.3 Polymerization reactor .....	18
3.1.4 Magnetic stirrer and heater .....	18
3.1.5 Vacuum pump.....	18
3.1.6 Polymerization line .....	19
3.1.7 Schlenk tube .....	19
3.2 Silica preparation.....	19
3.2.1 Synthesis of silica.....	20
3.2.1.1 Chemical .....	20
3.2.1.2 Procedure .....	20
3.2.2 Husk silica .....	20
3.2.3 Commercial silica.....	21
3.3 Preparation of MMAO/Modified silica .....	21
3.3.1 Chemical.....	21
3.3.2 Immobilization procedure .....	21

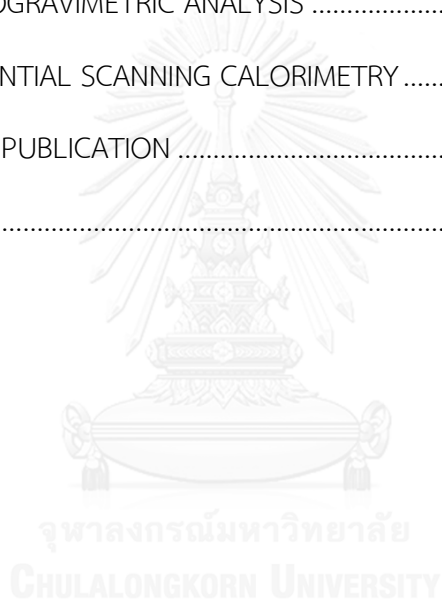


	Page
3.3.2.1 <i>Ex situ</i> immobilization.....	21
3.3.2.2 <i>In situ</i> immobilization.....	21
3.4 Polymerization on the support with <i>Ex situ</i> impregnation.....	22
3.4.1 Chemical.....	22
3.4.2 Polymerization procedure .....	22
3.4.2.1 Homopolymerization.....	22
3.4.2.2 Heteropolymerization .....	22
3.5 Characterization.....	24
3.5.1 Characterization silica support before immobilization .....	24
3.5.1.1 Scanning electron microscopy (SEM).....	24
3.5.1.2 X-ray diffraction (XRD).....	24
3.5.1.3 N <sub>2</sub> physisorption .....	24
3.5.1.4 Fourier transform infrared spectroscopy (FT-IR) .....	24
3.5.1.5 Thermogravimetric analysis - differential scanning calorimetry (TGA-DSC).....	24
3.5.1.6 X-ray fluorescence spectrometry (XRF).....	25
3.5.2 Characterization silica support after immobilization.....	25
3.5.2.1 Scanning electron microscopy (SEM) and energy dispersive X-ray spectroscopy (EDX).....	25
3.5.2.2 Fourier transform infrared spectroscopy (FT-IR) .....	25
3.5.2.3 Thermogravimetric analysis - differential scanning calorimetry (TGA-DSC).....	25
3.5.2.4 X-ray photoelectron spectroscopy (XPS).....	25
3.5.3 Characterization polyethylene coated-SiO <sub>2</sub> .....	26

	Page
3.5.3.1 Scanning electron microscopy (SEM).....	26
3.5.3.2 X-ray diffraction (XRD).....	26
3.5.3.3 Thermogravimetric analysis - differential scanning calorimetry (TGA-DSC).....	26
3.5.3.4 Transmission electron microscopy (TEM).....	26
3.5.3.5 Microtome .....	26
3.6 Benefits.....	26
Chapter IV.....	27
RESULTS AND DISCUSSIONS .....	27
4.1 Characterization of supports and supported MMAO. ....	27
4.1.1 Characterization of supports with X-ray fluorescence spectrometry (XRF).....	27
4.1.2 Characterization of supports with N <sub>2</sub> physisorption.....	28
4.1.3 Characterization of supports and supported MMAO with scanning electron microscope (SEM) and energy dispersive X- ray spectroscopy (EDX).....	30
4.1.4 Characterization of supports and supported MMAO with X-ray Powder Diffraction (XRD). ....	34
4.1.5 Characterization of supports and supported MMAO with Thermogravimetric Analysis (TGA) .....	36
4.1.6 Characterization of supported MMAO with X-ray photoelectron spectroscopy (XPS). ....	39
4.2 Catalytic activities and melting temperature of polymer.....	41
4.2.1 Catalytic activities of ethylene polymerization.....	41

4.2.2 Effect of various supports , immobilization method and polymerization temperature on the melting temperature and percent of crystallinity of polymer.....	43
4.3 Homopolymerization.....	45
4.3.1. Characterization of polyethylene with Scanning Eletron Microscopy (SEM) .....	45
4.3.2 Characterization of polyethylene with X-ray Powder Diffraction (XRD) .....	46
4.3.3 Characterization of polyethylene with Thermogravimetric Analysis (TGA).....	46
4.4 Polymerization via <i>ex situ</i> immobilization.....	48
4.4.1 Characterization of polyethylene with Scanning Electron Microscopy (SEM) with Energy Dispersive X-Ray Analysis (EDX) ....	48
4.4.2 Characterization of polyethylene with Transmission electron microscopy (TEM).....	57
4.4.3 Characterization of polyethylene by X-ray Powder Diffraction (XRD) .....	59
4.4.4. Characterization of polyethylene with Thermogravimetric Analysis (TGA).....	59
4.5 Polymerization via <i>in situ</i> immobilization.....	62
4.5.1 Characterization of polyethylene with SEM-EDX .....	62
4.5.2 Characterization of polyethylene with X-ray Powder Diffraction (XRD) .....	65
4.5.3 Characterization of polyethylene with Thermogravimetric Analysis (TGA).....	65
Chapter V.....	68

	Page
CONCLUSIONS AND RECOMMENDATIONS.....	68
5.1 Conclusions .....	68
5.2 Recommendations .....	68
REFERENCES .....	69
APPENDIX A : FOURIER TRANSFORM INFRARED SPECTROSCOPY .....	72
APPENDIX B : X-RAY PHOTOELECTRON SPECTROSCOPY .....	74
APPENDIX C : THERMOGRAVIMETRIC ANALYSIS .....	76
APPENDIX D : DIFFERENTIAL SCANNING CALORIMETRY .....	85
APPENDIX E : LIST OF PUBLICATION .....	89
VITA.....	91



## LIST OF FIGURE

<b>Figure 2.1</b> Structures of $Cp_2ZrCl_2$ : $(BuCp)_2ZrCl_2$ .....	5
<b>Figure 2.3</b> Structure of MMAO.....	9
<b>Figure 2.4</b> The active site formation of metallocene catalyst .....	11
<b>Figure 2.5</b> Propagation mechanism.....	11
<b>Figure 2.6</b> Chain transfer reactions .....	12
<b>Figure 2.7</b> Silanol group of silica surface .....	12
<b>Figure 3.1</b> Schlenk line .....	18
<b>Figure 3.2</b> Diagram of system in slurry phase polymerization.....	19
<b>Figure 3.3</b> Schlenk tube.....	19
<b>Figure 3.4</b> Methodology.....	23
<b>Figure 4.1</b> The $N_2$ adsorption-desorption isotherms for all supports.....	29
<b>Figure 4.2</b> The pore size distribution of silica .....	29
<b>Figure 4.4</b> SEM micrographs of $SiO_2$ -RH (a.), $SiO_2$ -Syn (b.), and $SiO_2$ -Com (c.) at 200X and 4kx magnification before immobilization.....	31
<b>Figure 4.5</b> SEM micrographs of $SiO_2$ -RH (a.), $SiO_2$ -Syn (b.), and $SiO_2$ -Com (c.) at 350X and 2.5kx magnification after immobilization. ....	32
<b>Figure 4.6</b> EDX of $SiO_2$ -RH (a.), $SiO_2$ -Syn (b.), and $SiO_2$ -Com (c.) .....	33
<b>Figure 4.7</b> XRD patterns of $SiO_2$ -RH, $SiO_2$ -Syn and $SiO_2$ -Com.....	34
<b>Figure 4.8</b> XRD patterns of $SiO_2$ -RH, $SiO_2$ -Syn and $SiO_2$ -Com.....	35
<b>Figure 4.9</b> XRD patterns of sample holder.....	35
<b>Figure 4.10</b> TGA profiles of $SiO_2$ before immobilization. ....	36
<b>Figure 4.11</b> DTA profiles of $SiO_2$ before immobilization.....	37
<b>Figure 4.12</b> TGA profiles of $SiO_2$ after immobilization.....	38

<b>Figure 4.13</b> DTA profiles of SiO <sub>2</sub> after immobilization.....	38
<b>Figure 4.14</b> The ethylene consumption of homopolymerization at 60 °C and 70 °C...	42
<b>Figure 4.15</b> SEM micrographs of polymer from homopolymerization at 60 °C and 70 °C at 500X and 4kX magnification (a.) PE-60 (b.) PE-70.....	45
<b>Figure 4.16</b> XRD pattern of polymer from Homopolymerization. ....	46
<b>Figure 4.17</b> TGA profiles of polymer from homopolymerization. ....	47
<b>Figure 4.18</b> DTA profiles of polymer from homopolymerization. ....	47
<b>Figure 4.19</b> SEM micrographs of PE-SiO <sub>2</sub> -RH60 (a.), PE-SiO <sub>2</sub> -Syn60 (b.) , PE-SiO <sub>2</sub> -Com60 (c.) at 350X and 7kX magnification at 60 °C of polymerization temperature....	49
<b>Figure 4.20</b> SEM micrographs of PE-SiO <sub>2</sub> -RH60 (a.), PE-SiO <sub>2</sub> -Syn60 (b.) , PE-SiO <sub>2</sub> -Com60 (c.) at 350X and 7kX magnification at 60 °C of polymerization temperature....	50
<b>Figure 4.21</b> EDX of PE-SiO <sub>2</sub> -RH60 (a.), PE-SiO <sub>2</sub> -Syn60 (b.) , PE-SiO <sub>2</sub> -Com60 (c.) at 60 °C of polymerization temperature. ....	51
<b>Figure 4.22</b> EDX of PE-SiO <sub>2</sub> -RH70 (a.), PE-SiO <sub>2</sub> -Syn70 (b.) , PE-SiO <sub>2</sub> -Com70 (c.) at 70 °C of polymerization temperature. ....	52
<b>Figure 4.23</b> The SEM micrographs of cross-sectional of polyethylene PE-SiO <sub>2</sub> -RH70 (a.), PE-SiO <sub>2</sub> -Syn70 (b.), PE-SiO <sub>2</sub> -Com70 (c.) obtained from polymerization at 70 °C via <i>ex situ</i> immobilization.....	54
<b>Figure 4.24</b> The EDX of cross-sectional of polyethylene PE-SiO <sub>2</sub> -RH70 (a.), PE-SiO <sub>2</sub> -Syn70 (b.), PE-SiO <sub>2</sub> -Com70 (c.) obtained from polymerization at 70 °C via <i>ex situ</i> immobilization.....	55
<b>Figure 4.25</b> The EDX of cross-sectional of polyethylene PE-SiO <sub>2</sub> -RH70 (a.), PE-SiO <sub>2</sub> -Syn70 (b.), PE-SiO <sub>2</sub> -Com70 (c.) obtained from polymerization at 70 °C via <i>ex situ</i> immobilization.....	56
<b>Figure 4.26</b> The TEM of PE-SiO <sub>2</sub> -RH60 (a.), PE-SiO <sub>2</sub> -RH70 (b.), PE-SiO <sub>2</sub> -Syn60 (c.), PE-SiO <sub>2</sub> -Syn70 (d.), PE-SiO <sub>2</sub> -Com60 (e.), and PE-SiO <sub>2</sub> -Com70 (f.) obtained from polymerization via <i>ex situ</i> immobilization .....	58

<b>Figure 4.27</b> XRD patterns of polyethylene obtained from polymerization via <i>ex situ</i> immobilization.....	59
<b>Figure 4.28</b> TGA profiles of polymer obtained from polymerization via <i>ex situ</i> immobilization.....	60
<b>Figure 4.29</b> DTA profiles of polymer obtained from polymerization via <i>ex situ</i> immobilization.....	61
<b>Figure 4.30</b> SEM micrographs of INPE-SiO <sub>2</sub> -RH70 (a.), INPE-SiO <sub>2</sub> -Syn70 (b.) , INPE-SiO <sub>2</sub> -Com70 (c.) at 350X and 500X magnification at 70°C of polymerization temperature.....	63
<b>Figure 4.31</b> The EDX of INPE-SiO <sub>2</sub> -RH70 (a.), INPE-SiO <sub>2</sub> -Syn70 (b.) , INPE-SiO <sub>2</sub> -Com70 (c.) at 70°C of polymerization temperature.....	64
<b>Figure 4.32</b> XRD patterns of polyethylene obtained from polymerization at 70°C via <i>in situ</i> immobilization.....	65
<b>Figure 4.33</b> TGA profiles of polymer obtained from polymerization via <i>in situ</i> immobilization at 70°C.....	66
<b>Figure 4.34</b> TGA profiles of polymer obtained from polymerization via <i>in situ</i> immobilization at 70°C.....	66
<b>Figure A-1</b> FT-IR of SiO <sub>2</sub> before immobilization with MMAO.....	73
<b>Figure A-2</b> FT-IR of SiO <sub>2</sub> after immobilization with MMAO.....	73
<b>Figure B-1</b> XPS of SiO <sub>2</sub> after immobilization.....	75
<b>Figure C-1</b> TGA of SiO <sub>2</sub> -RH before immobilization.....	77
<b>Figure C-3</b> TGA of SiO <sub>2</sub> -Syn before immobilization.....	77
<b>Figure C-4</b> TGA of SiO <sub>2</sub> -Com before immobilization.....	78
<b>Figure C-5</b> TGA of SiO <sub>2</sub> -RH after immobilization.....	78
<b>Figure C-6</b> TGA of SiO <sub>2</sub> -Syn after immobilization.....	79
<b>Figure C-7</b> TGA of SiO <sub>2</sub> -Com after immobilization.....	79

<b>Figure C-8</b> TGA of PE-SiO <sub>2</sub> -RH60 obtained from polymerization via <i>ex situ</i> immobilization.....	80
<b>Figure C-9</b> TGA of PE-SiO <sub>2</sub> -RH70 obtained from polymerization via <i>ex situ</i> immobilization.....	80
<b>Figure C-10</b> TGA of PE-SiO <sub>2</sub> -Syn60 obtained from polymerization via <i>ex situ</i> immobilization.....	81
<b>Figure C- 11</b> TGA of PE-SiO <sub>2</sub> -Syn70 obtained from polymerization via <i>ex situ</i> immobilization.....	81
<b>Figure C- 12</b> TGA of PE-SiO <sub>2</sub> -Com60 obtained from polymerization via <i>ex situ</i> immobilization.....	82
<b>Figure C-13</b> TGA of PE-SiO <sub>2</sub> -Com70 obtained from polymerization via <i>ex situ</i> immobilization.....	82
<b>Figure C-14</b> TGA of INPE-SiO <sub>2</sub> -RH70 obtained from polymerization via <i>in situ</i> immobilization.....	83
<b>Figure C- 15</b> TGA of INPE-SiO <sub>2</sub> -Syn70 obtained from polymerization via <i>in situ</i> immobilization.....	83
<b>Figure C-16</b> TGA of INPE-SiO <sub>2</sub> -Com70 obtained from polymerization via <i>in situ</i> immobilization.....	84



## LIST OF TABLE

<b>Table 3.1</b> The chemicals used for synthesis of the silica. ....	20
<b>Table 3.2</b> The chemicals used for polymerization .....	22
<b>Table 4.1</b> XRF of silica supports with different sources .....	27
<b>Table 4.3</b> N <sub>2</sub> physisorption of silica supports with different sources .....	28
<b>Table 4.4</b> EDX analysis expressed the average of O on silica supports.....	31
<b>Table 4.5</b> EDX analysis of Al on the silica supported .....	33
<b>Table 4.6</b> XPS data of Al 2p core level of cocatalyst. ....	39
<b>Table 4.7</b> Catalytic activities of various silica-supported zirconocene/MMAO catalyst via <i>ex situ</i> and <i>in situ</i> immobilization method. ....	41
<b>Table 4.8</b> Melting temperature and percent of crystallinity of polymer.....	43
<b>Table 4.9</b> The average amount of Al on SiO <sub>2</sub> surface in polyethylene via <i>ex situ</i> immobilization.....	53
<b>Table 4.10</b> The average amount of Al on SiO <sub>2</sub> surface in polyethylene via <i>in situ</i> polymerization. ....	57
<b>Table 4.11</b> Percent weight loss of polymer obtained from polymerization via <i>ex situ</i> immobilization.....	62
<b>Table 4.12</b> The average amount of Al on SiO <sub>2</sub> surface in polyethylene via <i>in situ</i> immobilization.....	64

## Chapter I

### INTRODUCTION

#### 1.1 General Introduction

Nowadays , natural rubber is used as a raw material to produce several products such as glove and tire due to its high specific stiffness , strength and availability from natural sources. However , raw natural rubber has limit to be used because of low mechanical property and unstable with high temperature. So, the natural rubber needs to be improved by adding some filler. There are variety of fillers such as fiber from banana stem , grass , coconut shell powder, husk fiber and silica [1]. Silica ( $\text{SiO}_2$ ) is one of the most attractive nanoparticles because of its inexpensive and nontoxic [2]. Adding silica is one of the most important reinforcements in rubber industry. Silica is the additive in tires as the rise and development of “green tire”. There are many applications of silica together with some special rubbers such as solution polymerized styrene-butadiene rubber (SSBR) in tires [3], which improve the rolling resistance and wet traction without any compromises in tread wear. Hall *et al.* [3] suggested that  $\text{SiO}_2$  nanoparticles were beneficial for increasing the abrasion resistance and wet grip, and reducing the rolling resistance.

Rice husk is an agricultural waste that mainly consists of amorphous silica about 55 to 97 weight% depending on the combustion conditions [4]. There are several advantages of rice husk such as easy to process , economic aspects and being a renewable resource. Nevertheless, the main drawback of silica is hydrophilicity. It needs altering to be more hydrophobic as the rubber matrix. Thermoplastic polymer such as polyethylene, which is hydrophobic as natural rubber, thus it could be used to improve the silica surface by *in situ* polymerization. The *in situ* polymerization is

the technique of producing polymer at condition of polymerization condition. This technique is able to produce the strong linkage between two parts of silica and natural rubber matrix [2].

In this study, the *in situ* polymerization of ethylene over metallocene catalyst with the presence of silica was investigated. Three types of silica obtained from rice husk, commercial and synthesized silica were used. The modified methylaluminoxanes (MMAO) is used as cocatalyst along with a zirconocene catalyst for polymerization. MMAO-modified silica was prepared by *ex situ* immobilization compared with *in situ* immobilization method. After the silica-supported MMAO was prepared, it was characterized by various techniques including scanning energy dispersive X-ray spectroscopy (SEM/EDX) in order to determine the morphology and amount of MMAO, X-ray powder diffraction (XRD) to determine the bulk crystalline phases. The surface area, average pore diameter and pore size of silica were determined by Brunauer Emmett Teller (BET) analysis via nitrogen adsorption/desorption. X-ray photoelectron spectroscopy (XPS) was used to determine the interaction between MMAO and silica. Infrared spectroscopy (IR) was used to determine the functional group and X-ray Fluorescence spectroscopy (XRF) was conducted to determine the amount of element. The polyethylene coated silica was characterized using various techniques including SEM, XRD, thermogravimetric analysis - differential scanning calorimetry (TGA-DSC) in order to determine the thermal properties and stability. Microtome technique was used to prepare cross-sectional PE-coated silica samples in order to analyze the morphology of them. Transmission electron microscopy (TEM) was used to determine the morphology of polyethylene. The activity of polymerization was also determined at different polymerization conditions.

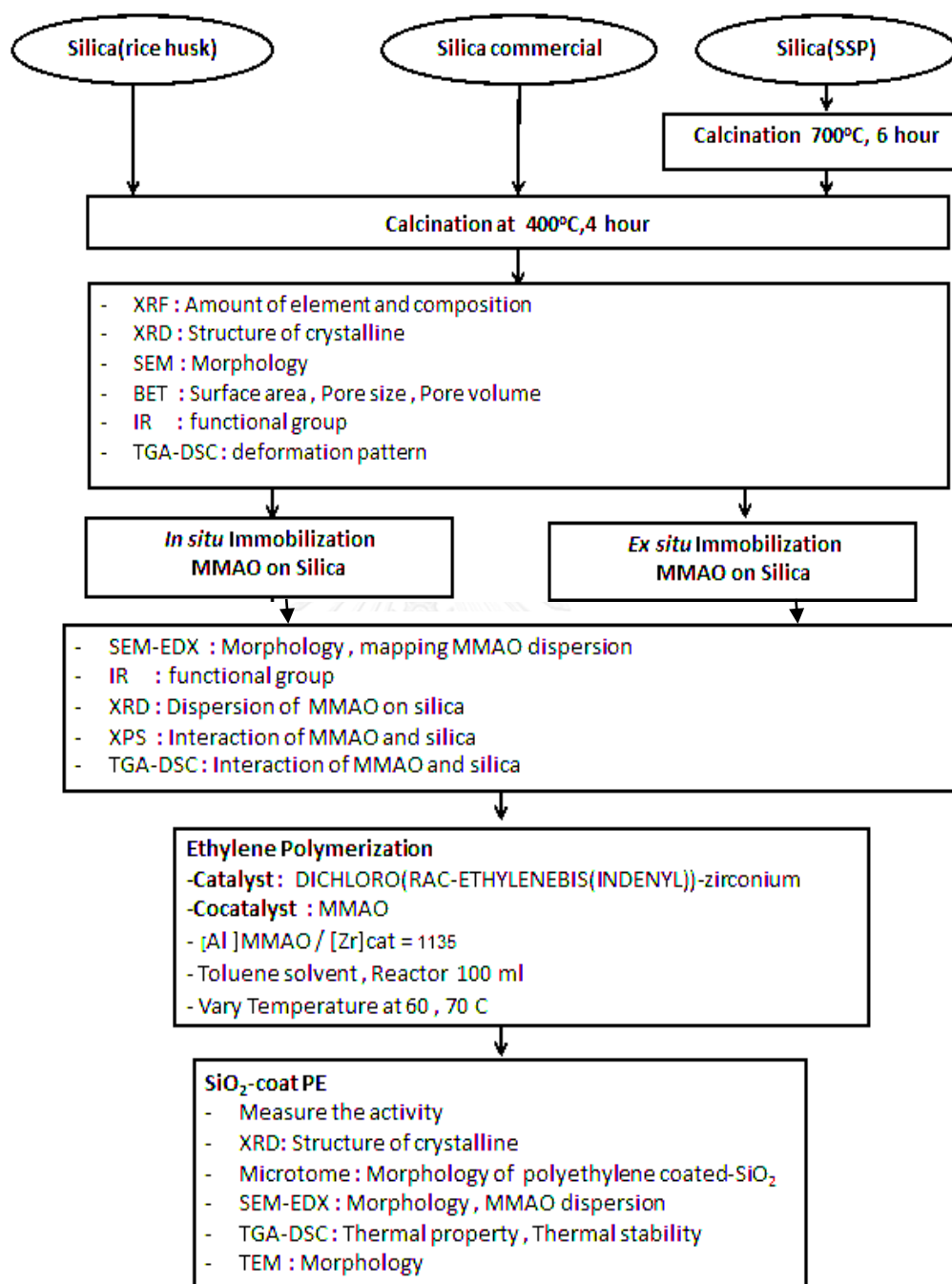
## 1.2 Research objectives

To find optimal condition for preparation of polyethylene coated-SiO<sub>2</sub> using *in situ* polymerization with zirconocene/MMAO catalyst.

## 1.3 Research scopes

- There are 3 silica supports (from rice husk , synthesis , and commercial) immobilized with MMAO.
- MMAO-modified silica was prepared by *ex situ* immobilization compared with *in situ* immobilization method.
- To test the catalytic activity of polymerization with zirconocene/MMAO catalyst under 3.5 bar at 60 °C and 70 °C in slurry process.
- Find optimal condition in order to produce polyethylene-coated SiO<sub>2</sub>.

## 1.4 Research methodology



## Chapter II

### THEORIES AND LITERATURE REVIEWS

#### 2.1 Metallocene catalyst

Metallocenes are organometallic compounds. The general name of metallocene is derived from ferrocene,  $(C_5H_5)_2Fe$  or  $Cp_2Fe$ . After Ziegler-Natta catalysts era, metallocene is one of the most important catalysts for olefin polymerization. Compared to Ziegler-Natta catalysts, metallocene has its unique catalytic characteristics. It has single active center, which produce polymers having narrow molecular weight distribution, and narrow chemical composition distribution. Because of different structures of the catalysts, polymers have multi properties and can be used in various applications [5].

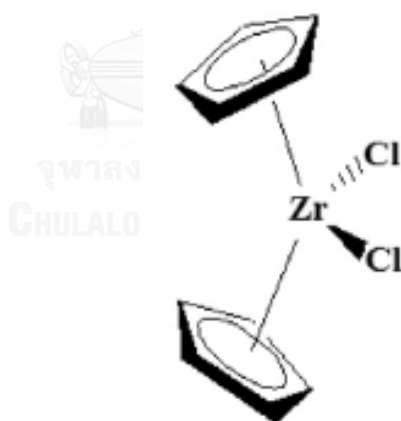


**Figure 2.1** Structures of  $Cp_2ZrCl_2$ :  $(BuCp)_2ZrCl_2$  [5]

In 1976 Kaminsky and Sinn [6] found that a highly active catalyst with a metallocene complex and MAO. The polymers produced with metallocene catalysts have narrower molecular weight distributions and more uniform incorporation of co-monomers than polymers produced with Ziegler catalysts.

However, the main drawback of metallocene catalyst is low activity polymerization, so it has to use the high molar of Al to transition metal ratio to achieve the high activity [7].

## 2.2 Polymerization reaction

Polymerization is a process of reacting monomer molecules together in a chemical reaction to form polymer chains [6].

In 1935, Perrin [6] discovered that ethylene could be polymerized at very high pressure into a semi crystalline solid.

In 1938, The ICI laboratories [6] found that low-density polyethylene is produced in supercritical ethylene pressure at 600 till 3500 bar and temperature at 200 till 350°C. This radical polymerization leads to a highly branched.

In 1950, Hogan and Banks at the Phillips Petroleum Company [6] found that temperature at 70 till 100°C and pressure at 30 till 40 bar with a catalyst containing chromium oxide on a silica support produced highly crystalline polyethylene.

Chatuma Suttivutnarubet [1] studied synthesis of polyethylene/coir dust hybrid filler via in situ polymerization with zirconocene/MAO catalyst for natural rubber biocomposites by using 0.0083 g ( $1.98 \times 10^{-5}$  moles) of  $\text{Et}(\text{Ind})_2\text{ZrCl}_2$  in 20 ml of toluene solution, stirred at room temperature. The polymerization reaction was operated in a 100 ml semi-batch stainless steel autoclave reactor with a magnetic stirrer. 1.1 ml of methylaluminoxane(MAO) ( $[\text{Al}]_{\text{TMA}}/[\text{Zr}]_{\text{cat}}=1135$ ) were mixed and stirred for 30 min at room temperature. The polymerization reaction was occurred at 70°C, 6 psi. The acidic methanol (0.1% HCl in methanol) was added and stirred overnight. Finally, the polymer was filtered and washed by methanol and dried at room temperature. The dried hybrid filler was obtained as whited powder. It was found that the catalytic activities decreased when increasing amount of the coir dust because of negative supporting effects.

Introducing the PE/coir-dust is more compatible with the natural rubber matrix than the pure coir dust because of the hydrophobicity of the polyethylene. Introducing hybrid filler with the natural rubber provided a greater storage modulus than the pure coir dust because it enhanced stiffness.

Mingkwan wannaborworn [8] studied copolymerization of ethylene/1-octene over gallium-modified silica-supported metallocene catalyst. MMAO-modified silica was prepared by ex situ immobilization method by immobilizing 0.1 g of thermally treated silica at 400°C under vacuum for 4 h with the desired amount of MMAO in 10 ml toluene with magnetic stirring at room temperature for 30 min. The solid part was separated followed by drying in vacuum at room temperature. The white powder of supported cocatalyst (MMAO/support) was then obtained and 0.2 g of the Ga-modified silica supports contacted with 1.14 ml of MMAO for 30 min with magnetic stirring in 100 ml reactor. Zirconocene and TMA ( $[Al]_{TMA}/[Zr]_{cat}=1135$ ) were mixed and then toluene was introduced in to reactor to make a total volume of 30 ml. The reactor was frozen in liquid nitrogen to stop reaction, and then 0.018 mol of 1-octene was injected into the reactor. To remove argon, the reactor was evacuated, then it was heated up to 70°C. The polymerization was started by addition of ethylene gas at 50 psi until the concentration of ethylene at 0.018 mol (6 psi). The polymerization was terminated with acidic methanol. It was found that *in situ* impregnation exhibited higher polymerization activity than the *ex situ* method.

### 2.3 Polyethylene

Polyethylene (PE), light, versatile synthetic resin made from the polymerization of ethylene. Polyethylene is a member of the important family of polyolefin resins. It is the most widely used plastic in the world, being made into products ranging from clear food wrap and shopping bags to detergent



bottles and automobile fuel tanks. Polyethylene has been used in many applications such as pipe film or etc. Polyethylene is the most common plastic produced in the world. It comes in a wide variety of physical properties. Polyethylene can be hard and rigid or soft and pliable. In the packaging industry soft and pliable films are often used to package and store a large variety of products and even waste. The low cost of polyethylene production has encouraged producers to prefer its use over many other plastics. Polyethylene offers the lowest softening point of the basic packaging plastics. The lower softening point results in lower processing energy costs. There are three types of polyethylene commonly used in the packaging industry: High-Density Polyethylene (HDPE), Low-Density Polyethylene (LDPE), and Linear Low-Density Polyethylene [9].

#### 2.3.1 High-Density Polyethylene (HDPE)

High density polyethylene has density more or equal  $0.941 \text{ g/cm}^3$ . This polyethylene has low branching in structure which cause high impact strength. High-density polyethylene has a variety of advantages over other polymers. HDPE offers low cost, easy processing, a good High-Density Polyethylene Clear Bottle High-Density Polyethylene Oil Bottle moisture barrier, and the ability to produce an opaque packaging product for example shampoo bottles, oil bottles, household cleaning bottles, blown mold drums, flower pots, and more.

#### 2.3.2 Low-Density Polyethylene (LDPE) and Linear Low-Density Polyethylene (LLDPE)

By far the most common types of polyethylene used in the packaging industry. A large variety of packaging products are made with LDPE and LLDPE. Low production costs, high clarity, heat seal-ability, high elongation, and softness are primary reasons these forms of polyethylene are often chosen for packaging. Linear low density polyethylene has density in range 0.915-0.925

$\text{g/cm}^3$ . LLDPE has higher tensile strength than LDPE. Low density polyethylene has density in range 0.91-0.94  $\text{g/cm}^3$ . Low density polyethylene has short chain and long chain branching than LLDPE. One of the most common uses for polyethylene bundling film is for wrapping water bottles and canned goods. The polyethylene bundling film is thicker and offers more strength than polyolefin or PVC shrink film.

## 2.4 Modified methylaluminoxanes , MMAO

MMAO is composed of aluminoxanes for use in single-site catalyst technology. It contains modifiers, which provide stability for long-term storage. Modifiers also often provide solubility in aliphatic hydrocarbons.

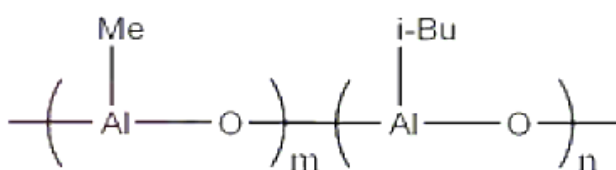
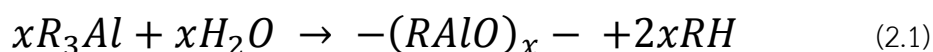


Figure 2.2 Structure of MMAO [8]

Modified methylaluminoxanes (MMAO) have also been offered commercially since the early 1990s. It is a generic term encompassing all products wherein some of the methyl groups are replaced by other alkyl groups. The most commonly used modifiers are isobutyl and n-octyl groups.

Most MMAO are prepared by reaction with water as equation 1. There are several formulations of MMAO. One commercially available MMAO is produced by the nonhydrolytic.



All modified methylaluminoxanes contain  $\geq 65\%$  methyl groups and, as such, remain predominantly methylaluminoxanes. Indeed, one MMAO formulation contains 95% methyl groups. MMAO exhibit much improved storage

stability and several are highly soluble in aliphatic hydrocarbons. MMAO give yields higher and less costly than MAO. However, since MMAO contain other types of alkylaluminumoxane in some single site catalyst systems. Consequently, MMAO should be considered as cocatalysts for single site catalysts. All commercially available methylaluminumoxanes employ trimethyl aluminum as the starting material [8].

## 2.5 Mechanism of Polymerization with single site catalysts.

There are substantial differences between the mechanisms of polymerization with single site catalysts. Most notably, the active centers of single site catalysts are believed to be cationic. Cocatalysts are used in all commercial process using single site catalysts. Active site generation is the essential first step with the relatively simple system of dimethylzirconocene and methylaluminumoxane. Cocatalysts function as agents to create cationic active centers by ligand abstraction. It has been shown that the counterion in the ion pair resulting from abstraction must be weakly coordinated to the cationic active center. Normally, polymerization mechanism with metallocene catalyst consists of three steps; initiation, propagation and termination [10].

### (i) Initiation

For initiation step, it is the step of formation of cationic active species on metallocene catalyst. The cocatalyst abstracts a methyl group from metal atom in metallocene catalyst, which generates the cationic metallocene species and coordinated anion. The mechanism in this step is shown in Figure 2.3.

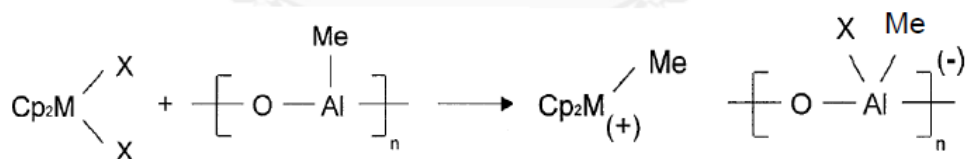


**Figure 2.3** The active site formation of metallocene catalyst [10]

(ii) Propagation

The propagation step is the step of insertion of monomer unit in the cationic active site. The strained four transition state allows for the breaking of bond between metal atom and polymer chain which cause the polymer chain growth by one monomer unit and a new vacant site formation which allows another monomer addition until polymer chain termination occurs. The mechanism in the propagation step is presented in Figure 2.4.

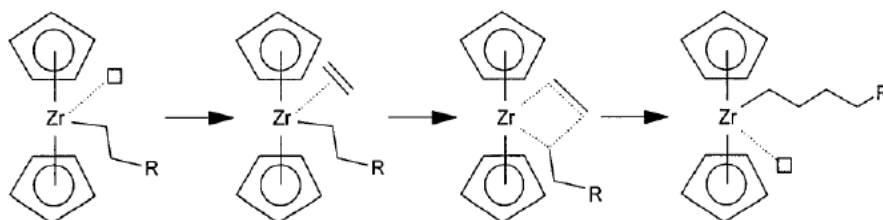


**Figure 2.4** Propagation mechanism [10]

(III) Chain termination reaction

Chain transfer to aluminum is transferred from alkyl group in cocatalyst to the cationic active center and the  $-\text{AlR}_2$  is attached to the polymer chain. The bond between  $-\text{AlR}_2$  and polymer chain can be removed by the addition of acidic methanol. Hydrogen is a common agent used to control the molecular weight of olefin polymerizations. A hydrogen molecule inserts to the growing polymer chain resulting in a dead polymer chain. The chain transfer reactions are demonstrated in Figure 2.5.

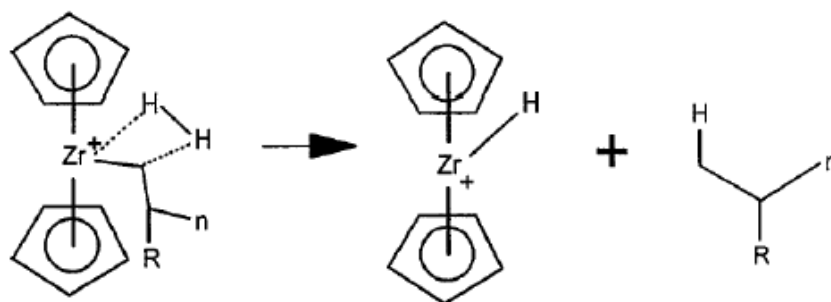


Figure 2.5 Chain transfer reactions [10]

## 2.6 Silica

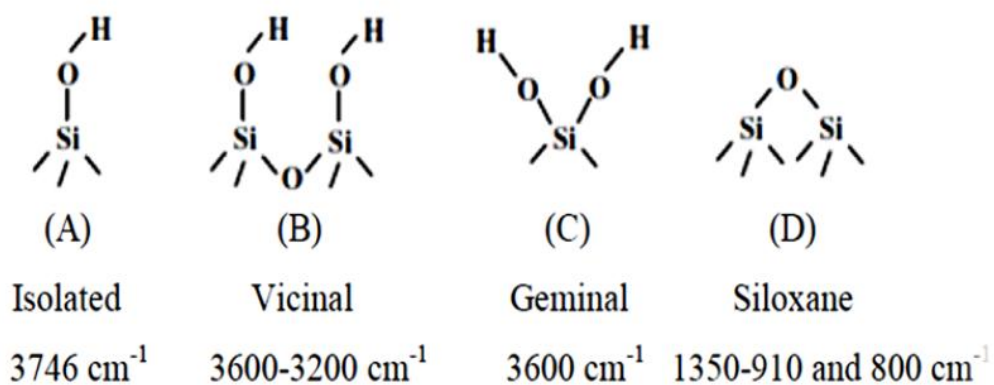


Figure 2.6 Silanol group of silica surface [11]

Silica is a hydrophilic material, which usually contains 2 - 5 weight% of adsorbed water from the moisture in the air. Silica usually has high surface area, porosity and good mechanical properties which appropriate to be support or template in supporting system through the controllable of polymer morphology. Isolated, Vicinal, Geminal and hydroxyl groups were silanol group on the surface of silica [11].

### 2.6.1 Silica synthesis

Maurice *et al.* [12] studied synthesis and characterization of amorphous silica nanoparticles from aqueous silicates using cationic surfactants. In this work amorphous silica was synthesized using sodium silicate and hydrochloric acid by precipitation according to Stober method. A system of chemical reactions has been developed which permits the controlled growth of silica particles using two different cationic surfactants as the dispersing agents. These surfactants were cetyltrimethylammonium bromide [CTAB] and dodecyltrimethylammonium bromide [DTAB]. Addition of a dispersing agent in the reaction reduced the particle size of the silica produced. The average size of silica nanoparticles can be finely tuned in the range 148–212 nm by changing the chain length of cationic surfactant. XRD results showed that the synthesized silica was predominantly amorphous.

Bangchao Zhong *et al.* [2] studied surface modification of silica with N-cyclohexyl-2-benzothiazole sulfenamide for styrene–butadiene rubber composites with dramatically improved mechanical property. Accelerator N-cyclohexyl-2-benzothiazole sulfonamide (CZ) was chemically bonded onto the surface of (3-glycidoxypropyl) trimethoxy silane modified silica(m-silica) to obtain CZ modified silica(silica-s-CZ).

### 2.6.2 Silica with MAO

Chatuma Suttivutnarubet *et al.* [1] studied synthesis of polyethylene/coir dust hybrid filler via in situ polymerization with zirconocene/MAO catalyst for natural rubber biocomposites. The synthesizing process of the filler was investigated with variation of coir dust loadings. It was found that increasing amount of the coir dust decreased the catalytic activities due to negative supporting effects. When introducing the PE/coir-dust hybrid filler into natural rubber, it can be observed from a scanning electron microscope (SEM) that the PE/coir-dust filler appeared to be

more compatible with the natural rubber matrix than the pure coir dust. This is because of the hydrophobicity of the polyethylene in the hybrid filler. The results from a dynamic mechanical analysis (DMA) showed that the natural rubber biocomposites with the hybrid filler provided a greater storage modulus than that with the pure coir dust. This suggests the enhanced stiffness of the natural rubber biocomposites probably due to the strong interaction between the hybrid filler and the natural rubber matrix. The strong interaction inside the biocomposite can be confirmed by the low value of a loss factor ( $\tan \delta$ ), which indicated a low degree of molecular mobility of the polymer, resulted from good adhesion on the filler surfaces.

### 2.6.3 Silica from Husk

Pongdong *et al.* [4] studied property correlations for dynamically cured rice husk ash filled epoxidized natural rubber/thermoplastic polyurethane blends: influences of RHA loading. Novel thermoplastic vulcanizates based on thermoplastic polyurethane (TPU) and epoxidized natural rubber (ENR) were prepared with rice husk ash (RHA) filler. It was found that the RHA showed good dispersion and was mainly localized in the ENR phase. Increasing the RHA loading led to the formation of larger ENR domains dispersed in the TPU matrix. Also, migration of the RHA particles from ENR to TPU phases was observed, resulting in reduced strength properties. It was found that the RHA acted as a nucleating agent in the TPU matrix and could accelerate the crystallization of TPU. Higher relaxation stresses or raised relaxation curves were observed with increased RHA loadings in the dynamically vulcanized ENR/TPU blends.

Khalil Ahmed *et al* [13] studied reinforcement of natural rubber hybrid composites based on marble sludge/silica and marble sludge/rice husk derived silica. The use of both industrial and agricultural waste such as marble sludge and rice husk derived silica has the primary advantage of being eco-friendly, low cost and easily

available as compared to other expensive fillers. The results from this study showed that the performance of natural rubber hybrid composites with marble sludge /silica and marble sludge / rice husk derived silica as fillers is extremely better in mechanical and swelling properties as compared with the case where marble sludge used as single filler. The study suggests that the use of recently developed silica and marble sludge as industrial and agricultural waste is accomplished to provide a probable cost effective, industrially prospective, and attractive replacement to the general purpose used fillers like china clay, calcium carbonate, and talc.

#### 2.6.4 Silica for rubber composite

Yong Lin *et al.* [3] studied silica/reduced graphene oxide ( $\text{SiO}_2@\text{rGO}$ ) hybrids were fabricated by an electrostatic assembly, and subsequently,  $\text{SiO}_2@\text{rGO}$  was incorporated into styrene butadiene rubber (SBR) to fabricate SBR composites. It was found that the greater the volume fraction of constrained region has possessed, the stronger the interfacial interaction has had. Moreover, the contribution of constrained region to the performance of composites was quantitatively analyzed by the mechanical analysis and the tube model, and the results showed that it is the effect of constrained region, rather than the contents of  $\text{SiO}_2@\text{rGO}$ , which controls the reinforcement of composites. Specifically, the higher the volume fraction of constrained region is, the better the mechanical properties of composites will be. Also,  $\text{SiO}_2@\text{rGO}$  can be utilized as novel reinforcing filler for fabricating the green tire materials with high performance.

Shamsiah Awang Ngah *et al.* [14] studied toughening performance of glass fibre composites with core-shell. The rubber and silica nanoparticle modified matrices the fracture energies of glass fibre composites with an anhydride-cured epoxy matrix modified using core-shell rubber (CSR) particles and silica nanoparticles were investigated. The quasi-isotropic laminates with a central  $0^\circ/0^\circ$  ply interface were produced using resin infusion. The composite toughness at initiation increased



approximately linearly with increasing particle concentration, from 328 J/m<sup>2</sup> for the control to 842 J/m<sup>2</sup> with 15 wt% of CSR particles. All of the CSR particles cavitated, giving increased toughness by plastic void growth and shear yielding. However, the toughness of the silica-modified epoxies is lower as the literature shows that only 14% of the silica nanoparticles undergo debonding and void growth. The size of CSR particles had no influence on the composite toughness. The propagation toughness was dominated by the fibre toughening mechanisms, but the composites achieved full toughness transfer from the bulk.



## Chapter III

### EXPERIMENTAL

In this chapter, equipment used in these experiments, chemicals used with each method, synthesis of support, immobilization procedure ,and polymerization procedures as well as characterizations are specified as follows.

#### 3.1 Equipment

According to the metallocene system is extremely sensitive to the oxygen and moisture. Thus, the special equipments were required to handle while performing the preparation and polymerization process. For example, glove box: equipped with the oxygen and moisture protection system was used to generate the inert atmosphere. Schlenk techniques (vacuum and purge with inert gas) are the other set of the equipment used to handle air-sensitive product.

##### 3.1.1 Schlenk line

Schlenk line was used to protect oxygen and moisture in all operations [10]. It was composed of nitrogen gas line and vacuum line with several stopcocks. The experiment was operated under vacuum . Solvent vapors or gas from evacuation was trapped by liquid nitrogen cold trap to prevent contaminating the vacuum pump. The Schlenk line is shown in **Figure 3.1**.

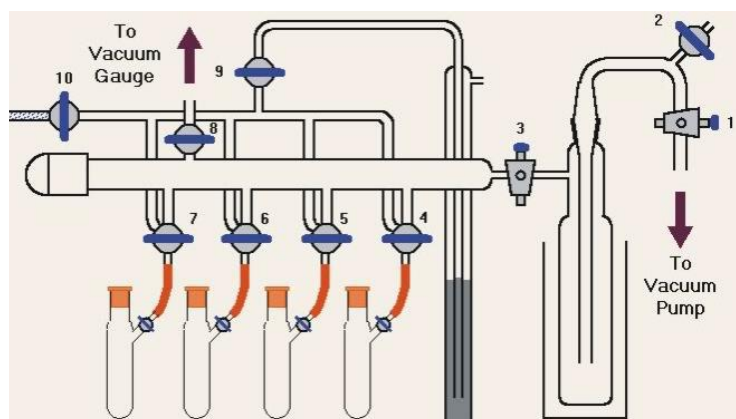


Figure 3.1 Schlenk line [10]

### 3.1.2 Gas supply

Ethylene gas (99.96%) was devolved from National Petrochemical Co., Ltd., Thailand and used as received.

Ultra high purity argon gas (99.999%) was purchased from Thai Industrial Gas Co., Ltd., and further purified by passing through columns packed with molecular sieve 3 A, sodium hydroxide (NaOH) and phosphorus pentoxide ( $P_2O_5$ ) to remove traces of oxygen and moisture. The argon gas was passed through glove box to remove oxygen and moisture.

### 3.1.3 Polymerization reactor

A 100 ml stainless steel autoclave was used as polymerization reactor equipped with a magnetic stirrer.

### 3.1.4 Magnetic stirrer and heater

The magnetic stirrer and heater model RTC basis from IKA Labortechnik were used.

### 3.1.5 Vacuum pump

The vacuum pump model 195 from Labconco Corporation was used. A pressure of  $10^{-1}$  to  $10^{-3}$  mmHg was adequate for the vacuum supply to the vacuum line in the Schlenk line.

### 3.1.6 Polymerization line

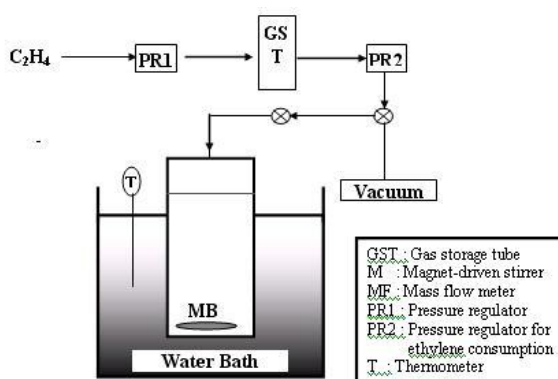


Figure 3.2 Diagram of system in slurry phase polymerization [8]

### 3.1.7 Schlenk tube

A tube with a ground glass joint and side arm, which is three-way glass valve as shown in Figure 3.3. Sizes of Schlenk tubes are 50, 100 and 200 ml used to prepare support in the immobilization process.



Figure 3.3 Schlenk tube [8]

## 3.2 Silica preparation

There are 3 silica supports, which is from rice husk , synthesis , and commercial immobilized with MMAO.

### 3.2.1 Synthesis of silica

#### 3.2.1.1 Chemical

**Table 3.1** The chemicals used for synthesis of the silica.

Chemical	Supplier	Purification
1. CTAB (Cetyltrimethyl ammonium bromide/hexadecyltrimethylammonium bromide)	Aldrich Chemical Company	Used as received
2. Tetraethyl orthosilicate grade 98%	Aldrich Chemical Company	Used as received
3. Ethanol 99% Mw 46.07g/mol Absolute Denatured	Qrec New zeaand	Used as received
4. Ammonia 30%	Aldrich Chemical Company	Used as received
5. DI Water		Used as received

#### 3.2.1.2 Procedure

3.3 g of CTAB was introduced into the beaker , then 11.45 ml ammonia and DI water were introduced into the beaker with magnetic bar and stirred for 30 minutes. After that 6.3 g of TEOS was introduced into the solution and stirred at room temperature for 2 hours. The slurry was filtered by vacuum pump and dried at room temperature for 12 hours , then the white powder was obtained and dried overnight in the oven at 70°C in order to remove the moisture. After that the white powder was calcined under oxygen at 700 °C , atmospheric pressure , heating rate of 10 °C /minute for 6 hours in order to remove solvent and impurities.

#### 3.2.2 Husk silica

Husk silica was prepared by soaking raw husk into the water for 2 days, followed by hydrochloric acid at 80 °C for 1 hour. Adjusted pH to be neutral and dried

in the oven. The silica was calcined under oxygen at 700 °C for 5 hours. The white powder was obtained. Finally, thermally treated silica at 400 °C under vacuum for 4 hours in order to remove OH-group.

### 3.2.3 Commercial silica

Silica Hisil-233 from PPG-Siam Silica Co. Ltd., Thailand was used, and then thermally treated silica at 400 °C under vacuum for 4 hours in order to remove OH-group.

## 3.3 Preparation of MMAO/Modified silica

### 3.3.1 Chemical

Modified- methylaluminoxane (MMAO) 6.5% in toluene supply from Tosoh Finechem Co.Ltd.

### 3.3.2 Immobilization procedure

#### 3.3.2.1 *Ex situ* immobilization

MMAO-modified silica was prepared by *ex situ* immobilization method by immobilizing 0.3 g of thermally treated silica at 400 °C under vacuum for 4 hours with the desired amount of MMAO in 10 ml toluene with magnetic stirring at room temperature for 30 min. The solid part was separated followed by drying in vacuum at room temperature. The white powder of supported cocatalyst (MMAO/support) was then obtained.

#### 3.3.2.2 *In situ* immobilization

0.3 g of thermally treated silica at 400 °C under vacuum for 4 h with the desired amount of 1.14 ml of MMAO with magnetic stirring at room temperature for 30 min in 100 ml of reactor. After this period of time, the suspension was mixed with the zirconocene at ratio of  $[Al]_{MMAO}/[Zr]_{cat} = 1135$ . Then to make a total volume of 30 ml, toluene was introduced into the reactor. The next step is heteropolymerization reaction.

### 3.4 Polymerization on the support with *Ex situ* impregnation

#### 3.4.1 Chemical

**Table 3.2** The chemicals used for polymerization

Chemical	Supplier	Purification
rac-Ethylenebis(indenyl) zirconiumdichloride (Et(Ind) <sub>2</sub> ZrCl <sub>2</sub> )	Aldrich Chemical Company, Inc.	Used as received
Hydrochloric acid (Fuming 36.7%)	Aldrich Chemical Company	Used as received
Methanol (Commercial grade)	S.R. lab	Used as received
Toluene (purity 99.5%)	Quality Reagent Chemical	Soak in molecular sieve

#### 3.4.2 Polymerization procedure

##### 3.4.2.1 Homopolymerization

The ethylene polymerization reaction was performed in a 100 ml semi-batch stainless steel autoclave reactor equipped with magnetic stirrer. In the glove box, MMAO and  $5 \times 10^{-5}$  M of rac-Et[Ind]<sub>2</sub>ZrCl<sub>2</sub> was introduced into the reactor corresponding to  $[Al]_{MMAO}/[Zr]_{cat} = 1135$ . Then, toluene was added into the reactor to make a total volume of 30 ml at room temperature. Polymerization was started by the addition of ethylene gas and was operated under 3.5 bar under vacuum. The rate of ethylene consumption was monitored by a mass flow meter. The polymerization was terminated with acidic methanol and stirred for 15 minutes. The resulting polymer was filtrated and dried at room temperature.

##### 3.4.2.2 Heteropolymerization

The ethylene polymerization reaction was performed in a 100 ml semi-batch stainless steel autoclave reactor equipped with magnetic stirrer. In the glove box, 0.3

g of MMAO/support were introduced into the reactor corresponding to  $[Al]_{MMAO}/[Zr]_{cat} = 1135$ . Then,  $5 \times 10^{-5}$  M of  $rac\text{-Et}[\text{Ind}]_2\text{ZrCl}_2$  was introduced into reactor. Toluene was added into the reactor to make a total volume of 30 ml at room temperature. Polymerization was started by the addition of ethylene gas and was operated under 3.5 bar under vacuum. The rate of ethylene consumption was monitored by a mass flow meter. The polymerization was terminated with acidic methanol and stirred for 15 minutes. The resulting polymer was filtrated and dried at room temperature. Details of immobilization on and polymerization are illustrated in **Figure 3.4**.

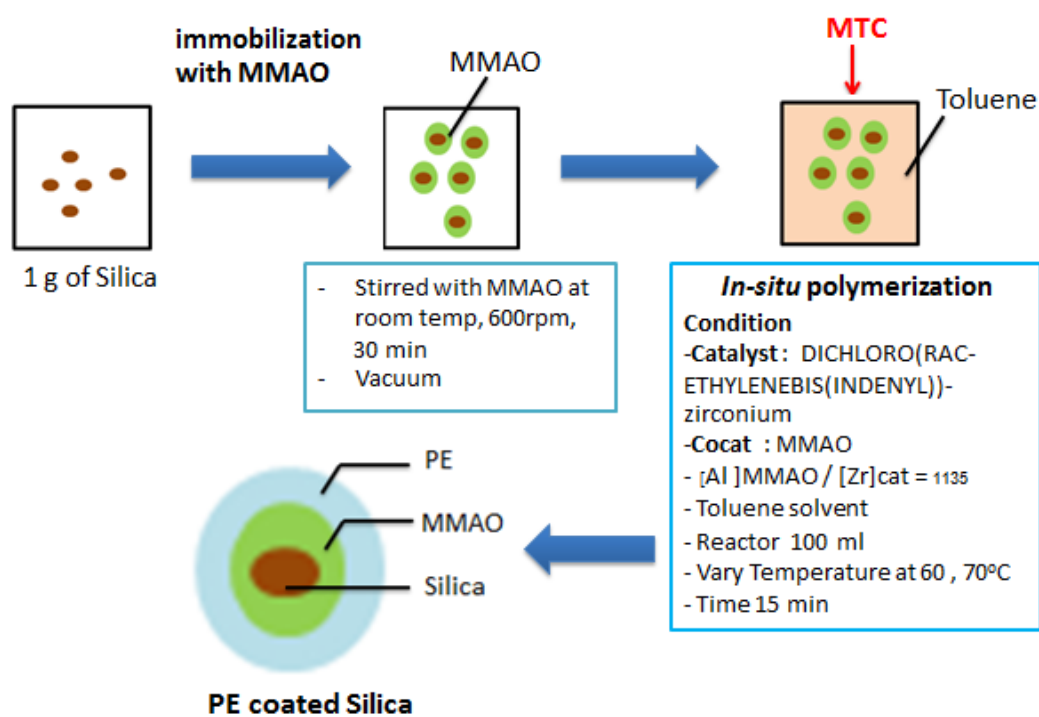


Figure 3.4 Methodology



### 3.5 Characterization

#### 3.5.1 Characterization silica support before immobilization

##### 3.5.1.1 Scanning electron microscopy (SEM)

SEM was used to determine the morphologies. The SEM of JEOL mode JSM-6400 was applied.

##### 3.5.1.2 X-ray diffraction (XRD)

XRD was performed to determine the bulk crystalline phases of sample. It was conducted using a SIEMENS D-5000 X-ray diffractometer with  $\text{CuK}\alpha$  radiation with Ni filter in the  $2\theta$  range of 20 to 80 degrees.

##### 3.5.1.3 $\text{N}_2$ physisorption

Measurement of BET surface area, average pore diameter, pore volume and pore size distribution of silica support were determined by  $\text{N}_2$  physisorption using a Micromeritics ASAP 2000 automated system.

##### 3.5.1.4 Fourier transform infrared spectroscopy (FT-IR)

The powder samples for IR analysis were casted as thin films on NaCl disks under the argon gas protection from moisture and oxygen. The prepared samples were analyzed by Nicolet 6700 FTIR spectrometer with ATR mode. The spectra were collected in the scanning range from  $400\text{-}4000\text{ cm}^{-1}$  with 100 numbers of scans at a resolution of  $4\text{ cm}^{-1}$ . The FTIR spectra were recorded on ATI Mattson Infinity Series spectrometer.

##### 3.5.1.5 Thermogravimetric analysis - differential scanning calorimetry (TGA-DSC)

TGA was performed to determine thermal stability of silica. It was conducted using TA Instruments SDT Q 600 analyzer. The samples of 10-20 mg and a temperature ramping from 25 to  $700^\circ\text{C}$  at  $10^\circ\text{C}/\text{min}$  were used in the operation. The carrier gas was  $\text{N}_2$  UHP

### 3.5.1.6 X-ray fluorescence spectrometry (XRF)

XRF using Panalytical minipal-4 instrument was performed to determine the composition and the amount of element on silica. Add sample into the mold and then put into the hydraulic press. The sample was analyzed by XRF.

## 3.5.2 Characterization silica support after immobilization

### 3.5.2.1 Scanning electron microscopy (SEM) and energy dispersive X-ray spectroscopy (EDX)

SEM and EDX were used to determine the morphologies and elemental distribution throughout the sample granules, respectively. The SEM of JEOL mode JSM-6400 was applied. The EDX was performed using Link Isis series 300 program.

### 3.5.2.2 Fourier transform infrared spectroscopy (FT-IR)

As mentioned in 3.5.1.4

### 3.5.2.3 Thermogravimetric analysis - differential scanning calorimetry (TGA-DSC)

As mentioned in 3.5.1.5, in order to determine the interaction force of the supported MMAO.

### 3.5.2.4 X-ray photoelectron spectroscopy (XPS)

XPS was performed to determine the interaction force of the supported MMAO. MMAO was evaluated using the AMICUS photoelectron spectrometer and a KRATOS VISION 2 software. The experiment was carried out at 0.1 eV/step of resolution, 75 eV pass energy and the operating pressure approximately  $1 \times 10^{-6}$  Pa. The sample was prepared in glove box and transferred to the XPS under an argon atmosphere.

### 3.5.3 Characterization polyethylene coated-SiO<sub>2</sub>

#### 3.5.3.1 Scanning electron microscopy (SEM)

As mentioned in 3.5.1.1

#### 3.5.3.2 X-ray diffraction (XRD)

As mentioned in 3.5.1.2

#### 3.5.3.3 Thermogravimetric analysis - differential scanning calorimetry (TGA-DSC)

As mentioned in 3.5.1.5, in order to determine thermal property of polyethylene.

#### 3.5.3.4 Transmission electron microscopy (TEM)

TEM was used to determine the Al distribution on polymer using Model 695 PIPS II.

#### 3.5.3.5 Microtome

Microtome was used to determine the morphology of polyethylene coated-SiO<sub>2</sub> using the Reichert-Jung ULTRACUT.

### 3.6 Benefits

- Obtain optimal condition in order to produce polyethylene coated-SiO<sub>2</sub> to be non-polar as the natural rubber.
- Realize the different properties of supports.
- Realize the different of immobilization method , prepared by *ex situ* immobilization and *in situ* immobilization.

## Chapter IV

### RESULTS AND DISCUSSIONS

#### Part1 : Effect of MMAO on SiO<sub>2</sub>-supported metallocene catalyst

In this part, SiO<sub>2</sub> supports before immobilization and after *ex situ* immobilization were investigated. In fact, the SiO<sub>2</sub> support was prepared, and then sequentially immobilized with MMAO. The MMAO- SiO<sub>2</sub> supports were then characterized using SEM-EDX, N<sub>2</sub> physisorption , XRF , XRD , TGA , and XPS.

#### 4.1 Characterization of supports and supported MMAO.

##### 4.1.1 Characterization of supports with X-ray fluorescence spectrometry (XRF)

The silica supports having different sources, such as SiO<sub>2</sub> from husk (SiO<sub>2</sub>-RH), SiO<sub>2</sub> from synthesis (SiO<sub>2</sub>-Syn), and SiO<sub>2</sub> from commercial (SiO<sub>2</sub>-Com) were characterized before immobilization with MMAO. The results are shown in Table 4.1.

**Table 4.1** XRF of silica supports with different sources

Compound	SiO <sub>2</sub> -RH	SiO <sub>2</sub> -Syn	SiO <sub>2</sub> -Com
SiO <sub>2</sub>	99.58	99.90	96.16
K <sub>2</sub> O	0.02	0	0.03
CaO	0.36	0.09	0.13
Fe <sub>2</sub> O <sub>3</sub>	0.01	0	0.04
Na <sub>2</sub> O	0	0	2.18
SO <sub>3</sub>	0	0	1.42
TiO <sub>2</sub>	0	0	0.03

From Table 4.1, it can be observed that SiO<sub>2</sub>-RH , SiO<sub>2</sub>-Syn , and SiO<sub>2</sub>-Com

were almost purity and be composed of some components such as CaO in SiO<sub>2</sub>-RH , Na<sub>2</sub>O and SO<sub>3</sub> in SiO<sub>2</sub>-Com , and CaO in SiO<sub>2</sub>-Syn.

#### 4.1.2 Characterization of supports with N<sub>2</sub> physisorption

The silica supports having different surface areas , pore size , and pore volume as shown in Table 4.2. It can be observed that SiO<sub>2</sub>-Syn exhibited the largest surface area of 1,081 m<sup>2</sup>/g and SiO<sub>2</sub>-Com exhibited the largest pore size of 169 Å.

**Table 4.2** N<sub>2</sub> physisorption of silica supports with different sources

Silica	Surface area (m <sup>2</sup> /g)	Pore size (Å)	Pore volume (cm <sup>3</sup> /g)
SiO <sub>2</sub> -RH	210	40	0.75
SiO <sub>2</sub> -Syn	1081	23	0.32
SiO <sub>2</sub> -Com	166	169	0.71

The N<sub>2</sub> adsorption-desorption isotherms for all supports are shown in Figure 4.1. The pore structure of SiO<sub>2</sub> exhibited the characteristic of mesoporous structure according to type IV classified by IUPAC (International Union of Pure and Applied Chemistry).

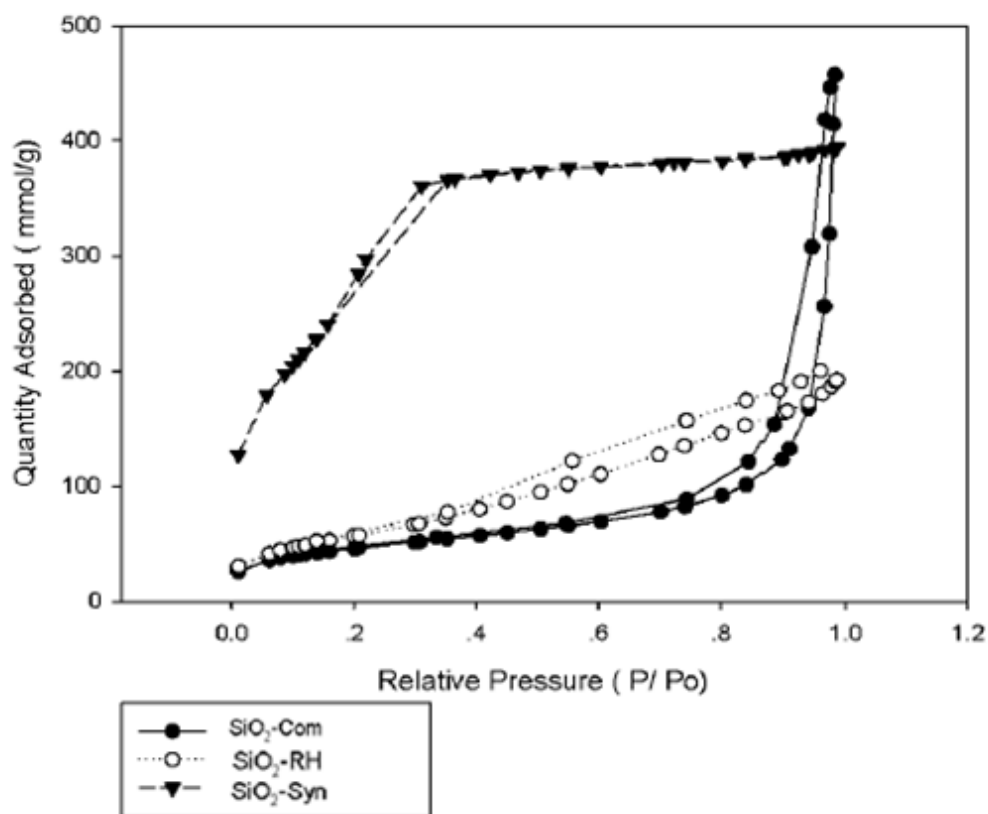


Figure 41 The N<sub>2</sub> adsorption-desorption isotherms for all supports.

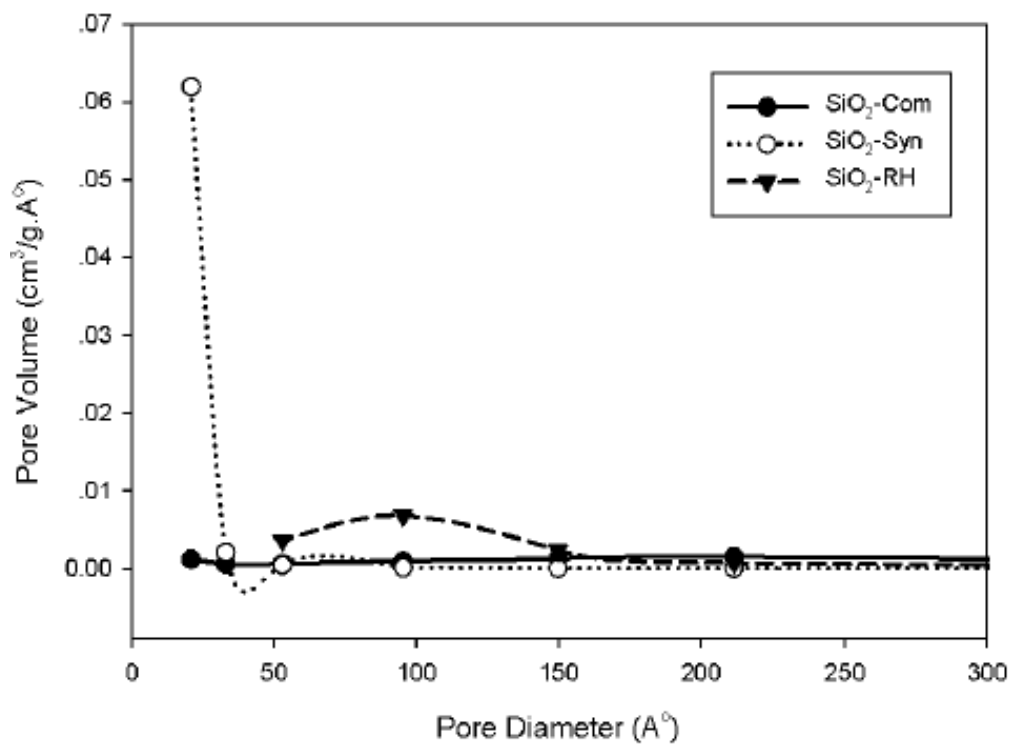


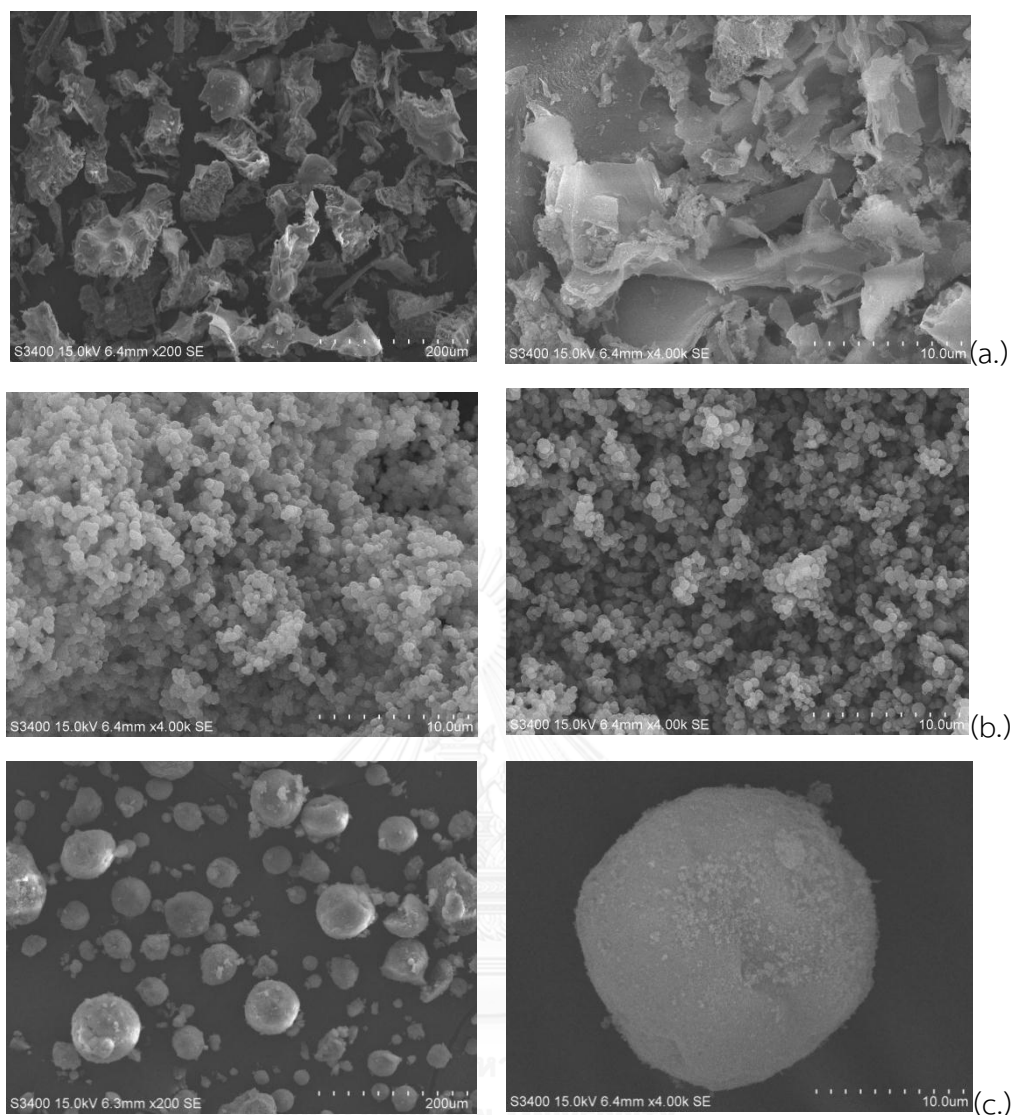
Figure 4.2 The pore size distribution of silica

Figure 4.2 shows the pore size distribution of silica , which were related to the pore structure as discussed from Figure 4.1. The average pore diameter of  $\text{SiO}_2\text{-RH}$  ,  $\text{SiO}_2\text{-Syn}$  , and  $\text{SiO}_2\text{-Com}$  was 40 , 23 , 169 Å , respectively.

#### 4.1.3 Characterization of supports and supported MMAO with scanning electron microscope (SEM) and energy dispersive X-ray spectroscopy (EDX)

In order to determine the morphologies of the supports and elemental distributions of the supports after immobilization, SEM and EDX were performed , respectively. The SEM micrographs of MMAO silica supports before immobilization with MMAO are shown in Figure 4.3.





**Figure 4.3** SEM micrographs of SiO<sub>2</sub>-RH (a.), SiO<sub>2</sub>-Syn (b.), and SiO<sub>2</sub>-Com (c.) at 200X and 4kx magnification before immobilization.

From Figure 4.3, it was observed that SiO<sub>2</sub>-Syn and SiO<sub>2</sub>-Com were spherical shape, while SiO<sub>2</sub>-RH was irregular shape.

**Table 4.3** EDX analysis expressed the average of O on silica supports.

	SiO <sub>2</sub> -RH	SiO <sub>2</sub> -Syn	SiO <sub>2</sub> -Com
Ratio of O/SiO <sub>2</sub>	0.83	0.86	1.06



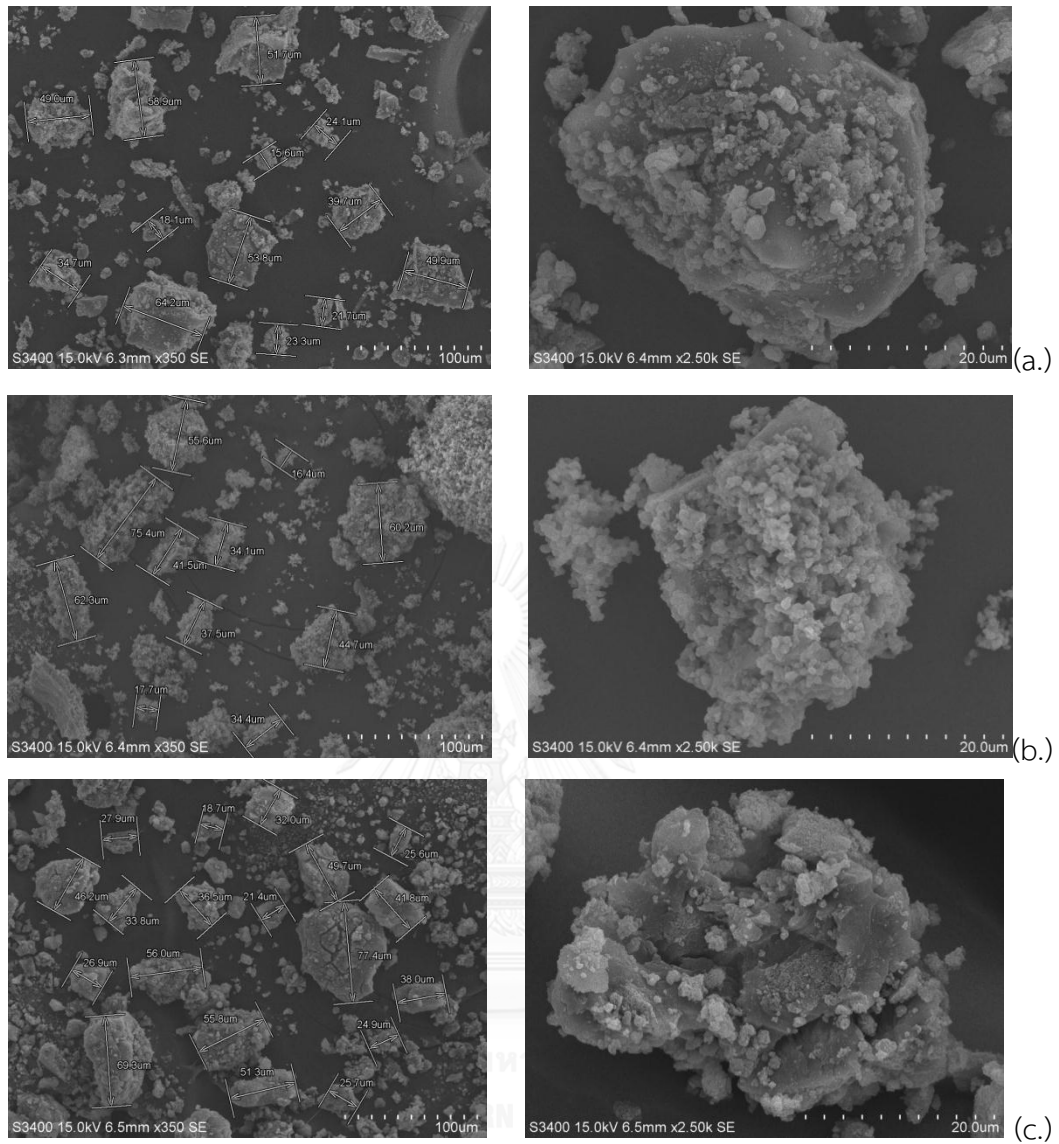


**Figure 4.4** SEM micrographs of  $\text{SiO}_2\text{-RH}$  (a.),  $\text{SiO}_2\text{-Syn}$  (b.), and  $\text{SiO}_2\text{-Com}$  (c.) at 350X and 2.5kx magnification after immobilization.

From Figure 4.4, it was observed that  $\text{SiO}_2\text{-RH}$ ,  $\text{SiO}_2\text{-Syn}$  and  $\text{SiO}_2\text{-Com}$  after immobilization with MMAO were irregular shape.

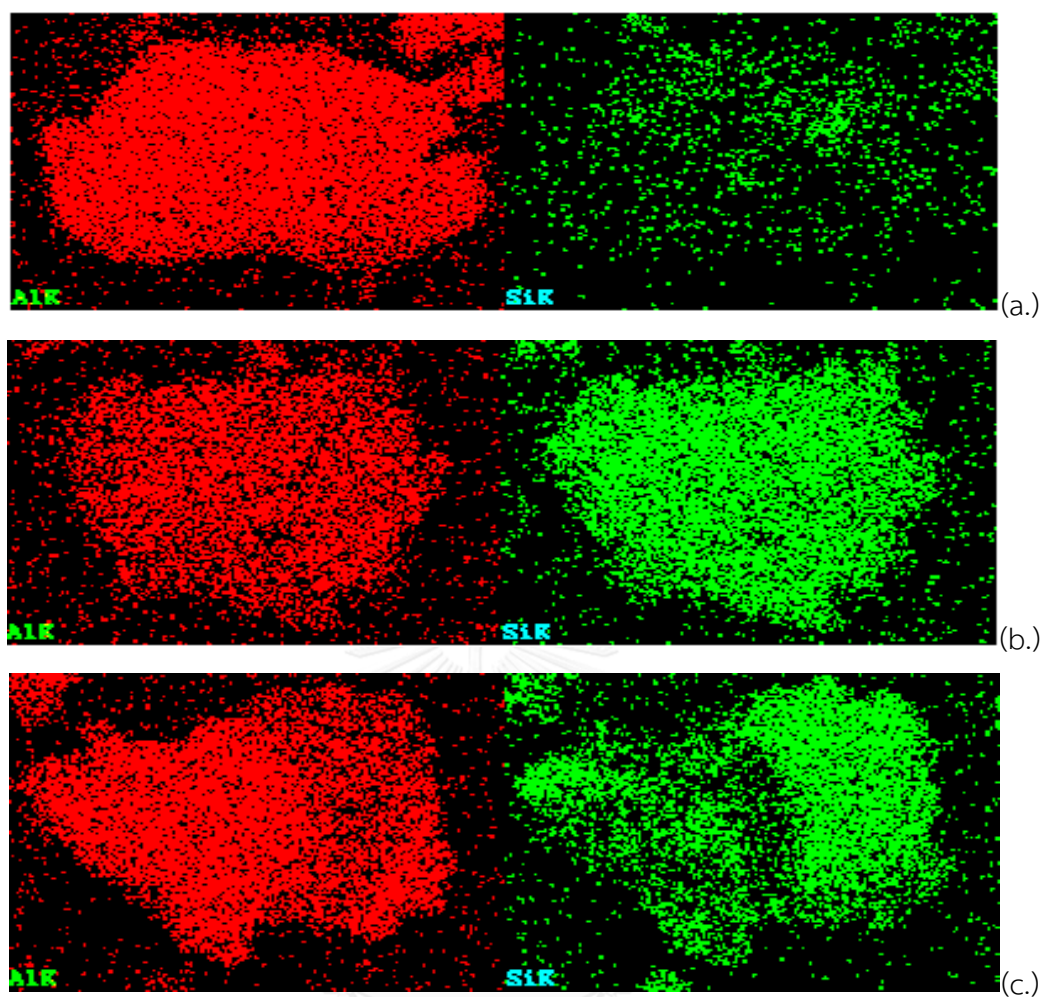


**Figure 4.5** EDX of SiO<sub>2</sub>-RH (a.), SiO<sub>2</sub>-Syn (b.), and SiO<sub>2</sub>-Com (c.)

From the Figure 4.5 , the EDX obtained is shown indicating good distribution of MMAO Al distribution. It was found that the average amount of  $[Al]_{MMAO} : SiO_2$  of SiO<sub>2</sub>-RH, SiO<sub>2</sub>-Syn and SiO<sub>2</sub>-Com was 9.63 , 0.62 , and 0.93, respectively as shown in Table 4.4. The largest amount of  $[Al]_{MMAO}$  indicated that SiO<sub>2</sub>-RH had the best Al distribution on the external surface of silica.

**Table 4.4** EDX analysis of Al on the silica supported

	SiO <sub>2</sub> -RH	SiO <sub>2</sub> -Syn	SiO <sub>2</sub> -Com
Al:SiO <sub>2</sub>	9.63	0.62	0.93

#### 4.1.4 Characterization of supports and supported MMAO with X-ray Powder Diffraction (XRD).

The SiO<sub>2</sub> supports were characterized before immobilization with MMAO. The XRD patterns of these supports are shown in Figure 4.6. It can be seen that all supports exhibited the similar XRD patterns indicating only a broad peak at 22° as seen typically for the conventional amorphous silica.

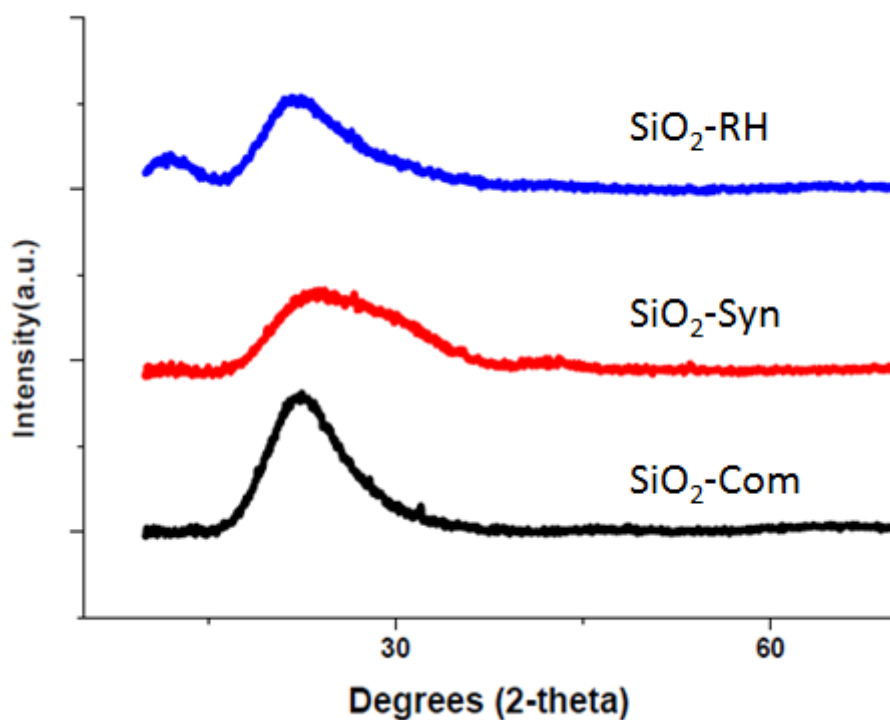
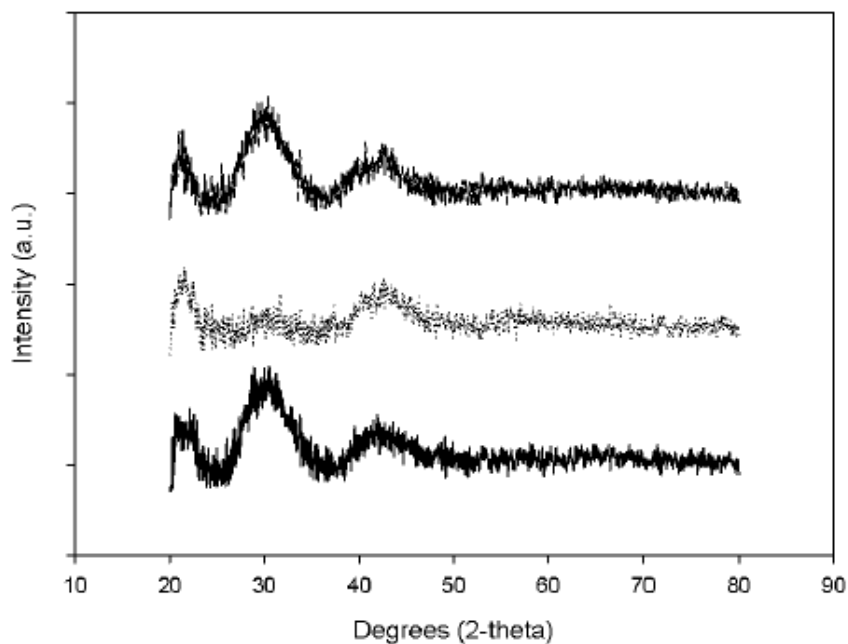
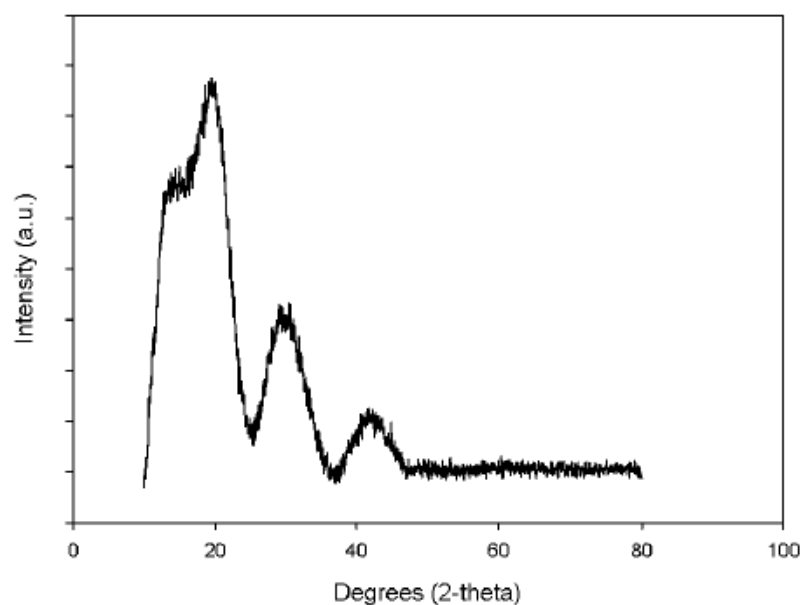


Figure 4.6 XRD patterns of SiO<sub>2</sub>-RH, SiO<sub>2</sub>-Syn and SiO<sub>2</sub>-Com before immobilization



**Figure 4.7** XRD patterns of SiO<sub>2</sub>-RH, SiO<sub>2</sub>-Syn and SiO<sub>2</sub>-Com after immobilization

After silica immobilization with MMAO, the support exhibited broad peak at 22°, which was similar to the silica before immobilization. It indicated that MMAO was in the highly dispersed form, which was invisible by XRD. As the peaks at 30° and 41.5° were the peak of sample holder, expressed in Figure 4.8.



**Figure 4.8** XRD patterns of sample holder.

#### 4.1.5 Characterization of supports and supported MMAO with Thermogravimetric Analysis (TGA)

In order to measure stability of silica supports before immobilization, the TGA measurement was performed. The TGA provides information on the degree of thermal stability of  $\text{SiO}_2$  supports in term of weight loss and temperature. The TGA profiles of  $\text{SiO}_2$  supports are shown in Figure 4.9. It was observed that the weight loss of the contents in supports were in the orders of  $\text{SiO}_2\text{-Com}$  (4.4%) >  $\text{SiO}_2\text{-Syn}$  (2.57%) >  $\text{SiO}_2\text{-RH}$  (1.72%). This indicated that  $\text{SiO}_2\text{-RH}$  had the strongest thermal stability among other supports.

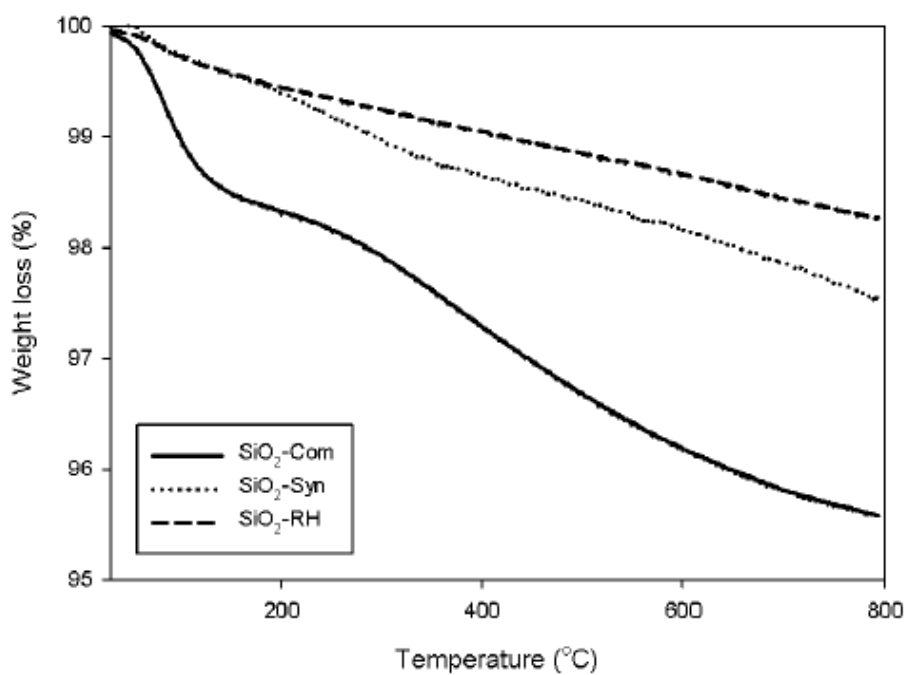
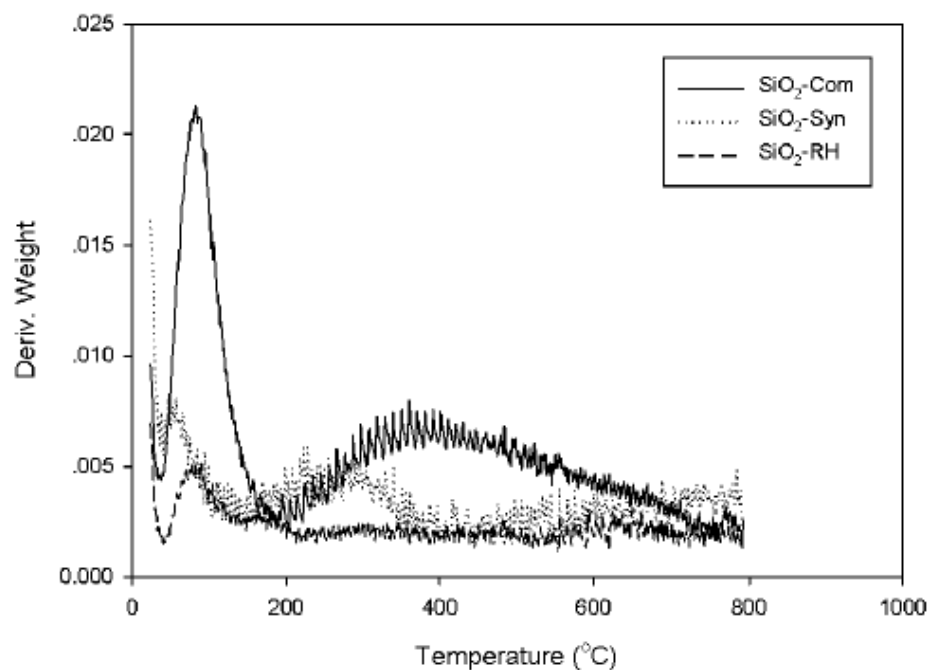


Figure 4.9 TGA profiles of  $\text{SiO}_2$  before immobilization.



**Figure 4.10** DTA profiles of SiO<sub>2</sub> before immobilization.

According to Figure 4.10, it can be seen that at 100°C, it exhibited percent weight loss of moisture and between 200-800°C assigned to percent weight loss of organic volatile content.

In order to identify the interaction of  $[Al]_{MMAO}$  on silica supports after immobilization with MMAO, the TGA measurement was performed to prove the degree of interaction between the cocatalyst (MMAO) and the support. The TGA provides information on the degree of interaction for MMAO bound to the supports in term of weight loss and temperature. The TGA profiles of  $[Al]_{MMAO}$  on various supports are shown in Figure 4.11. It was observed that the weight loss of  $[Al]_{MMAO}$  present on various supports were in the order of SiO<sub>2</sub>-Syn (26.13%) > SiO<sub>2</sub>-RH (24.33%) > SiO<sub>2</sub>-Com (23.11%). This indicated that  $[Al]_{MMAO}$  present on SiO<sub>2</sub>-Com had the strongest interaction among other supports.

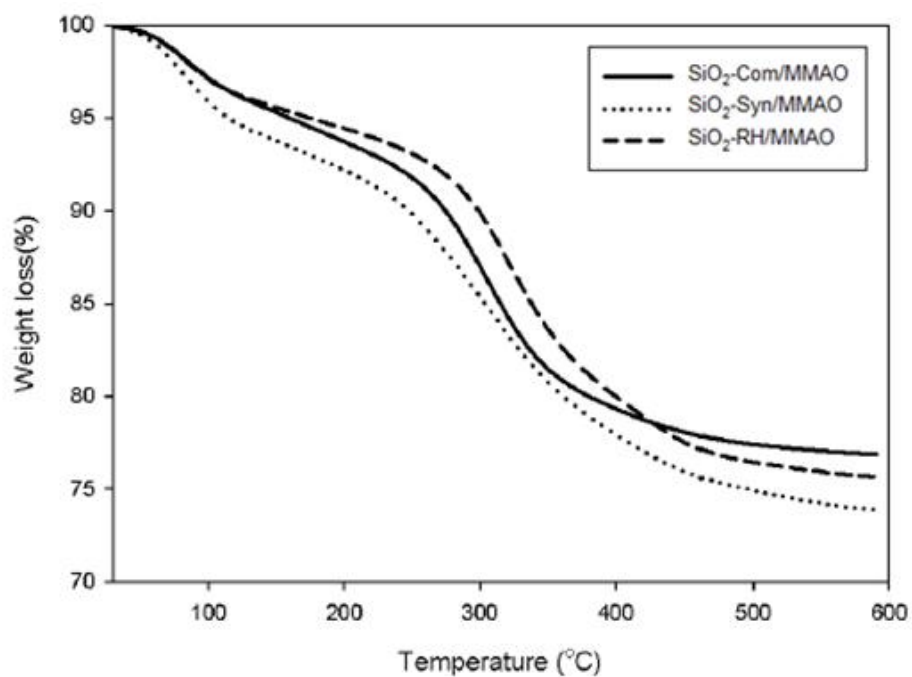


Figure 4.11 TGA profiles of SiO<sub>2</sub> after immobilization.

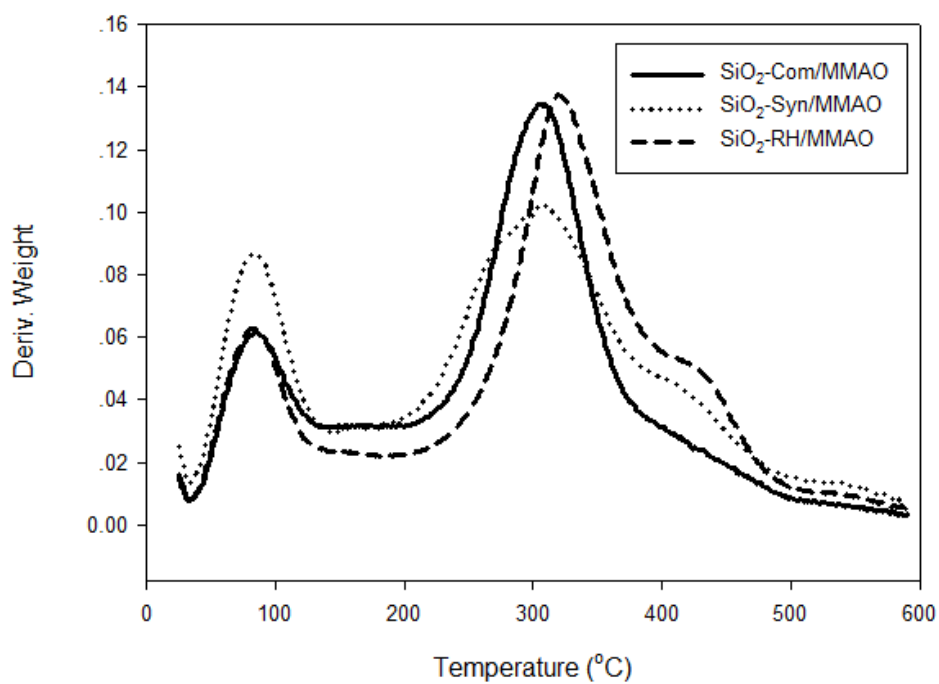


Figure 4.12 DTA profiles of SiO<sub>2</sub> after immobilization.

According to Figure 4.12 , it can be seen that at 100°C, it exhibited percent weight loss of volatile organic compounds and during 250-420°C, it exhibited percent weight loss of MMAO.

#### 4.1.6 Characterization of supported MMAO with X-ray photoelectron spectroscopy (XPS).

XPS was used to determine the binding energy (BE) and amount of Al on silica-supported surfaces. In fact, the binding energy of Al 2p core-level of  $[Al]_{MMAO}$  was measured in each silica-supported MMAO as shown in Table 4.5

**Table 4.5** XPS data of Al 2p core level of cocatalyst.

Cocatalyst	BE (ev) for $Al^{3+}$	Amount of $Al^{3+}$ at surface (%mass)
MMAO [15]	74.7	28.5
SiO <sub>2</sub> /MMAO [15]	74.6	25
SiO <sub>2</sub> -RH/MMAO	75.5	20.12
SiO <sub>2</sub> -Syn/MMAO	76	24
SiO <sub>2</sub> -Com/MMAO	76.1	25.07

From the Table 4.5 , it was found that no significant change in the oxidation state of  $[Al]_{MMAO}$  occurred in SiO<sub>2</sub>-RH/MMAO, SiO<sub>2</sub>-Syn/MMAO, and SiO<sub>2</sub>-Com/MMAO. SiO<sub>2</sub>-Com/MMAO expressed the highest amount of  $Al^{3+}$  at surface , so it exhibited the highest catalytic activity. Details of catalytic activities are illustrated in the second part.



## Part 2 : Catalytic activities of ethylene polymerization.

In this part , the catalytic activity during ethylene polymerization of silica - supported zirconocene/MMAO catalyst via different immobilization methods on the various silica-supported MMAO with different polymerization temperature was investigated.



## 4.2 Catalytic activities and melting temperature of polymer.

### 4.2.1 Catalytic activities of ethylene polymerization

**Table 4.6** Catalytic activities of various silica-supported zirconocene/MMAO catalyst via *ex situ* and *in situ* immobilization method.

	Immobilization method	Temperature Polymerization (°C)	Yield (g)	Catalytic activity (gPE/gZr.h)
Homogeneous	-	60	0.23	112
	-	70	0.83	400
PE-SiO <sub>2</sub> -RH	<i>Ex situ</i>	60	0.1	48
	<i>Ex situ</i>	70	0.11	52
	<i>In situ</i>	70	0.42	202
PE-SiO <sub>2</sub> -Syn	<i>Ex situ</i>	60	0.15	72
	<i>Ex situ</i>	70	0.16	77
	<i>In situ</i>	70	0.73	352
PE-SiO <sub>2</sub> -Com	<i>Ex situ</i>	60	0.09	43
	<i>Ex situ</i>	70	0.2	98
	<i>In situ</i>	70	0.31	150

From Table 4.6, the homopolymerization at 70°C expressed the highest catalytic activity (400 gPE/gZr.h), while at 60°C expressed the catalytic activity less than polymerization via *in situ* immobilization. The catalytic activity of SiO<sub>2</sub>-Syn at 60°C polymerization temperature via *ex situ* immobilization was the highest (72 gPE/gZr.h). At 70°C polymerization temperature, SiO<sub>2</sub>-Com expressed the highest

catalytic activity. Because the polymerization temperature at 70°C caused the higher catalytic activity than at 60°C and the ethylene consumption at 70°C was higher than at 60°C as shown in Figure 4.13. Therefore, the polymerization via *in situ* immobilization would be studied at 70°C. It was found that the catalytic activity of polymerization via *in situ* immobilization was higher than the catalytic activity of polymerization via *ex situ* immobilization and the catalytic activity of SiO<sub>2</sub>-Syn at 70°C was the highest.

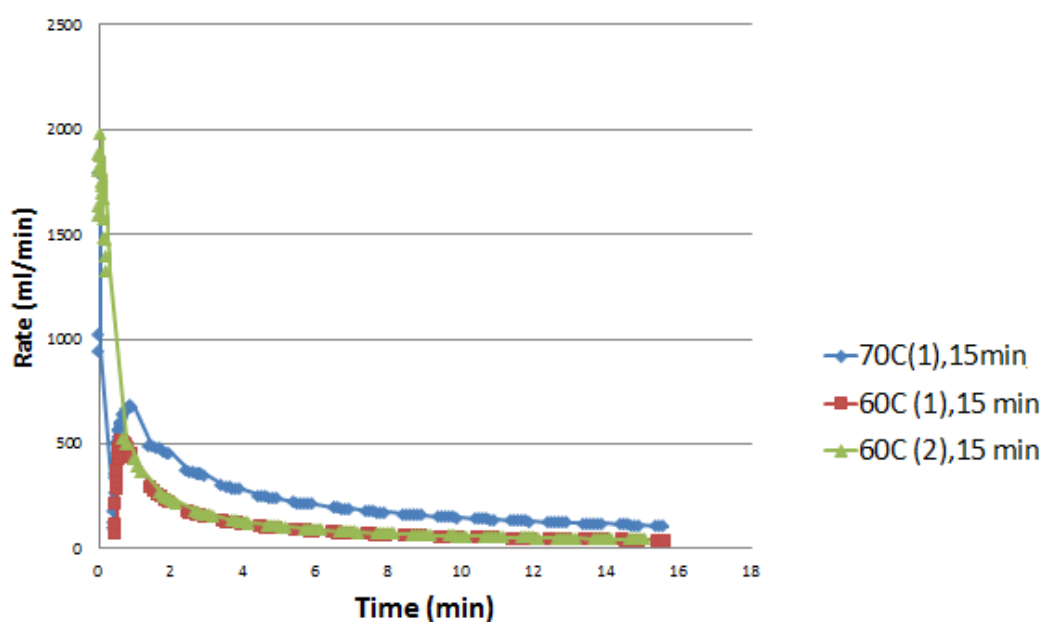


**Figure 4.13** The ethylene consumption of homopolymerization at 60 °C and 70 °C

Base on the surface concentrations of Al 2p in Table 4.5, SiO<sub>2</sub>-Com expressed the highest value, so it exhibited the highest catalytic activity of polymerization via *ex situ* immobilization. However the catalytic activity of SiO<sub>2</sub>-Com at 60 °C was the lowest. This was indicating the optimum polymerization temperature was at 70 °C.

4.2.2 Effect of various supports , immobilization method and polymerization temperature on the melting temperature and percent of crystallinity of polymer.

Table 4.7 Melting temperature and percent of crystallinity of polymer.

	Immobilization method	Temperature Polymerization (°C)	T <sub>m</sub> (°C)	Crystallinity (%)
Homogeneous	-	70	124.02	48.95
PE-SiO <sub>2</sub> -RH	<i>Ex situ</i>	60	n.o.	n.o.
	<i>Ex situ</i>	70	n.o.	n.o.
	<i>In situ</i>	70	125.95	19
PE-SiO <sub>2</sub> -Syn	<i>Ex situ</i>	60	n.o.	n.o.
	<i>Ex situ</i>	70	n.o.	n.o.
	<i>In situ</i>	70	124.47	23.96
PE-SiO <sub>2</sub> -Com	<i>Ex situ</i>	60	125.35	32.78
	<i>Ex situ</i>	70	125.35	25.59
	<i>In situ</i>	70	125.95	14.14

n.o. refers to not observe.

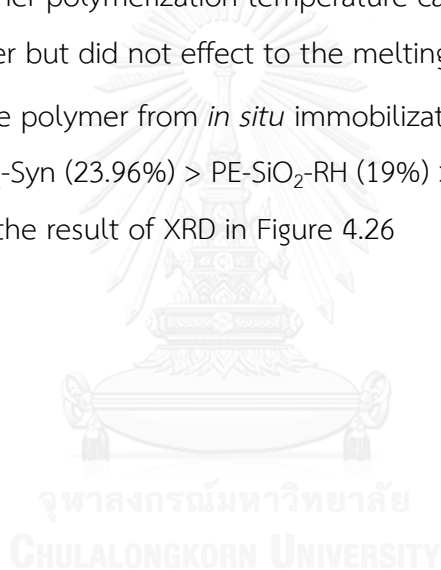
From the characterization of polymer in Table 4.7, it revealed that no melting temperature was found in PE-SiO<sub>2</sub>-RH60 , PE-SiO<sub>2</sub>-RH70 , PE-SiO<sub>2</sub>-Syn60 , and PE-SiO<sub>2</sub>-Syn70 from the *ex situ* immobilization, indicating non-crystalline or amorphous polymer. This was corresponded to the result of XRD in Figure 4.26

It was found the melting temperature of PE-SiO<sub>2</sub>-Com60 and PE-SiO<sub>2</sub>-Com70 from the *ex situ* immobilization, which were almost similar to polymer from homogeneous reaction and *in situ* immobilization.

Considered the crystallinity of polymer, it was observed that the polymer from homogeneous reaction expressed the highest crystallinity. It was indicated the crystallinity of polymer decreased when SiO<sub>2</sub> supported were used in the polymerization system.

The crystallinity of PE-SiO<sub>2</sub>-Com from *ex situ* immobilization via polymerization temperature at 60°C (32.78%) higher than at 70°C (25.59%). It was indicated that the higher polymerization temperature caused the lower of crystallinity of polymer but did not effect to the melting temperature.

Considered the polymer from *in situ* immobilization , it was found that crystallinity of PE-SiO<sub>2</sub>-Syn (23.96%) > PE-SiO<sub>2</sub>-RH (19%) > PE-SiO<sub>2</sub>-Com (14.14%), which correspond to the result of XRD in Figure 4.26



### Part 3 : Characterization of Polyethylene

In this part, the polymers from homopolymerization , polymerization via *ex situ* and *in situ* immobilization were characterized by SEM-EDX, XRD, TGA-DSC and TEM.

#### 4.3 Homopolymerization

Homopolymerization was studied in order to determine the catalytic activity and morphology of polymer at 60°C and 70°C. Moreover it is important to identify the characteristics of polymer without silica support in order to compare.

##### 4.3.1. Characterization of polyethylene with Scanning Eletron Microscopy (SEM)

In order to determine the morphologies of the polymer, SEM was performed in Figure 4.14, which can be seen the net of polymer.

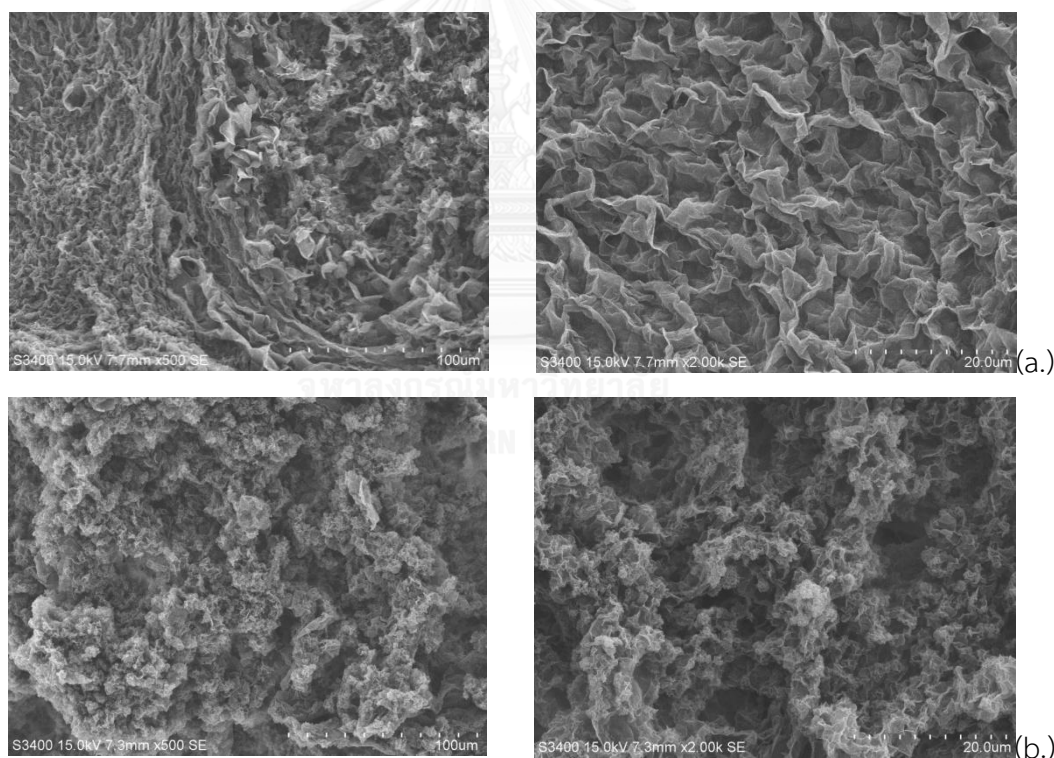


**Figure 4.14** SEM micrographs of polymer from homopolymerization at 60°C and 70°C at 500X and 4kX magnification (a.) PE-60 (b.) PE-70

### 4.3.2 Characterization of polyethylene with X-ray Powder Diffraction (XRD)

The polymer was characterized by XRD as shown in Figure 4.15. It was expressed the sharp peak at  $21.5^\circ$  and  $23.9^\circ$  as seen typically for the polyethylene.

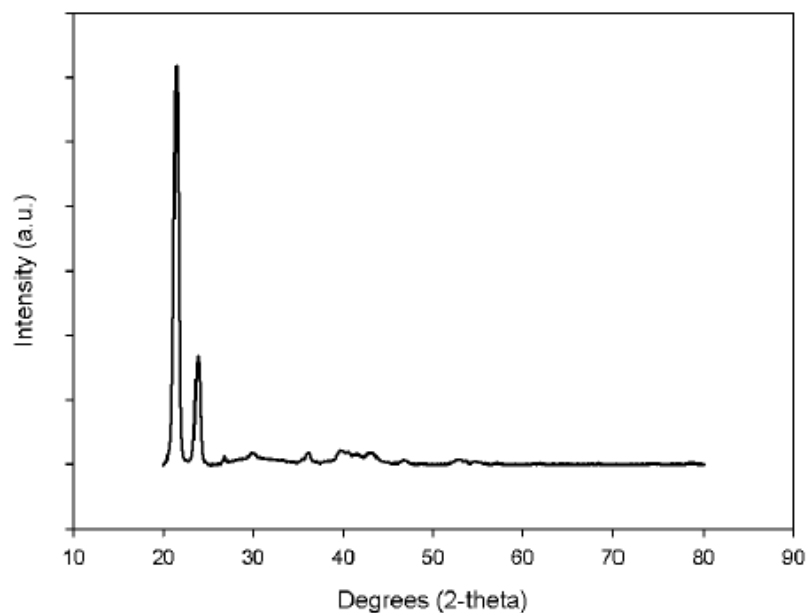


Figure 4.15 XRD pattern of polymer from Homopolymerization.

### 4.3.3 Characterization of polyethylene with Thermogravimetric Analysis (TGA)

In order to measure the thermal stability, the TGA measurement was performed. The TGA provides information on the degree of thermal stability of polymer in terms of weight loss and temperature. The TGA and DTA profiles of polymers are shown in Figures 4.16 and 4.17, respectively. It was observed that polymer was decomposed during  $400\text{-}500^\circ\text{C}$ , which was 95.38%wt.

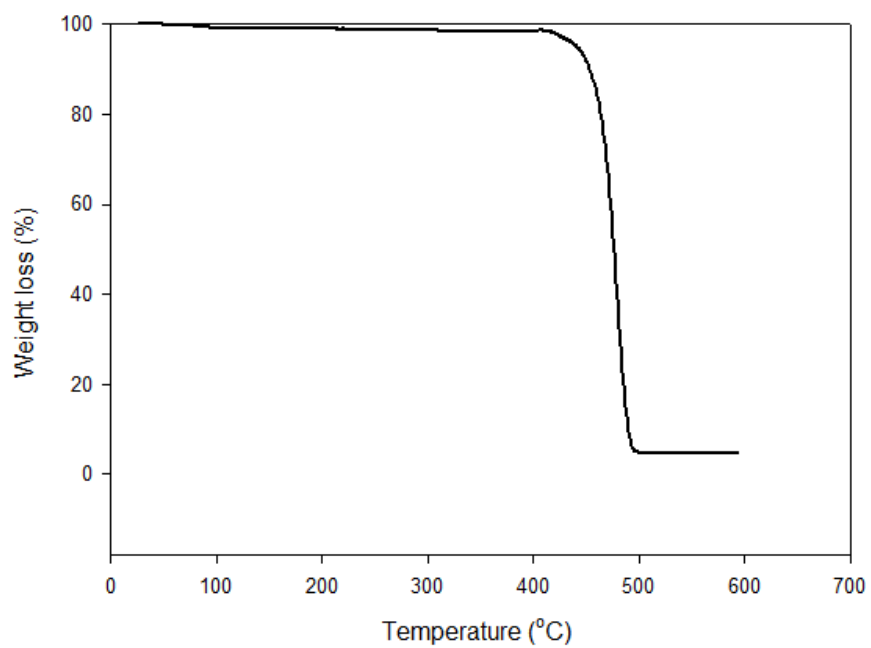


Figure 4.16 TGA profiles of polymer from homopolymerization.

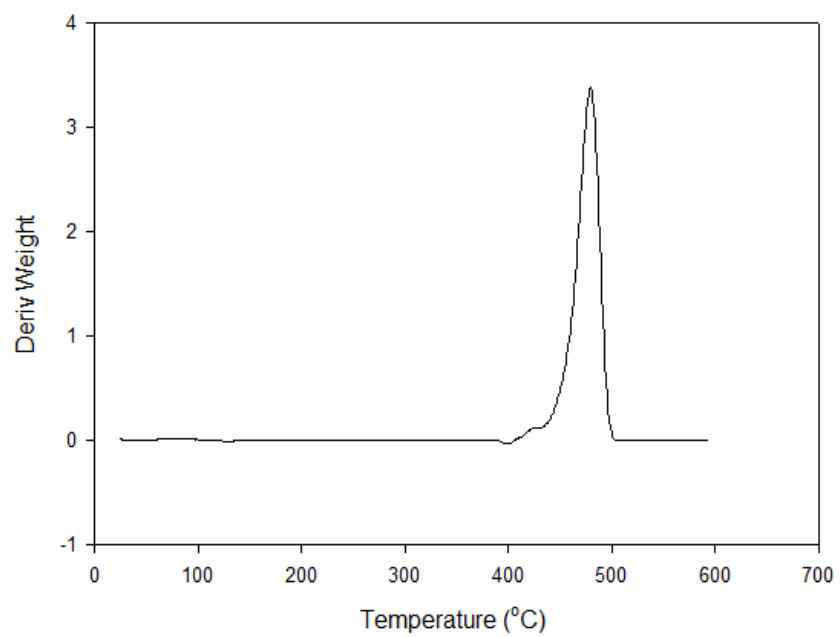


Figure 4.17 DTA profiles of polymer from homopolymerization.



#### 4.4 Polymerization via *ex situ* immobilization.

The polymerization via *ex situ* immobilization was studied at 60°C and 70°C using SiO<sub>2</sub>-RH, SiO<sub>2</sub>-Syn, and SiO<sub>2</sub>-Com as supported catalyst. The polymer was characterized by SEM-EDX, XRD, TGA-DSC, and TEM.

##### 4.4.1 Characterization of polyethylene with Scanning Electron Microscopy (SEM) with Energy Dispersive X-Ray Analysis (EDX)

In order to determine the morphologies and Al distribution of polymer, SEM-EDX was performed in Figures 4.18 - 4.21.



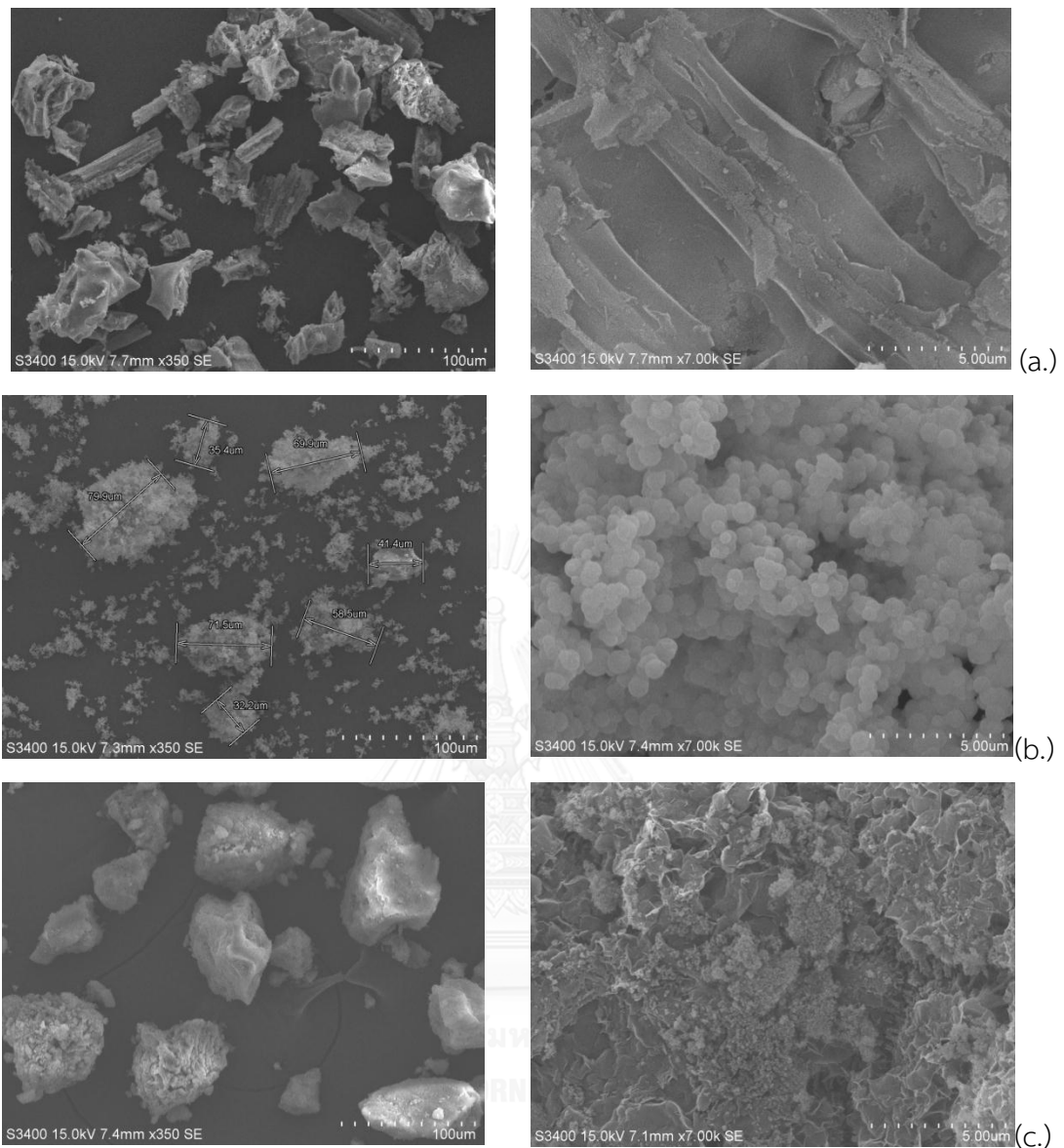


**Figure 4.18** SEM micrographs of PE-SiO<sub>2</sub>-RH60 (a.), PE-SiO<sub>2</sub>-Syn60 (b.) , PE-SiO<sub>2</sub>-Com60 (c.) at 350X and 7kX magnification at 60°C of polymerization temperature.

From the Figure 4.18 , it was observed that PE-SiO<sub>2</sub>-RH60 and PE-SiO<sub>2</sub>-Com60 were irregular shape ,while PE-SiO<sub>2</sub>-Syn60 was spherical shape.

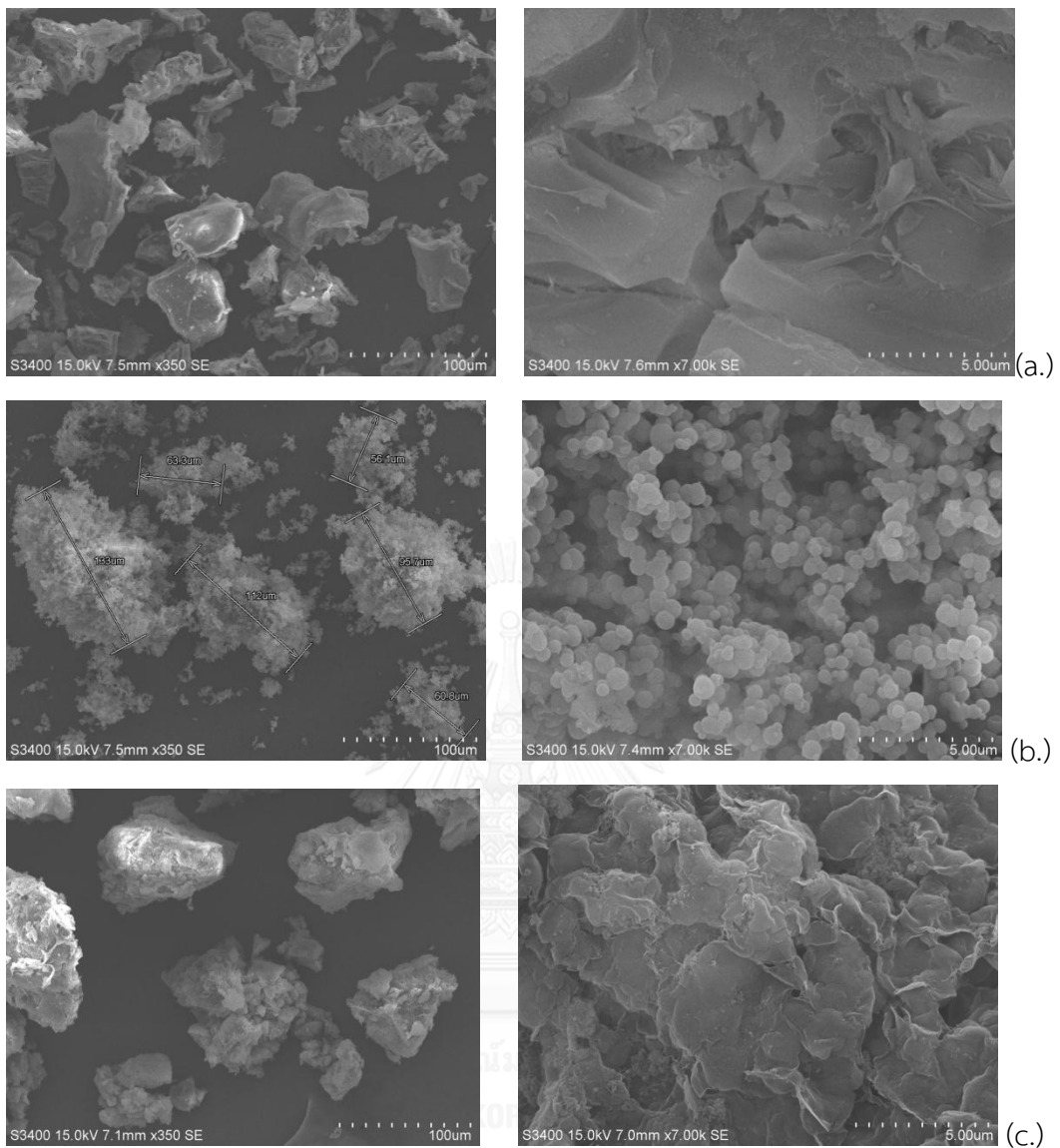


**Figure 4.19** SEM micrographs of PE-SiO<sub>2</sub>-RH60 (a.), PE-SiO<sub>2</sub>-Syn60 (b.) , PE-SiO<sub>2</sub>-Com60 (c.) at 350X and 7kX magnification at 60°C of polymerization temperature.

From the Figure 4.19 , it was observed that PE-SiO<sub>2</sub>-RH70 was more spheridoid shape than SiO<sub>2</sub> without coated by polyethylene, which was irregular shape. So, the morphologies of PE-SiO<sub>2</sub>-RH70 were improved.

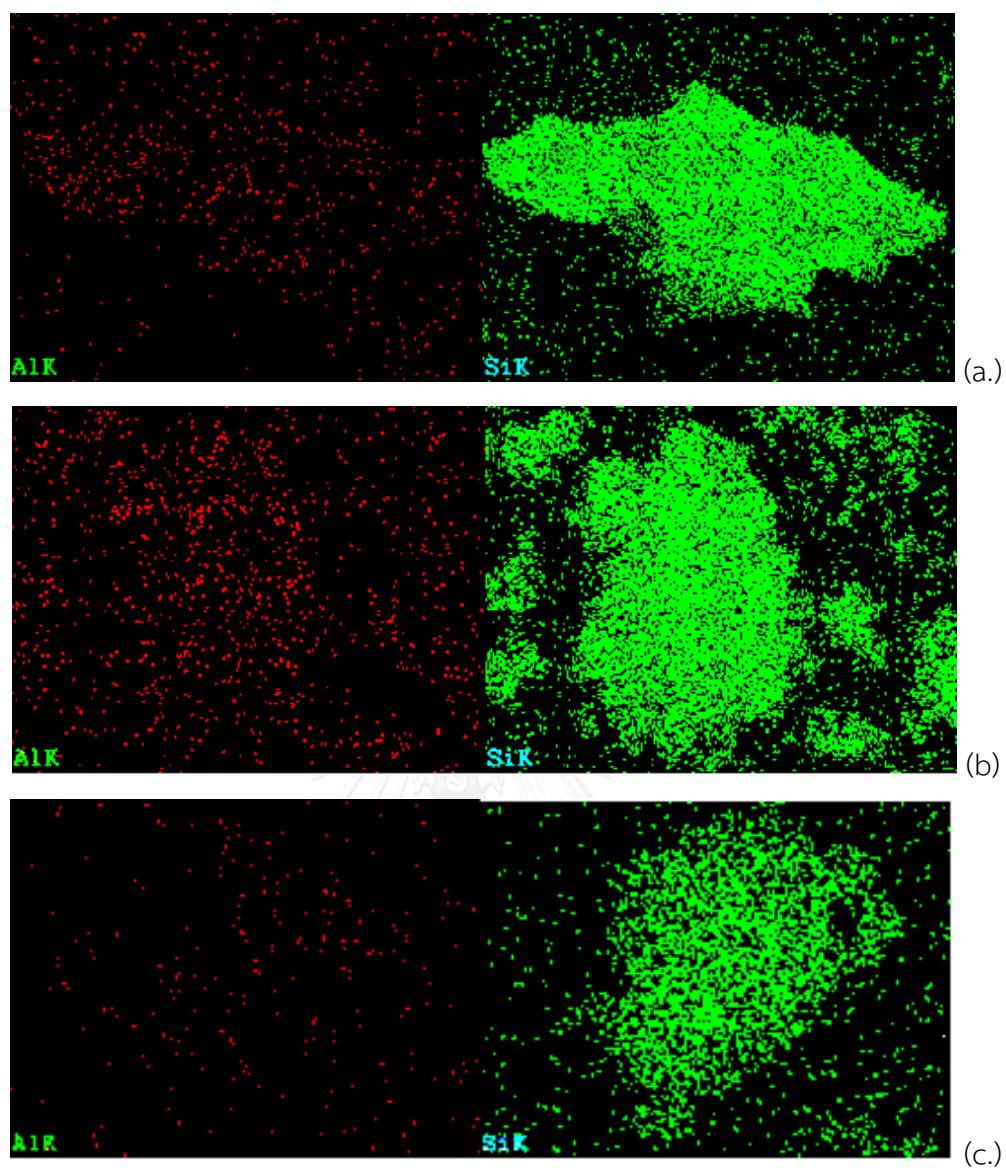


Figure 4.20 EDX of PE-SiO<sub>2</sub>-RH60 (a.), PE-SiO<sub>2</sub>-Syn60 (b.) , PE-SiO<sub>2</sub>-Com60 (c.) at 60°C of polymerization temperature.

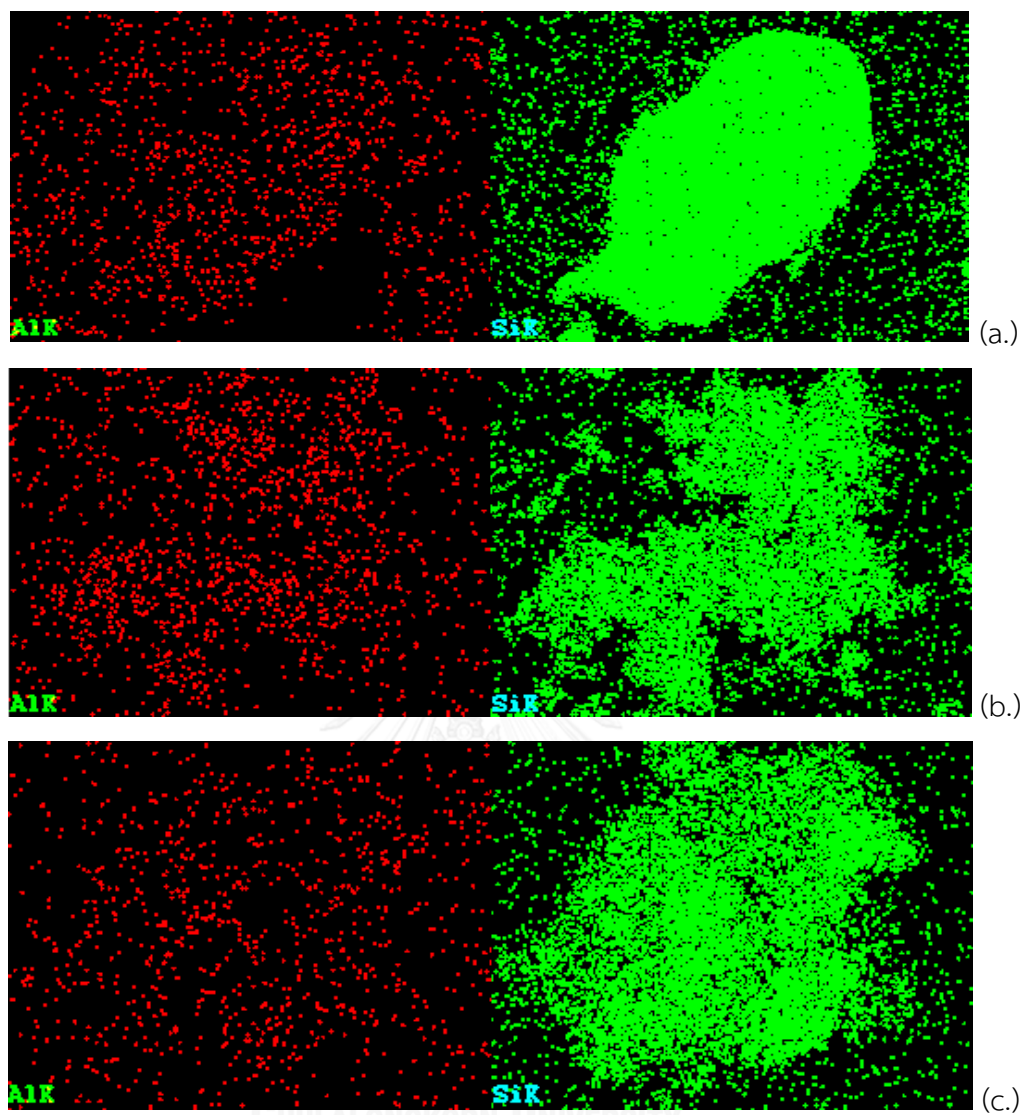


Figure 4.21 EDX of PE-SiO<sub>2</sub>-RH70 (a.), PE-SiO<sub>2</sub>-Syn70 (b.) , PE-SiO<sub>2</sub>-Com70 (c.) at 70°C of polymerization temperature.

**Table 4.8** The average amount of Al on SiO<sub>2</sub> surface in polyethylene via *ex situ* immobilization.

	Ratio of Al/SiO <sub>2</sub>
PE-SiO <sub>2</sub> -RH60	0.01
PE-SiO <sub>2</sub> -RH70	0.01
PE-SiO <sub>2</sub> -Syn60	0.03
PE-SiO <sub>2</sub> -Syn70	0.06
PE-SiO <sub>2</sub> -Com60	0.03
PE-SiO <sub>2</sub> -Com70	0.02

From Figures 20-21 and Table 4.8, the EDX obtained is shown indicating Al distribution in polymer, which had no significant difference among them.

The cross-sectional of polyethylene from polymerization at 70°C via *ex situ* immobilization was exhibited in Figure 4.22 in order to analyze the SiO<sub>2</sub>-coated by polyethylene morphology.

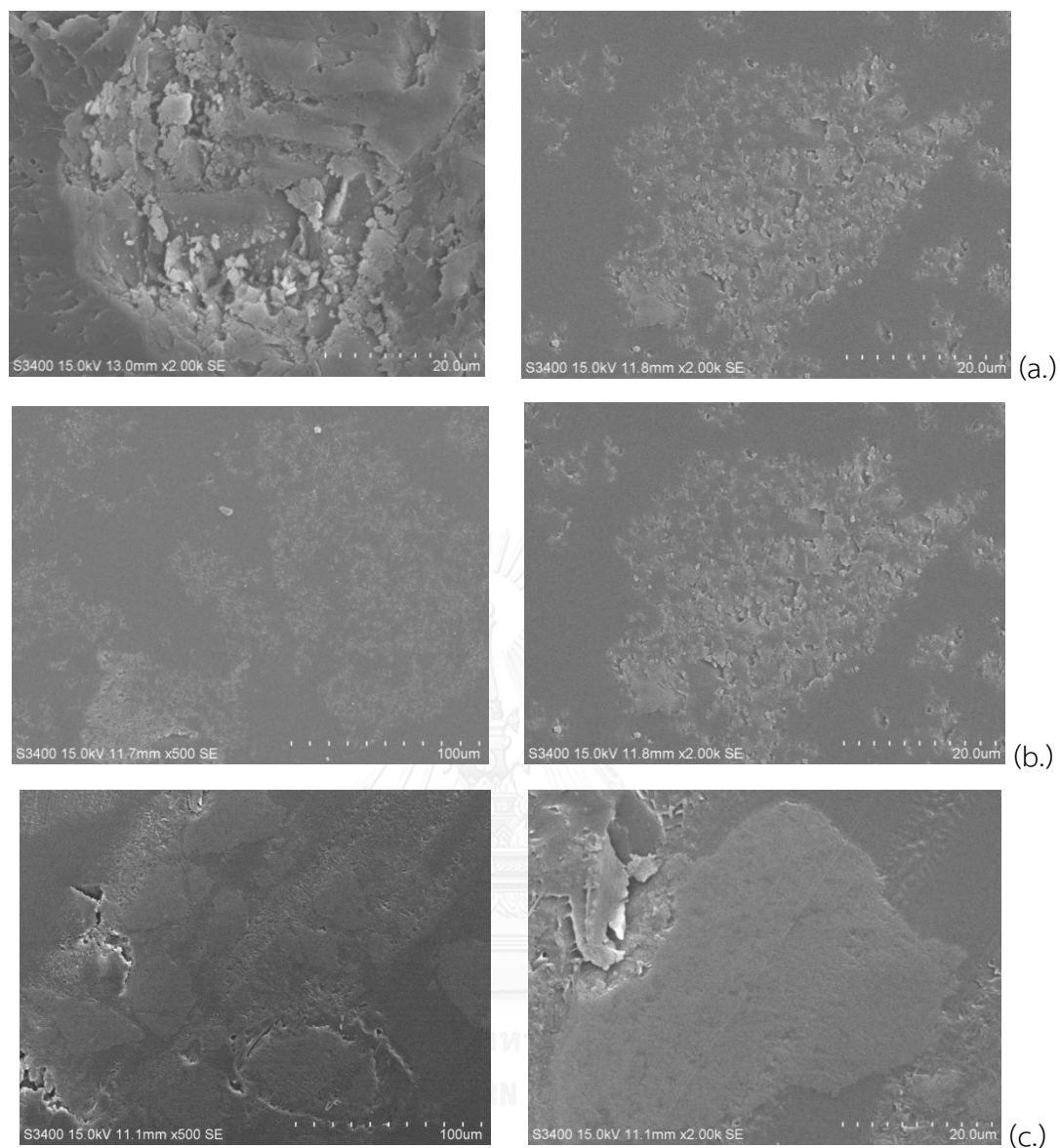


**Figure 4.22** The SEM micrographs of cross-sectional of polyethylene PE-SiO<sub>2</sub>-RH70 (a.), PE-SiO<sub>2</sub>-Syn70 (b.), PE-SiO<sub>2</sub>-Com70 (c.) obtained from polymerization at 70°C via *ex situ* immobilization

From the Figure 4.22 , it was clear that there was polyethylene coating on silica.

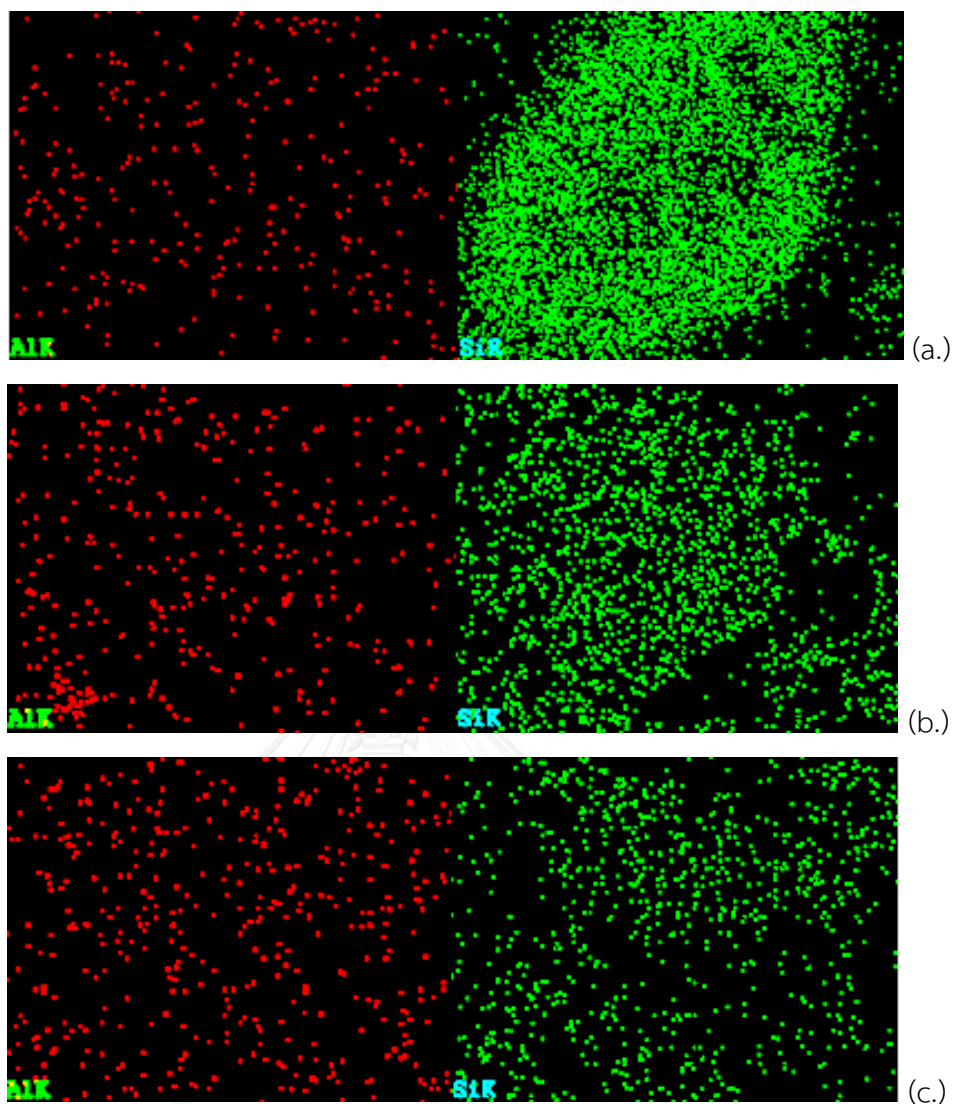


**Figure 4.23** The EDX of cross-sectional of polyethylene PE-SiO<sub>2</sub>-RH70 (a.), PE-SiO<sub>2</sub>-Syn70 (b.), PE-SiO<sub>2</sub>-Com70 (c.) obtained from polymerization at 70°C via *ex situ* immobilization



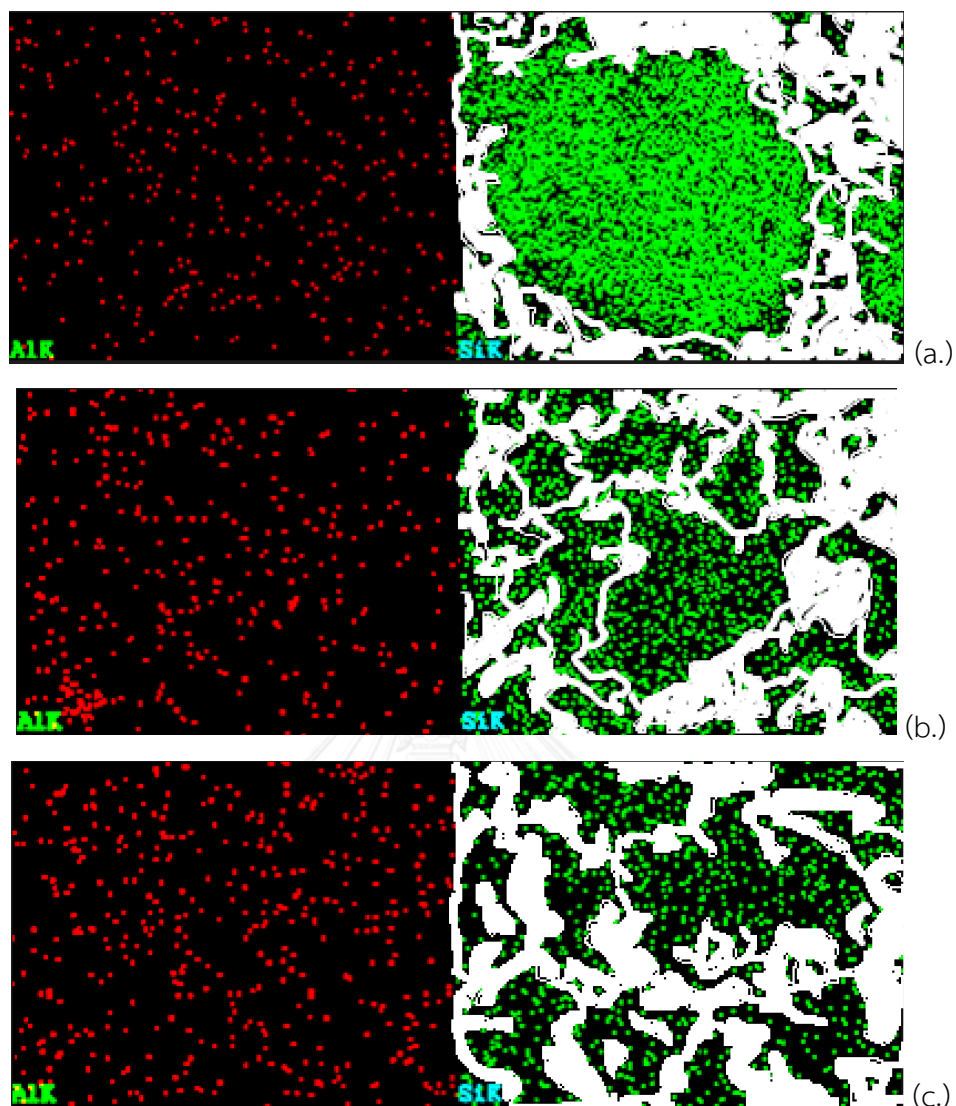


**Figure 4.24** The EDX of cross-sectional of polyethylene PE-SiO<sub>2</sub>-RH70 (a.), PE-SiO<sub>2</sub>-Syn70 (b.), PE-SiO<sub>2</sub>-Com70 (c.) obtained from polymerization at 70°C via *ex situ* immobilization

From Figure 4.24, in the right picture expressed the silica coated by polyethylene. The white color is polymer and the green color is silica.

**Table 4.9** The average amount of Al on SiO<sub>2</sub> surface in polyethylene via *in situ* polymerization.

	Ratio of Al/SiO <sub>2</sub>
PE-SiO <sub>2</sub> -RH70	0.01
PE-SiO <sub>2</sub> -Syn70	0.07
PE-SiO <sub>2</sub> -Com70	0.21

From Table 4.9 , it indicated that PE-SiO<sub>2</sub>-Com70 had the highest degree of Al distribution on the SiO<sub>2</sub> surface.

#### 4.4.2 Characterization of polyethylene with Transmission electron microscopy (TEM)

SiO<sub>2</sub>-coated PE samples were characterized by TEM in order to analyze the morphologies from polymerization at 60°C and 70°C as shown in Figure 4.25. The black and white color expressed the silica and polyethylene, respectively. It was found that SiO<sub>2</sub>-RH60, SiO<sub>2</sub>-RH70, SiO<sub>2</sub>-Com60, and SiO<sub>2</sub>-Com70 were coated throughout by Polyethylene, which was coated around each silica particle.

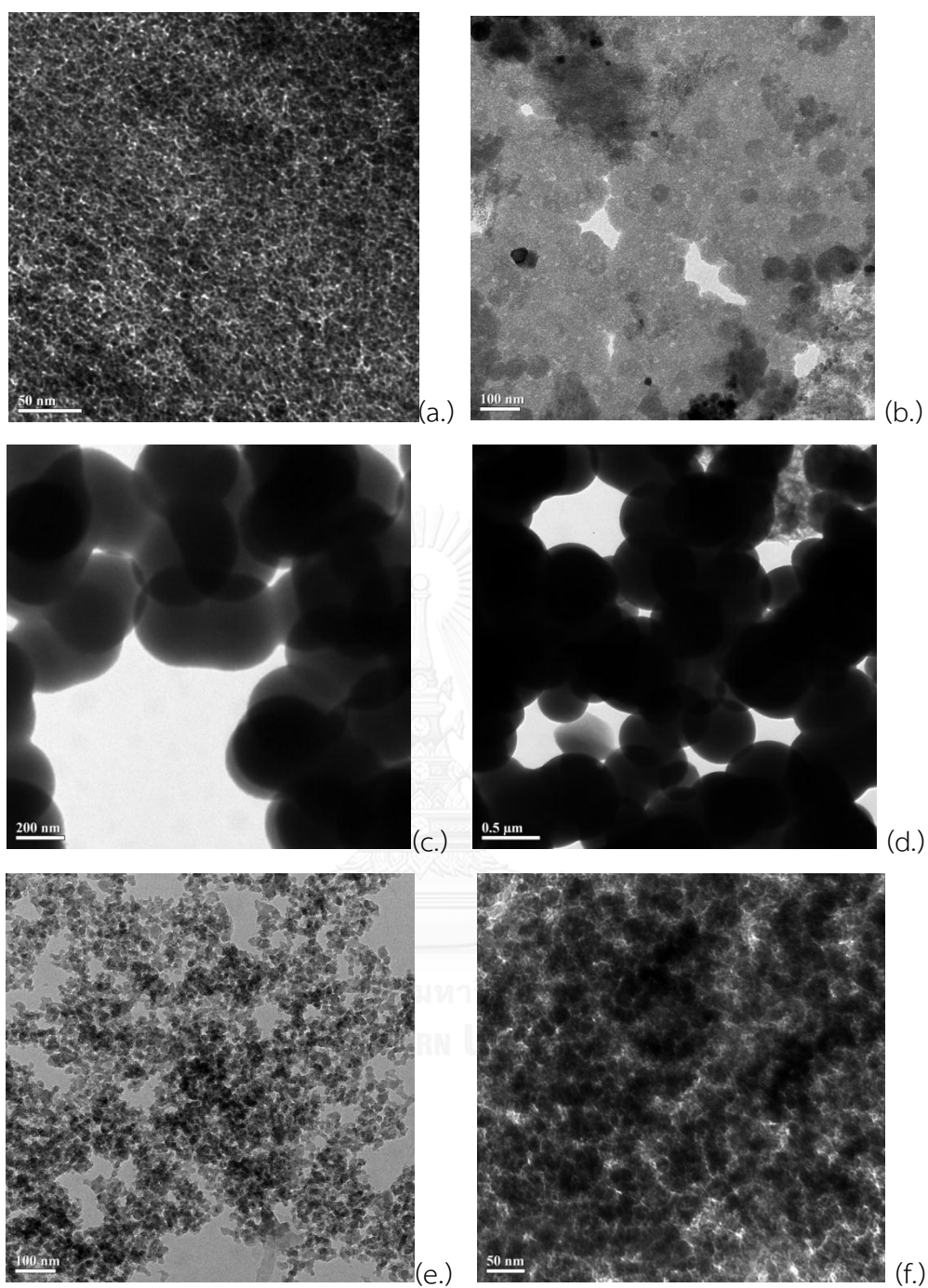


**Figure 4.25** The TEM of PE-SiO<sub>2</sub>-RH60 (a.), PE-SiO<sub>2</sub>-RH70 (b.), PE-SiO<sub>2</sub>-Syn60 (c.), PE-SiO<sub>2</sub>-Syn70 (d.), PE-SiO<sub>2</sub>-Com60 (e.), and PE-SiO<sub>2</sub>-Com70 (f.) obtained from polymerization via *ex situ* immobilization

#### 4.4.3 Characterization of polyethylene by X-ray Powder Diffraction (XRD)

The polymers obtained from polymerization via *ex situ* immobilization were characterized by XRD as shown in Figure 4.26. It was observed sharp peak at  $21.5^\circ$  and  $23.9^\circ$  in PE-SiO<sub>2</sub>-Com60 and PE-SiO<sub>2</sub>-Com70 as seen typically for the polyethylene, while PE-SiO<sub>2</sub>-RH60, PE-SiO<sub>2</sub>-RH70, PE-SiO<sub>2</sub>-Syn60, and PE-SiO<sub>2</sub>-Syn70 did not express any peak. It indicated that they were amorphous polyethylene, which were consistent with the results in Table 4.10 indicating that there were no melting temperature.

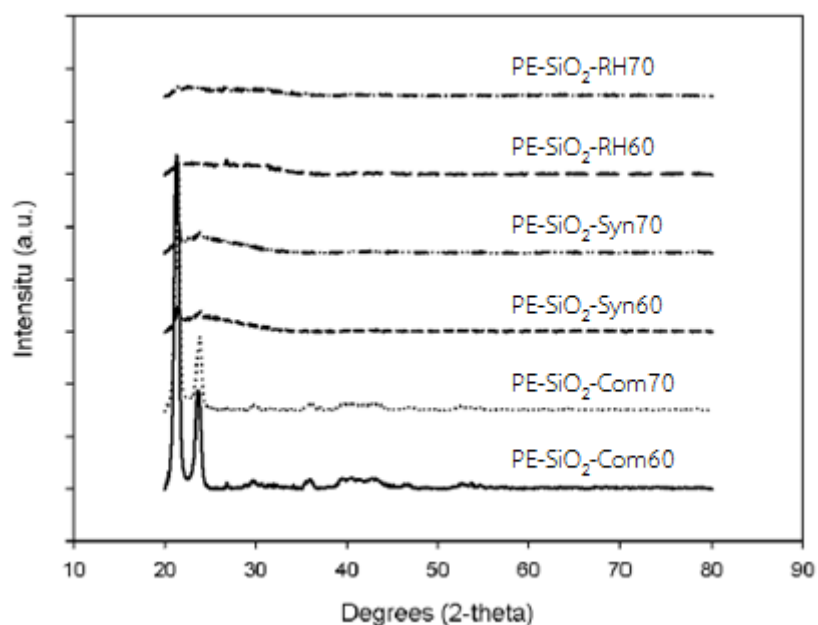


**Figure 4.26** XRD patterns of polyethylene obtained from polymerization via *ex situ* immobilization

#### 4.4.4. Characterization of polyethylene with Thermogravimetric Analysis (TGA)

In order to measure the stability of polymer obtained from polymerization via *ex situ* immobilization method, TGA measurement was performed. The TGA provides information on the degree of thermal stability of polymer in terms of weight loss and temperature. The TGA and DTA profiles of polymer are shown in Figures 4.27-4.28.

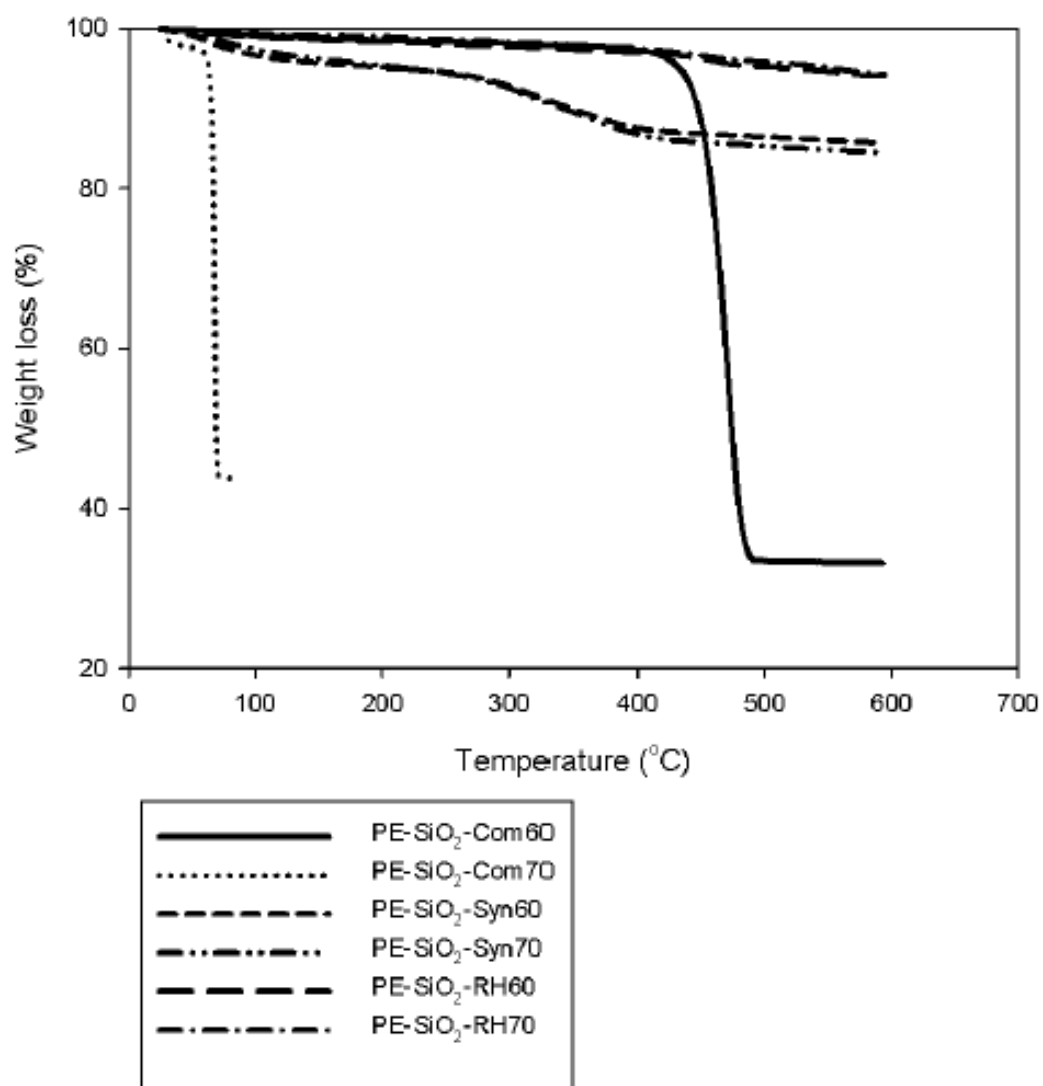


Figure 4.27 TGA profiles of polymer obtained from polymerization via *ex situ* immobilization.

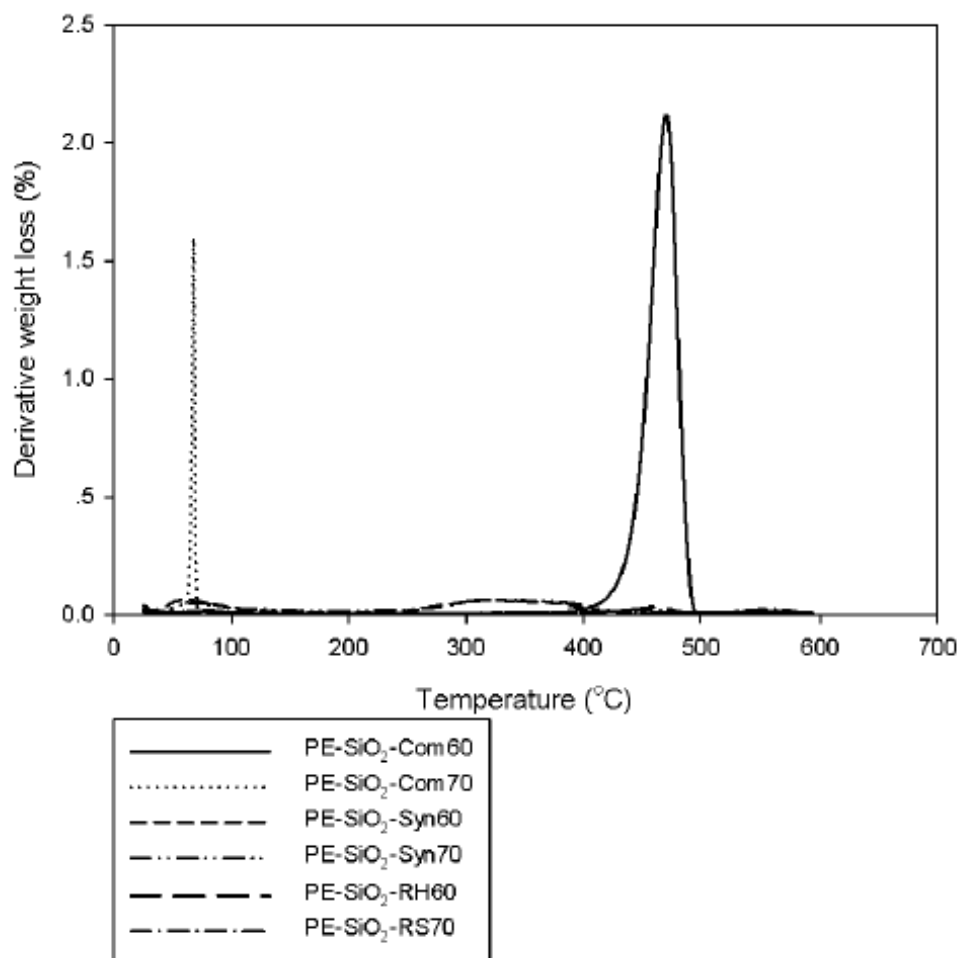


Figure 4.28 DTA profiles of polymer obtained from polymerization via *ex situ* immobilization.

From the DTA profiles from Figure 4.28, PE-SiO<sub>2</sub>-Com60 was decomposed at 470°C, which was very large different from PE-SiO<sub>2</sub>-Com70, that was decomposed at 70°C.

**Table 4.10** Percent weight loss of polymer obtained from polymerization via *ex situ* immobilization.

	%Weight loss
PE- SiO <sub>2</sub> -RH60	5.86
PE- SiO <sub>2</sub> -RH70	5.66
PE- SiO <sub>2</sub> -Syn60	14.18
PE- SiO <sub>2</sub> -Syn70	15.48
PE- SiO <sub>2</sub> -Com60	66.82
PE- SiO <sub>2</sub> -Com70	56.13

The percent weight loss is shown in Table 4.10 revealing the thermal stability of PE- SiO<sub>2</sub>-RH > PE- SiO<sub>2</sub>-Syn > PE- SiO<sub>2</sub>-Com. Weight loss of polymer at 60°C gave the similar value with at 70°C for PE- SiO<sub>2</sub>-Syn and PE- SiO<sub>2</sub>-RH. It was observed that PE- SiO<sub>2</sub>-RH70 had the most thermal stability.

#### 4.5 Polymerization via *in situ* immobilization.

As the results of polymerization via *ex situ* immobilization at 60 and 70°C, it was found that the catalytic activity and yield at 70°C was higher than at 60°C. Thus, polymerization via *in situ* immobilization using SiO<sub>2</sub>-RH, SiO<sub>2</sub>-Syn, and SiO<sub>2</sub>-Com as supported catalyst was studied at 70°C. The polymer was characterized by SEM-EDX, XRD, and TGA.

##### 4.5.1 Characterization of polyethylene with SEM-EDX

In order to determine the morphology and Al distribution on the polymer surface, SEM-EDX was performed in Figures 4.29-4.30

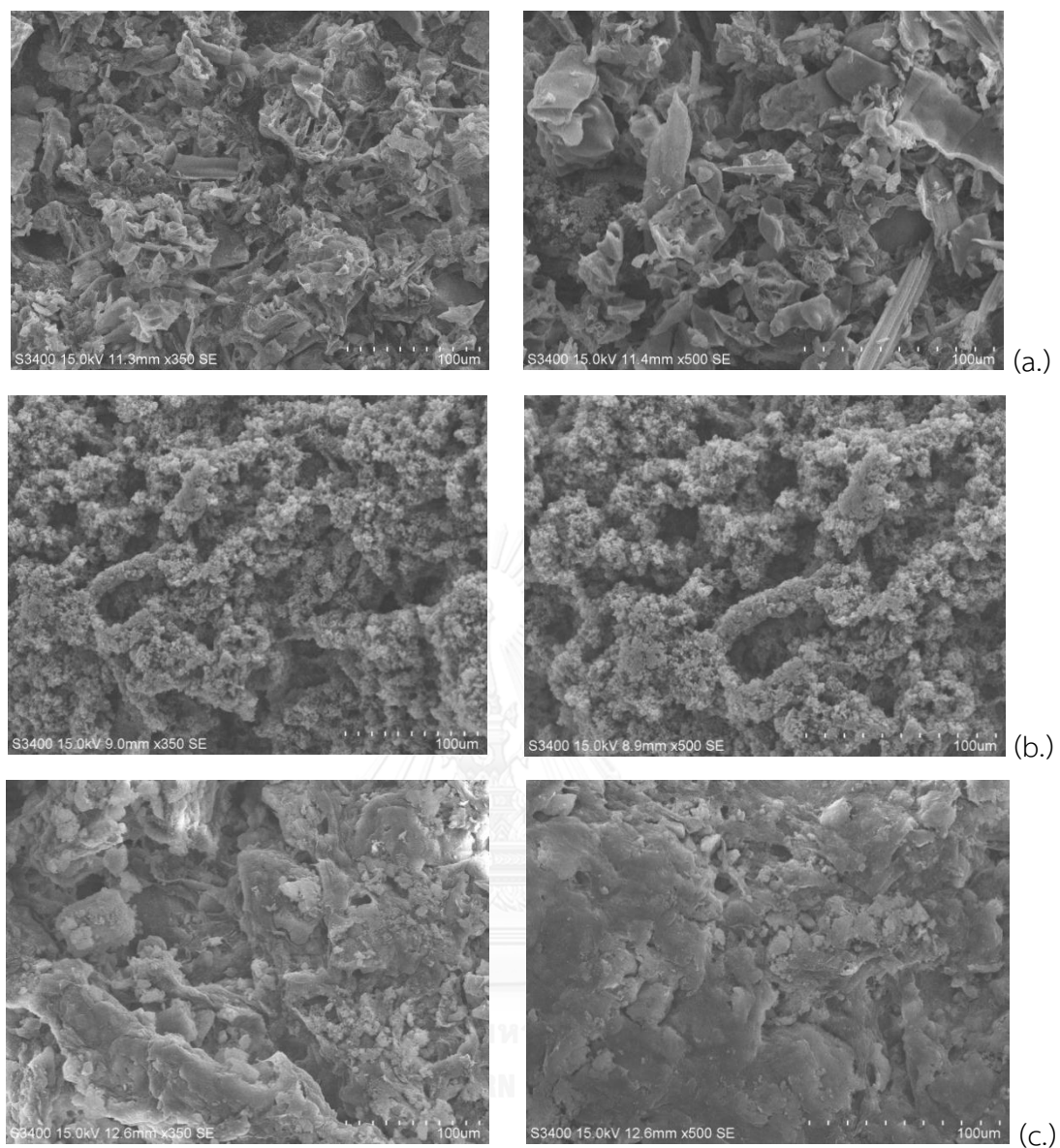


**Figure 4.29** SEM micrographs of INPE-SiO<sub>2</sub>-RH70 (a.), INPE-SiO<sub>2</sub>-Syn70 (b.) , INPE-SiO<sub>2</sub>-Com70 (c.) at 350X and 500X magnification at 70°C of polymerization temperature.



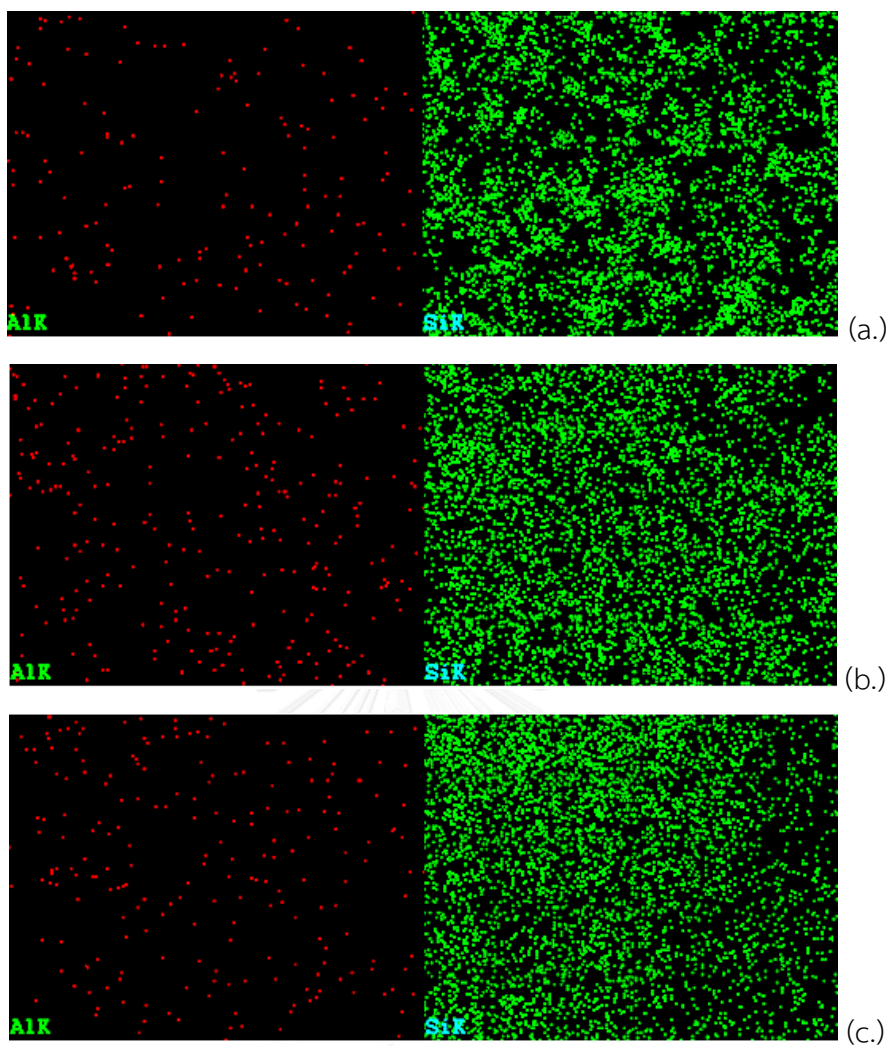


**Figure 4.30** The EDX of INPE-SiO<sub>2</sub>-RH70 (a.), INPE-SiO<sub>2</sub>-Syn70 (b.) , INPE-SiO<sub>2</sub>-Com70 (c.) at 70 °C of polymerization temperature.

**Table 4.11** The average amount of Al on SiO<sub>2</sub> surface in polyethylene via *in situ* immobilization.

	INPE-SiO <sub>2</sub> -RH70	INPE-SiO <sub>2</sub> -Syn70	INPE-SiO <sub>2</sub> -Com70
Ratio of Al/SiO <sub>2</sub>	0.02	0.02	0.02

From the Figure 4.29, it was observed that INPE-SiO<sub>2</sub>-RH70, INPE-SiO<sub>2</sub>-Syn70, and INPE-SiO<sub>2</sub>-Com70 were irregular shape and agglomerate. As the results of EDX in Figure 4.30 and Table 4.11, it was found that Al distribution of all polymer were equal.

#### 4.5.2 Characterization of polyethylene with X-ray Powder Diffraction (XRD)

The polymer were characterized by XRD as shown in Figure 4.31. It can be seen sharp peak at  $21.5^\circ$  and  $23.9^\circ$  as seen typically for the polyethylene. It indicated that MMAO was in the highly dispersed form, which was invisible by XRD

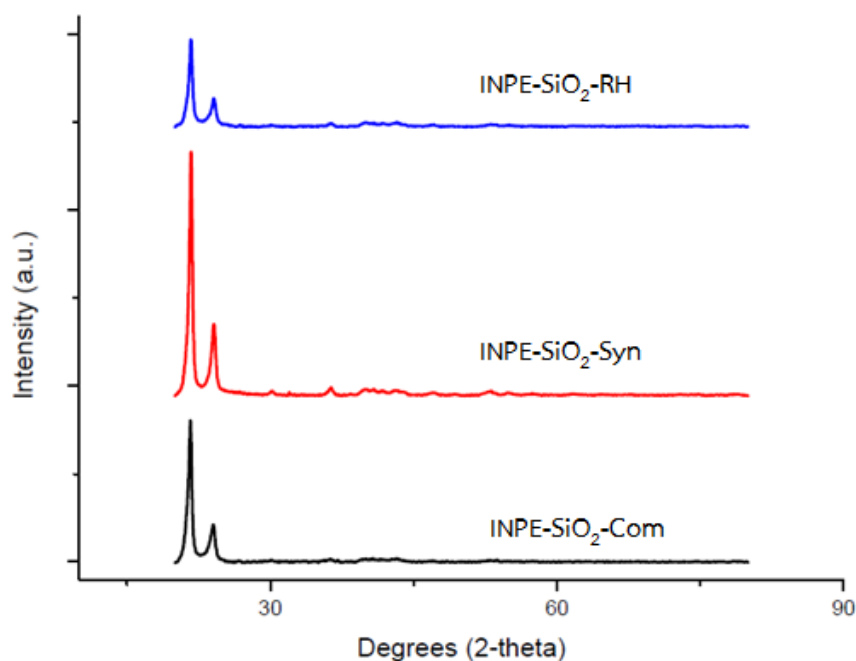


**Figure 4.31** XRD patterns of polyethylene obtained from polymerization at  $70^\circ\text{C}$  via *in situ* immobilization

From the Table 4.7, it was found that all of polymer from *in situ* immobilization method had the same value of melting temperature ( $125^\circ\text{C}$ ) and percent of crystallinity of INPE-SiO<sub>2</sub>-Syn70 (23.96%) > INPE-SiO<sub>2</sub>-RH70 (19%) > INPE-SiO<sub>2</sub>-Com70 (14.14%). So, the polymer obtained from *in situ* immobilization had more crystallinity than the polymer obtained from *ex situ* immobilization method.

#### 4.5.3 Characterization of polyethylene with Thermogravimetric Analysis (TGA)

In order to measure the stability of polymer obtained from polymerization via *in situ* immobilization method, TGA measurement was performed. The TGA provides information on the degree of thermal stability of polymer in terms of weight loss

and temperature. The TGA and DTA profiles of polymer are shown in Figures 4.32-4.33

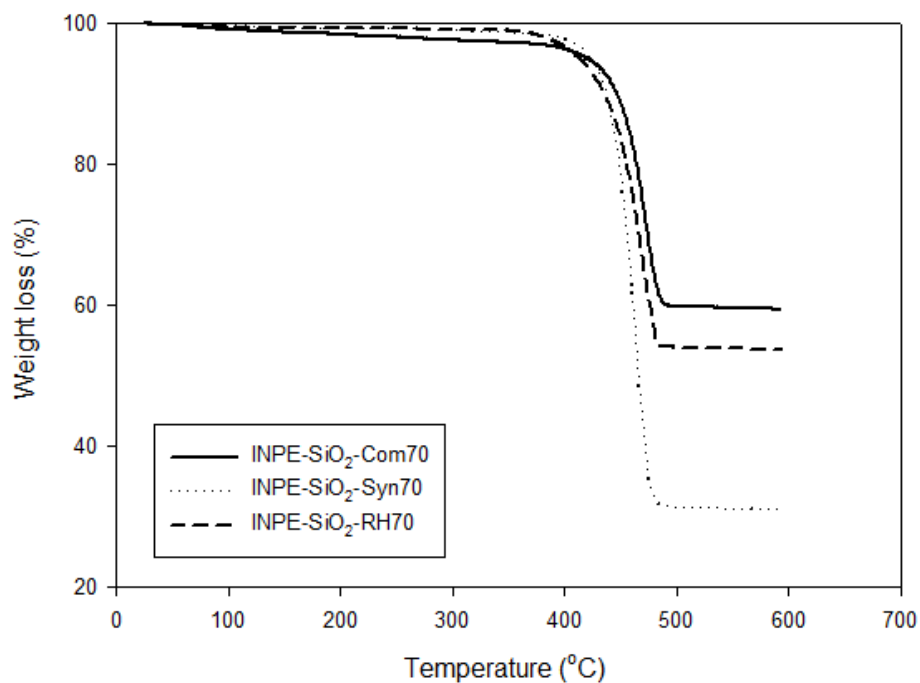


Figure 4.32 TGA profiles of polymer obtained from polymerization via in situ immobilization at 70°C.

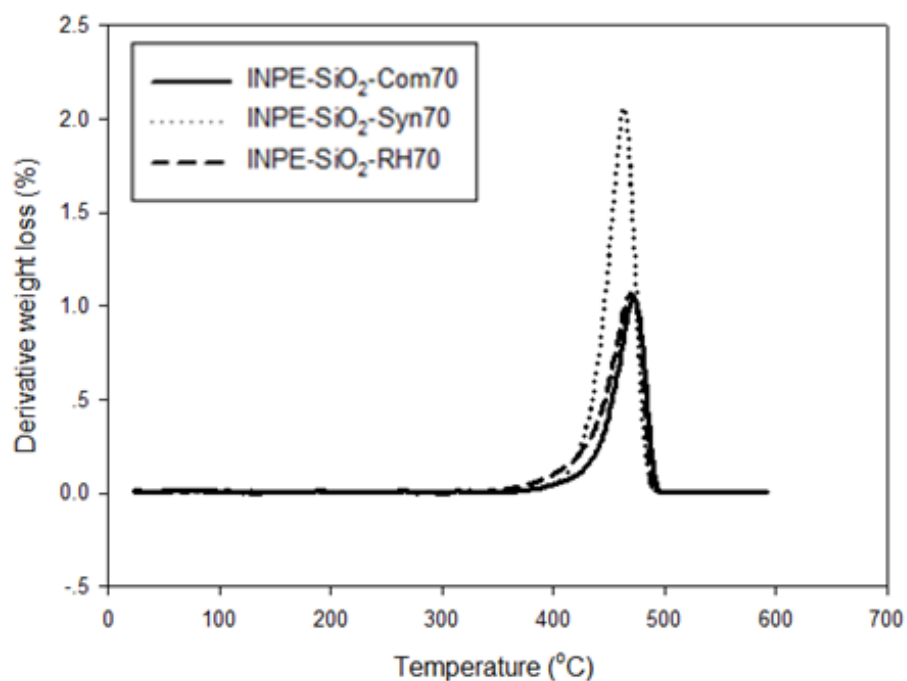


Figure 4.33 TGA profiles of polymer obtained from polymerization via in situ immobilization at 70°C.

It was found that thermal stability of INPE-SiO<sub>2</sub>-Com70 (40.56%) > INPE-SiO<sub>2</sub>-RH70 (46.27%) > INPE-SiO<sub>2</sub>-Syn70 (68.99%). They were decomposed at 470 °C.



## Chapter V

### CONCLUSIONS AND RECOMMENDATIONS

#### 5.1 Conclusions

The preparation of silica coated with polyethylene by *in situ* polymerization with metallocene catalyst was studied. It was found that the optimal polymerization temperature was at 70°C, leading the highest catalytic activity. The activity of polymerization via *ex situ* immobilization of SiO<sub>2</sub>-Com expressed the highest at 70°C and SiO<sub>2</sub>-Syn expressed the highest catalytic activity at 60°C. The *in situ* immobilization exhibited higher catalytic activity than the *ex situ* immobilization method. However, the morphologies of polymer with *ex situ* immobilization, which was spheroidal was better than those of *in situ* immobilization, which was irregular shape. It can be concluded that the SiO<sub>2</sub>-Com coated with polyethylene by *in situ* polymerization with metallocene catalyst at 70°C via *ex situ* immobilization expressed the highest catalytic activity, but it had the lowest thermal stability. SiO<sub>2</sub>-RH coated with polyethylene by *in situ* polymerization with metallocene catalyst at 70°C via *ex situ* immobilization expressed the lowest catalytic activity, but it had the highest thermal stability.

#### 5.2 Recommendations

Investigation of different properties of natural rubber with SiO<sub>2</sub> and PE coated-SiO<sub>2</sub> addition.

## REFERENCES

- [1] Suttivutnarubet, C., Jaturapiree, A., Chaichana, E., Prasertthdam, P., and Jongsomjit, B. Synthesis of polyethylene/coir dust hybrid filler via in situ polymerization with zirconocene/MAO catalyst for use in natural rubber biocomposites. Iranian Polymer Journal 25(10) (2016): 841-848.
- [2] Zhong, B., Jia, Z., Luo, Y., and Jia, D. Surface modification of silica with N-cyclohexyl-2-benzothiazole sulfenamide for styrene-butadiene rubber composites with dramatically improved mechanical property. Materials Letters 145 (2015): 41-43.
- [3] Lin, Y., Liu, S., Peng, J., and Liu, L. The filler-rubber interface and reinforcement in styrene butadiene rubber composites with graphene/silica hybrids: A quantitative correlation with the constrained region. Composites Part A: Applied Science and Manufacturing 86 (2016): 19-30.
- [4] Pongdong, W., Kummerlöwe, C., Vennemann, N., Thitithammawong, A., and Nakason, C. Property correlations for dynamically cured rice husk ash filled epoxidized natural rubber/thermoplastic polyurethane blends: Influences of RHA loading. Polymer Testing (2016).
- [5] Shi, Y., Yuan, Y., Xu, Q., and Yi, J. Preparation, characterization, and activity of  $\alpha$ -Ti (HPO 4) 2 supported metallocene catalysts. Applied Surface Science 383 (2016): 126-132.
- [6] Bergstra, M.F. Catalytic ethylene polymerization. University of Twente, 2004.
- [7] Kaleel, S.A., Bahuleyan, B.K., De, S.K., Khan, M.J., Sougrat, R., and Al-Harhi, M.A. Effect of Mn doped-titania on the activity of metallocene catalyst by in situ ethylene polymerization. Journal of Industrial and Engineering Chemistry 18(5) (2012): 1836-1840.
- [8] Wannaborworn, M. Copolymerization of ethylene/1-octene over gallium-modified silica-supported metallocene catalyst. (2008).
- [9] Ramrauytham, C. Effect of particle size of silica and SiO<sub>2</sub>/MMAO ratios on heterogeneous metallocene catalyst performance and polyethylene properties. Master degree, Chemical Engineering Chulalongkorn university, 2014.

- [10] Jantasee, S. Olefin polymerization with modified spherical zirconia supported metallocene catalysts. Doctoral dissertation, Chemical Engineering chulalongkorn university, 2013.
- [11] Mäkelä-Vaarne, N.I., Nicholson, D.G., and Ramstad, A.L. Supported metallocene catalysts—interactions of (n-BuCp)<sub>2</sub>HfCl<sub>2</sub> with methylaluminumoxane and silica. Journal of Molecular Catalysis A: Chemical 200(1) (2003): 323-332.
- [12] Rida, M.A. and Harb, F. Synthesis and characterization of amorphous silica nanoparticles from aqueous silicates using cationic surfactants. Journal of Metals, Materials and Minerals 24(1) (2014).
- [13] Ahmed, K., Nizami, S.S., and Raza, N.Z. Characteristics of natural rubber hybrid composites based on marble sludge/carbon black and marble sludge/rice husk derived silica. Journal of Industrial and Engineering Chemistry 19(4) (2013): 1169-1176.
- [14] Ngah, S.A. and Taylor, A.C. Toughening performance of glass fibre composites with core-shell rubber and silica nanoparticle modified matrices. Composites Part A: Applied Science and Manufacturing 80 (2016): 292-303.
- [15] Ketloy, C., Jongsomjit, B., and Praserttham, P. Characteristics and catalytic properties of [t-BuNSiMe<sub>2</sub>Flu]TiMe<sub>2</sub>/dMMAO catalyst dispersed on various supports towards ethylene/1-octene copolymerization. Applied Catalysis A: General 327(2) (2007): 270-277.

# APPENDICES



จุฬาลงกรณ์มหาวิทยาลัย  
CHULALONGKORN UNIVERSITY



# APPENDIX A : FOURIER TRANSFORM INFRARED SPECTROSCOPY



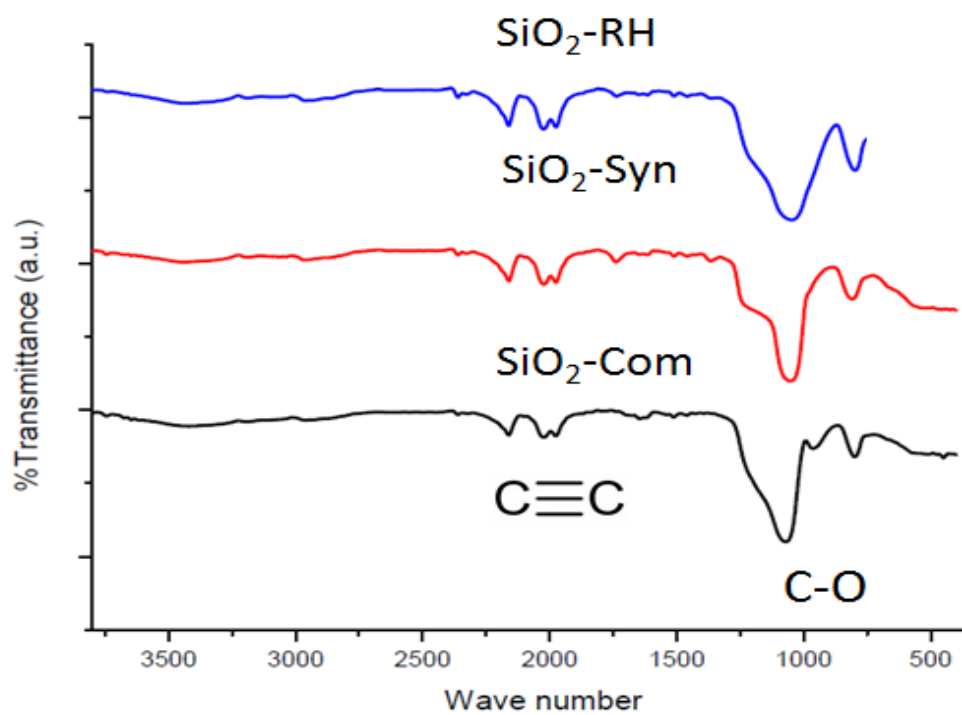


Figure A-1 FT-IR of SiO<sub>2</sub> before immobilization with MMAO

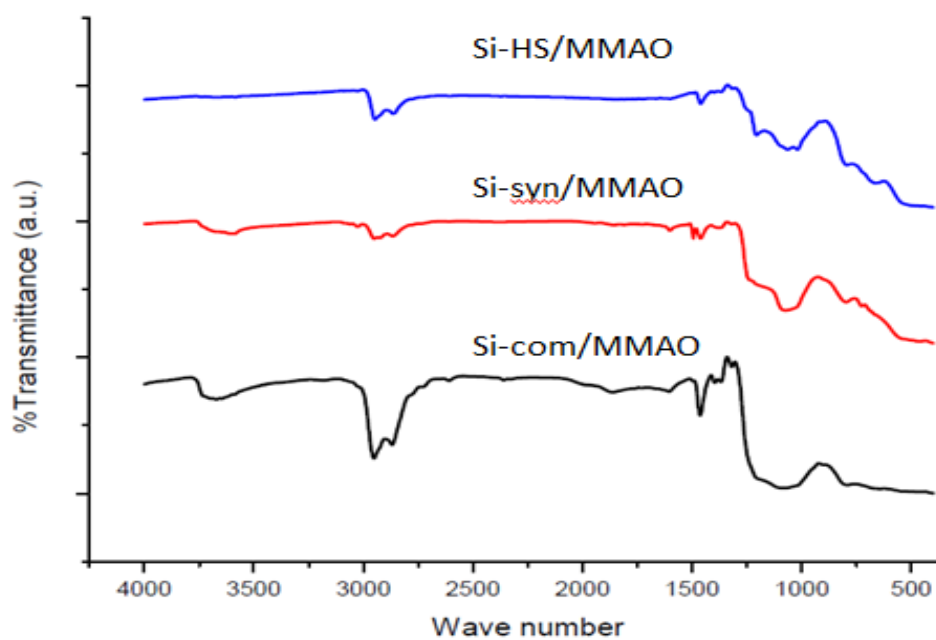


Figure A-2 FT-IR of SiO<sub>2</sub> after immobilization with MMAO

## APPENDIX B : X-RAY

## PHOTOELECTRON SPECTROSCOPY



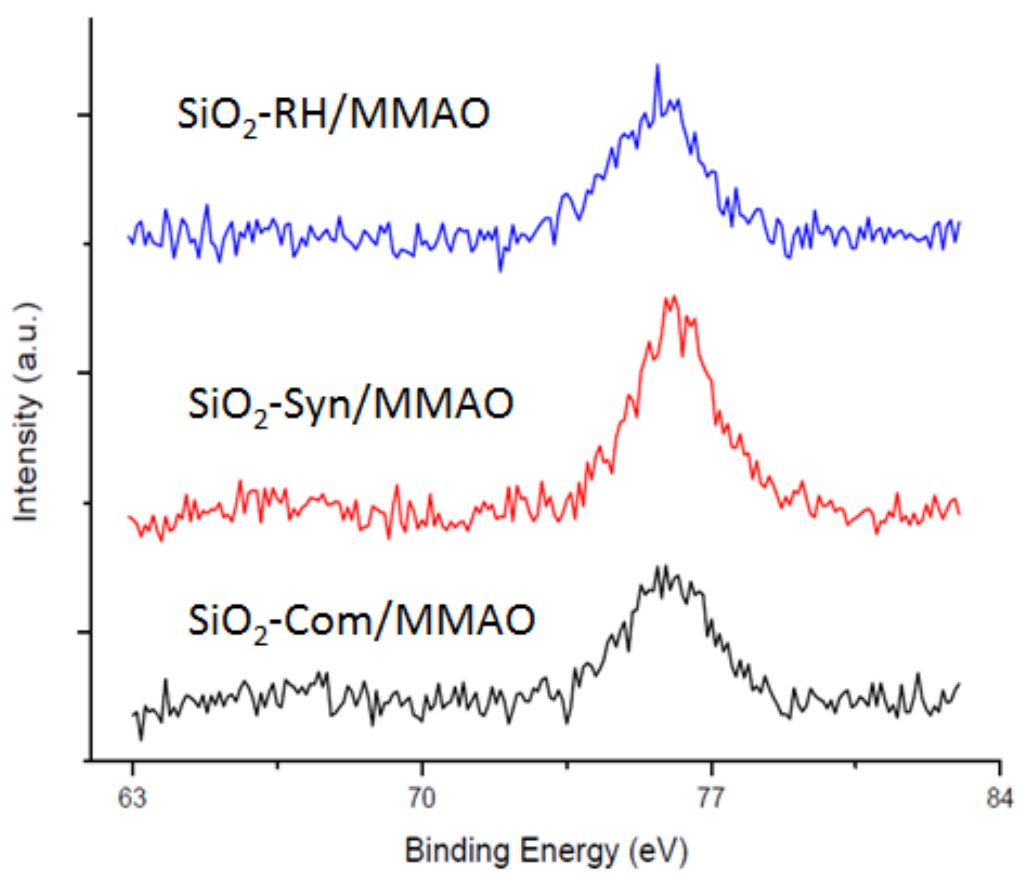
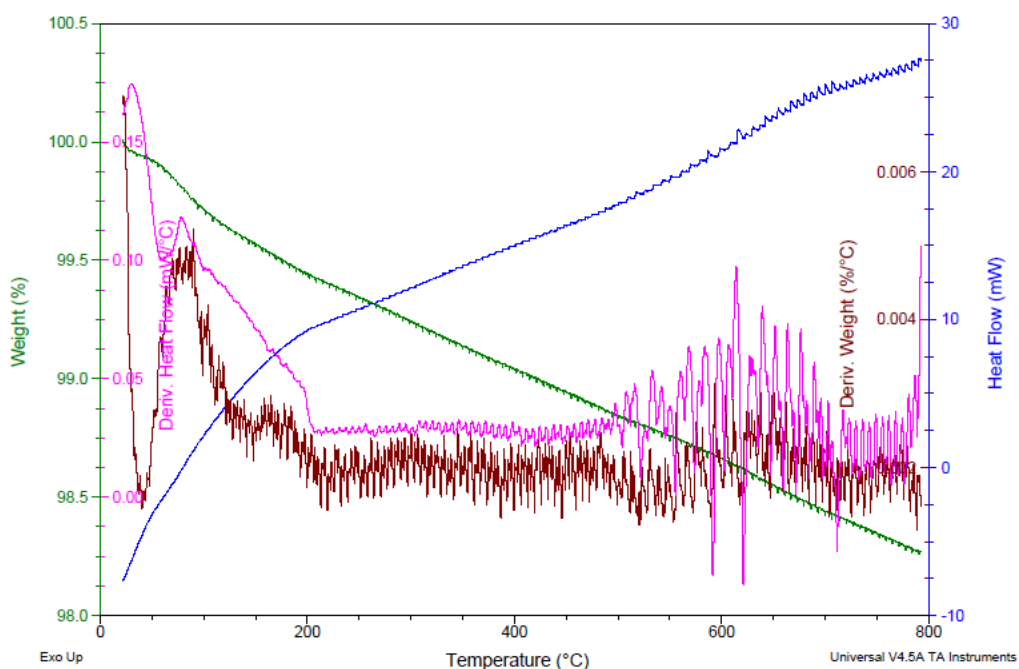
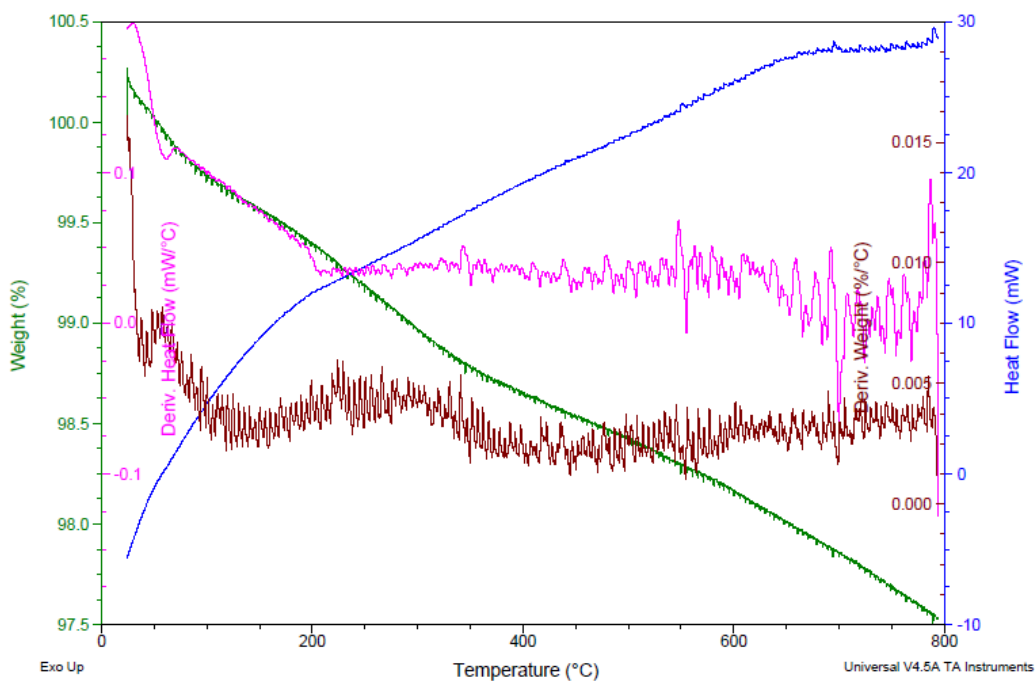


Figure B-1 XPS of SiO<sub>2</sub> after immobilization

# APPENDIX C : THERMOGRAVIMETRIC ANALYSIS



Figure C-1 TGA of SiO<sub>2</sub>-RH before immobilizationFigure C-2 TGA of SiO<sub>2</sub>-Syn before immobilization

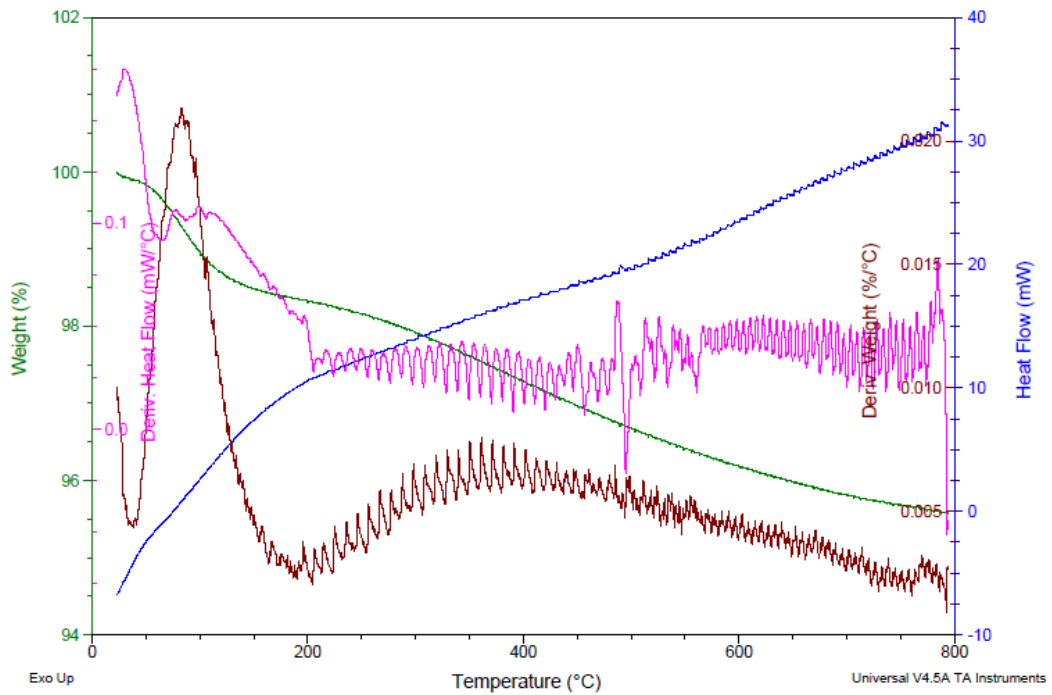


Figure C-3 TGA of SiO<sub>2</sub>-Com before immobilization

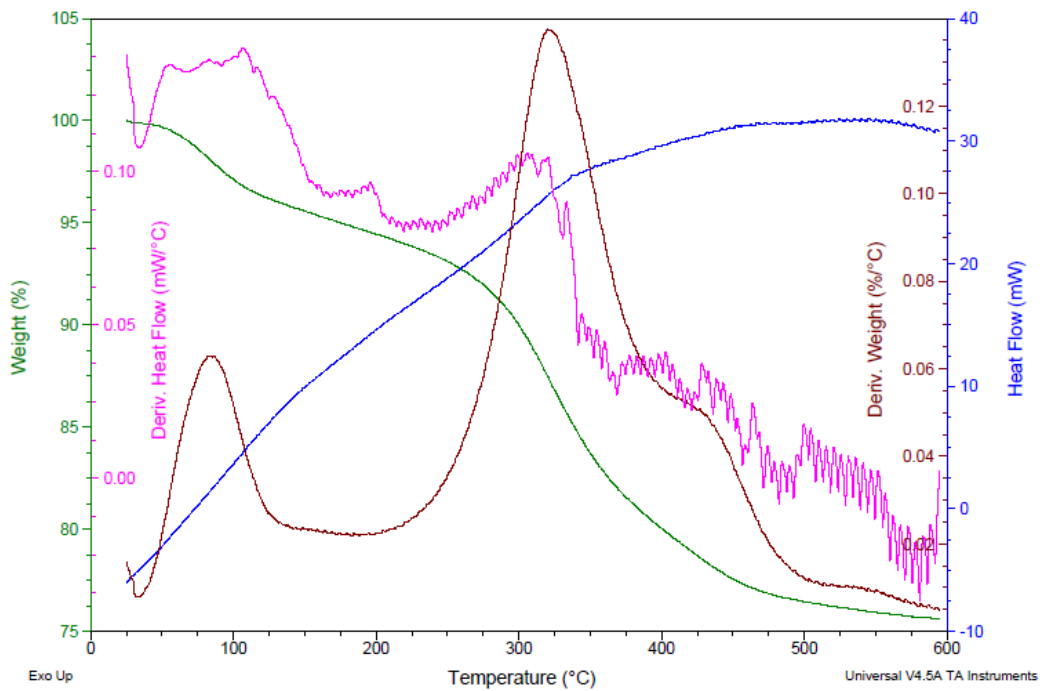


Figure C-4 TGA of SiO<sub>2</sub>-RH after immobilization

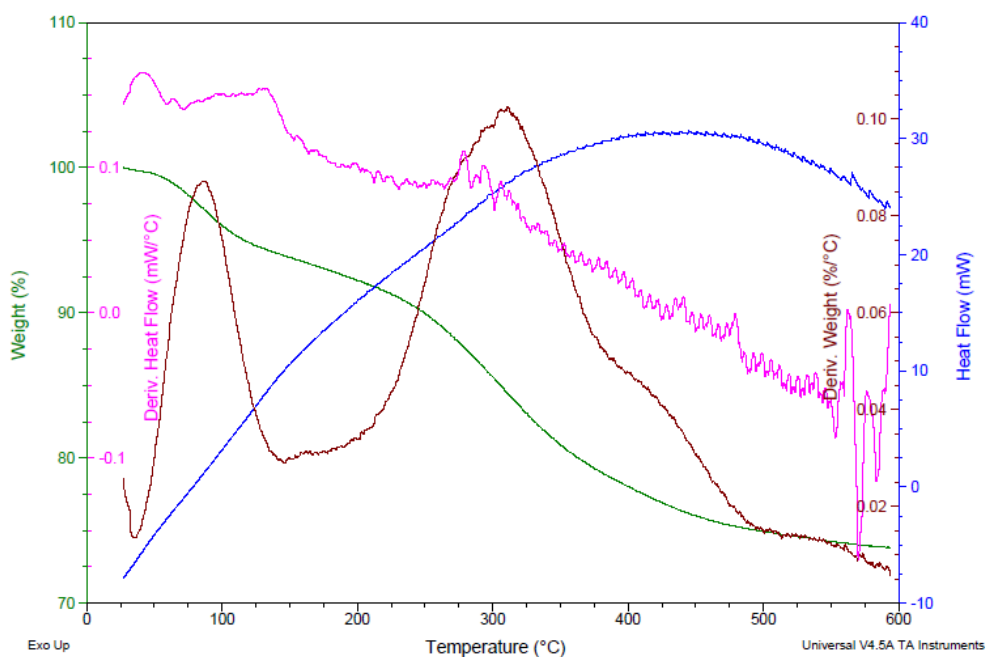


Figure C-5 TGA of SiO<sub>2</sub>-Syn after immobilization

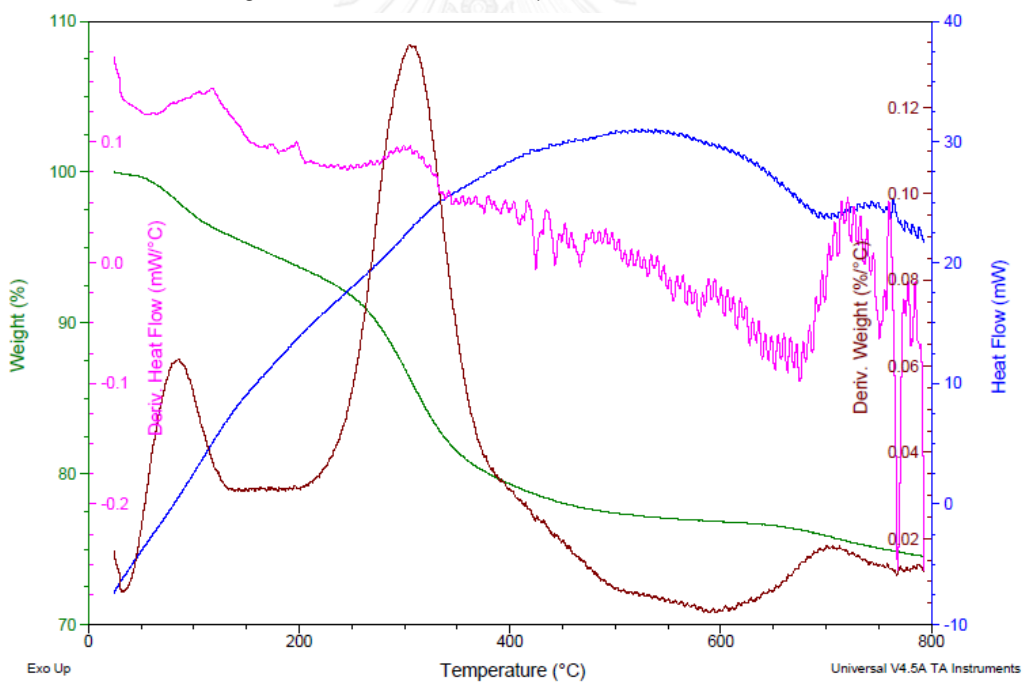


Figure C-6 TGA of SiO<sub>2</sub>-Com after immobilization



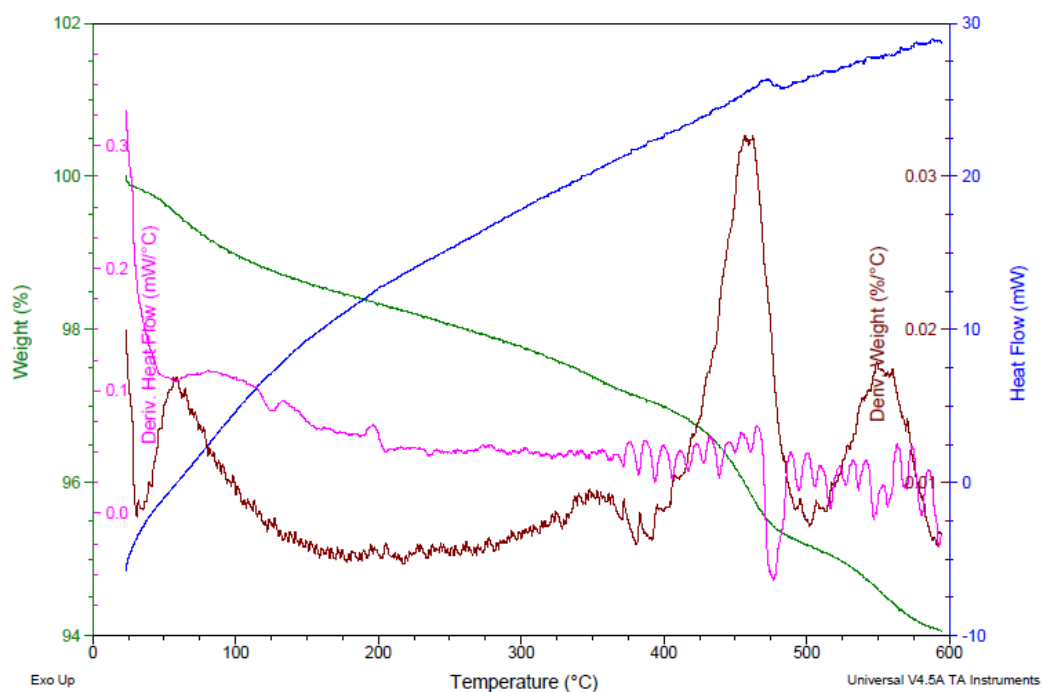


Figure C-7 TGA of PE-SiO<sub>2</sub>-RH60 obtained from polymerization via *ex situ* immobilization

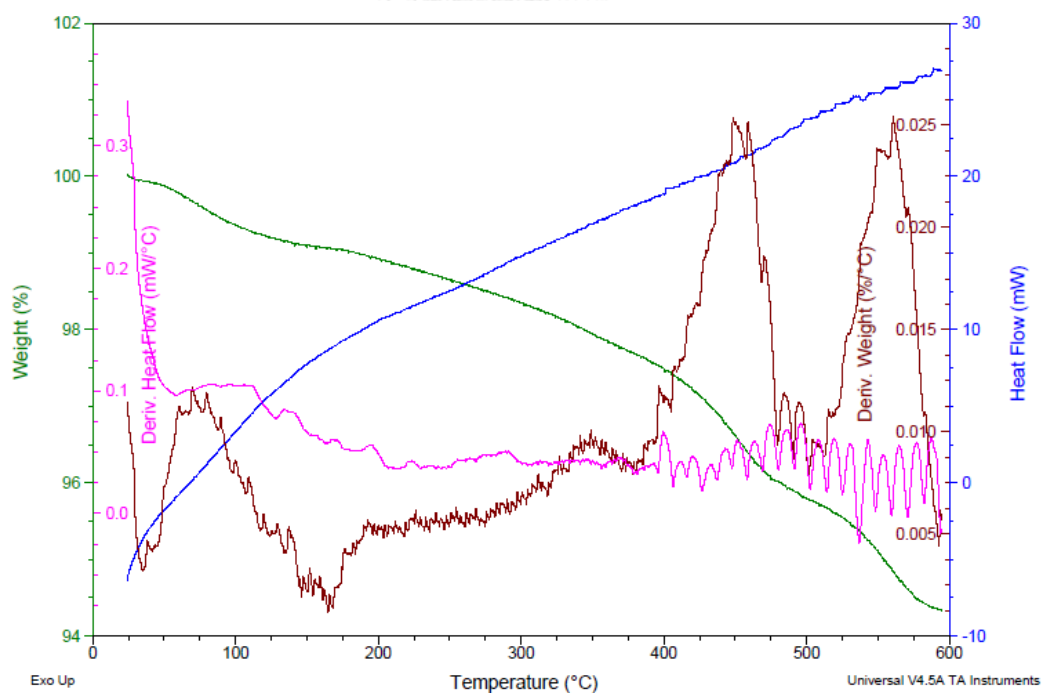


Figure C-8 TGA of PE-SiO<sub>2</sub>-RH70 obtained from polymerization via *ex situ* immobilization

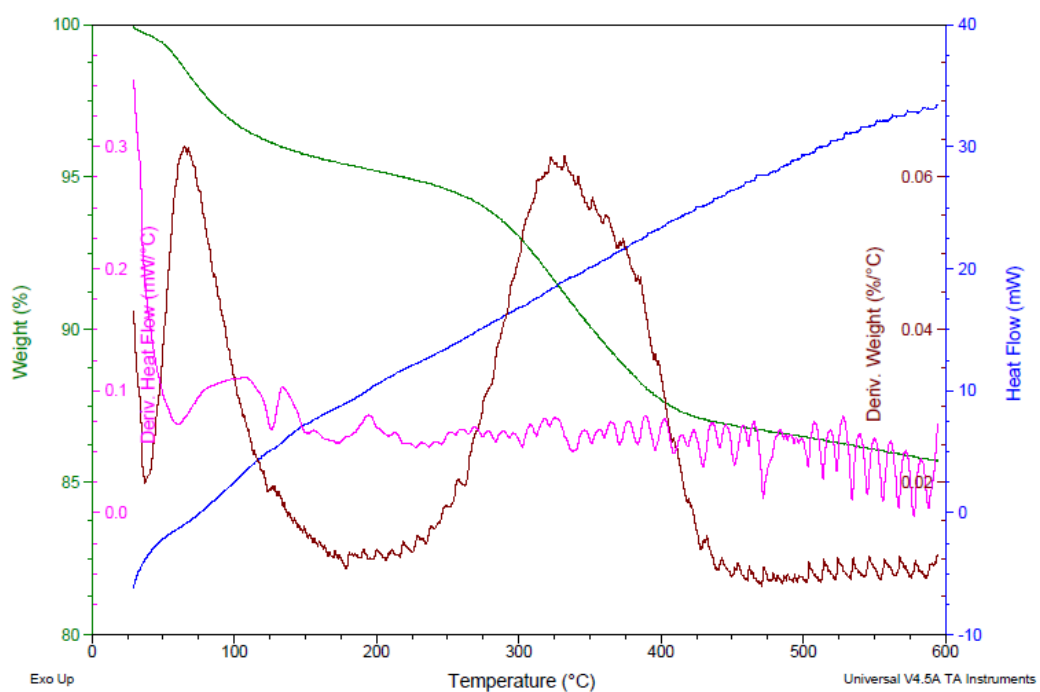


Figure C-9 TGA of PE-SiO<sub>2</sub>-Syn60 obtained from polymerization via *ex situ* immobilization

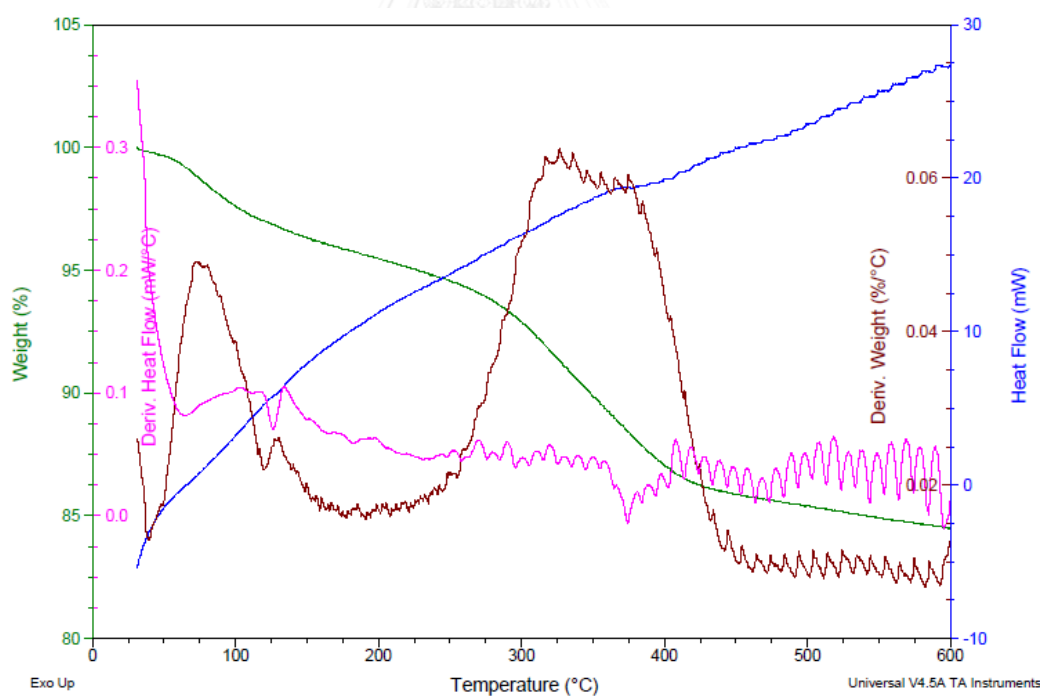


Figure C- 10 TGA of PE-SiO<sub>2</sub>-Syn70 obtained from polymerization via *ex situ* immobilization

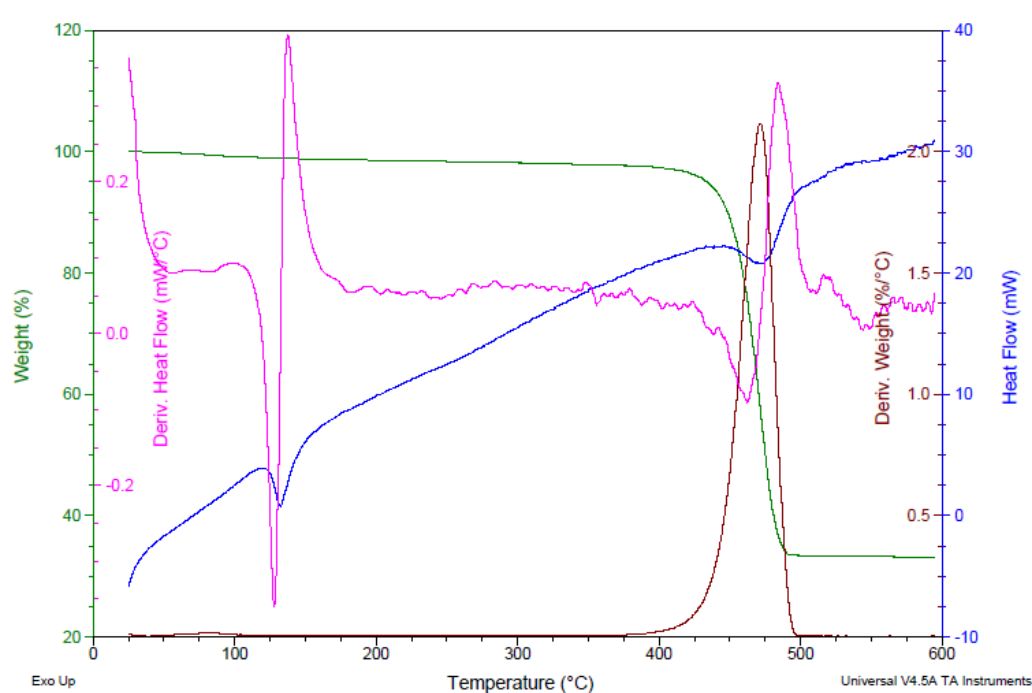


Figure C- 11 TGA of PE-SiO<sub>2</sub>-Com60 obtained from polymerization via *ex situ* immobilization

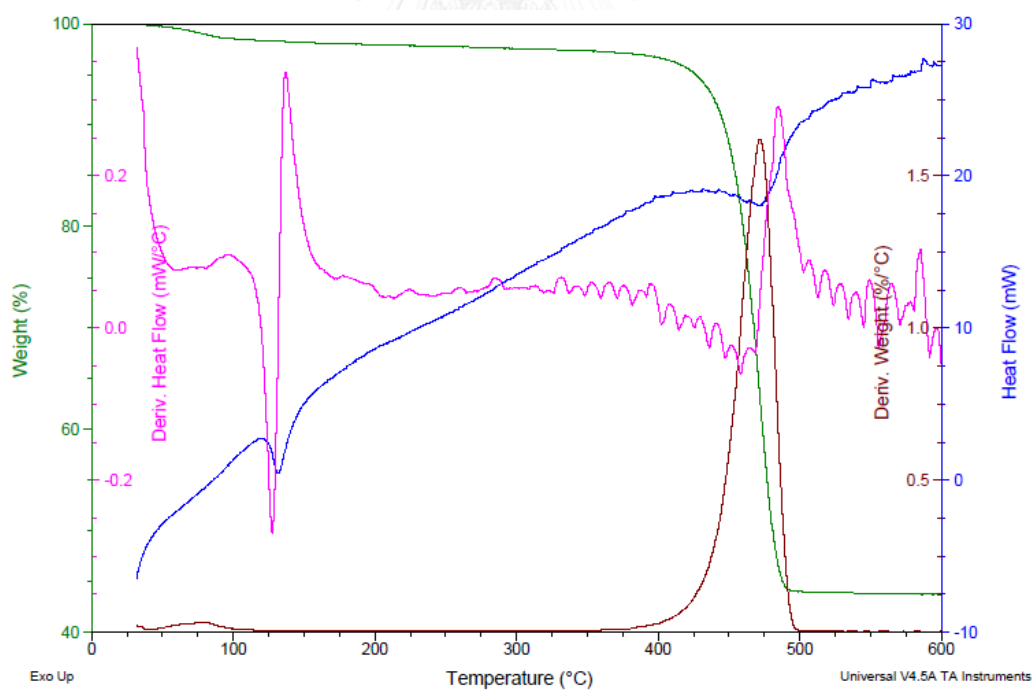


Figure C-12 TGA of PE-SiO<sub>2</sub>-Com70 obtained from polymerization via *ex situ* immobilization

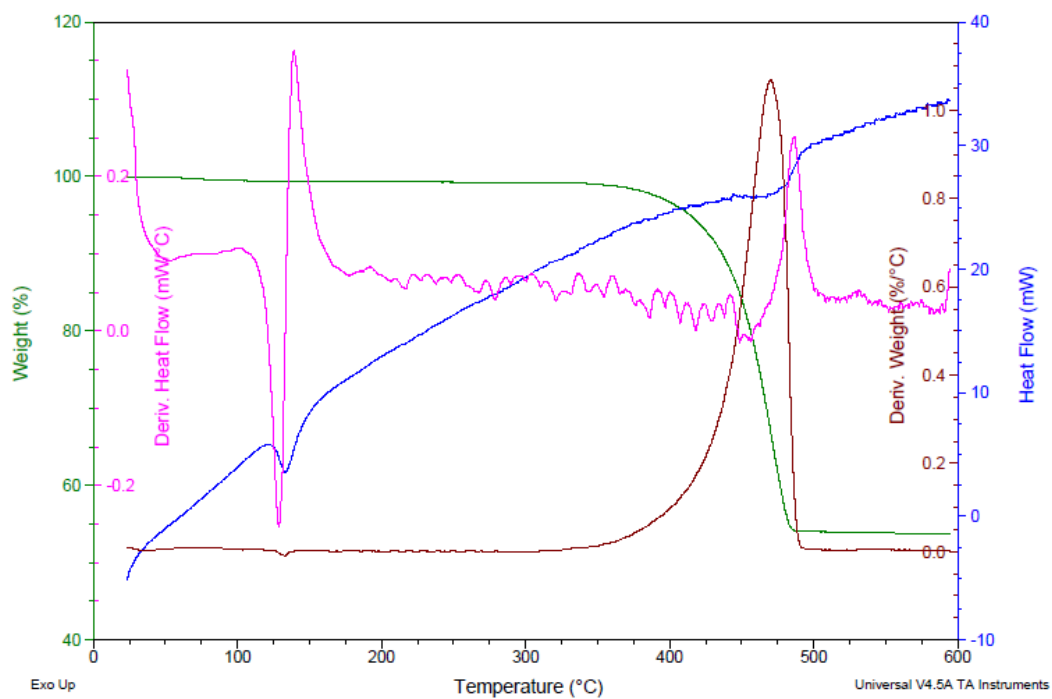


Figure C-13 TGA of INPE-SiO<sub>2</sub>-RH70 obtained from polymerization via *in situ* immobilization

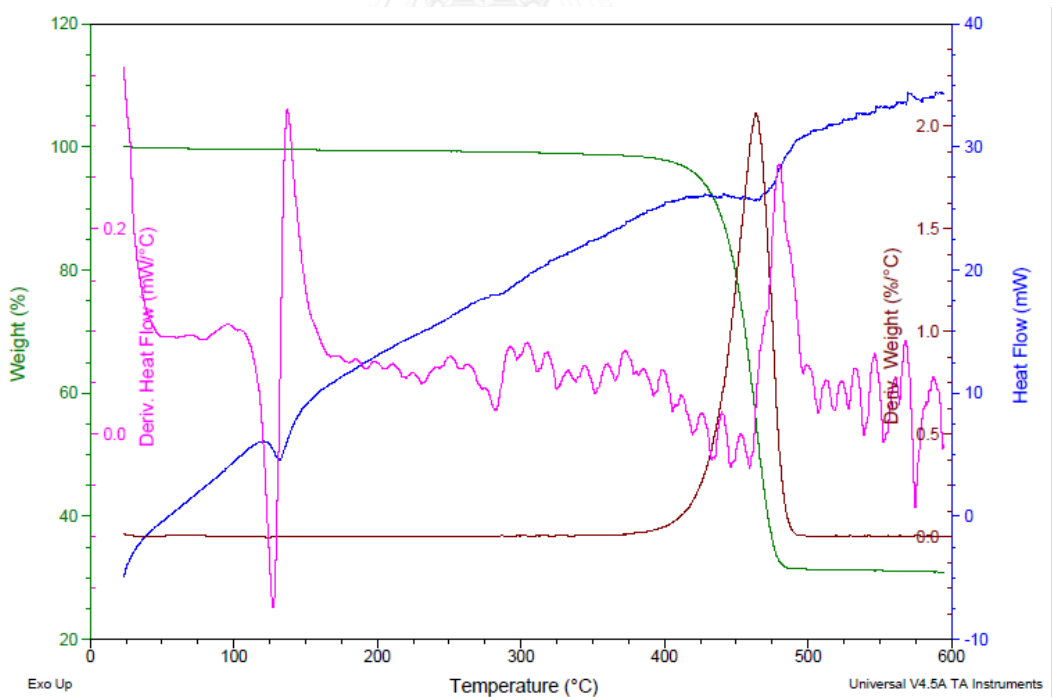


Figure C-14 TGA of INPE-SiO<sub>2</sub>-Syn70 obtained from polymerization via *in situ* immobilization

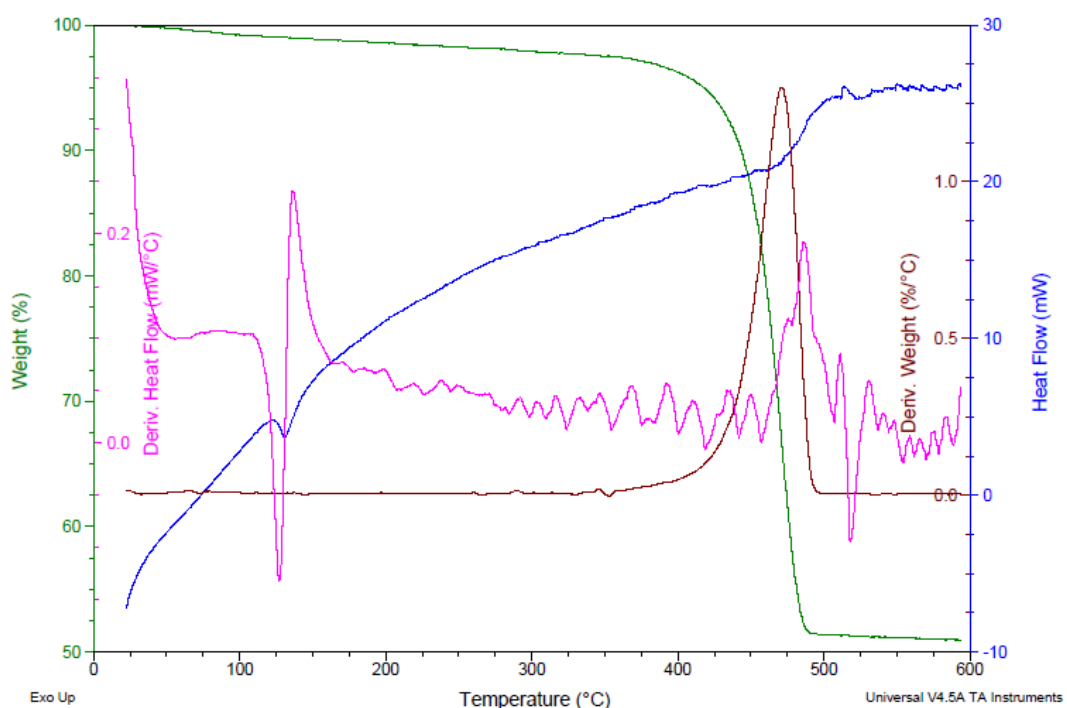
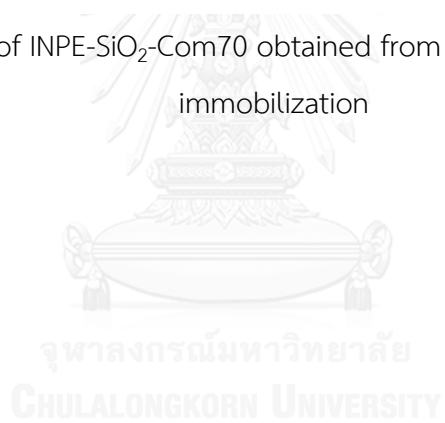


Figure C-15 TGA of INPE-SiO<sub>2</sub>-Com70 obtained from polymerization via *in situ* immobilization



# APPENDIX D : DIFFERENTIAL SCANNING CALORIMETRY



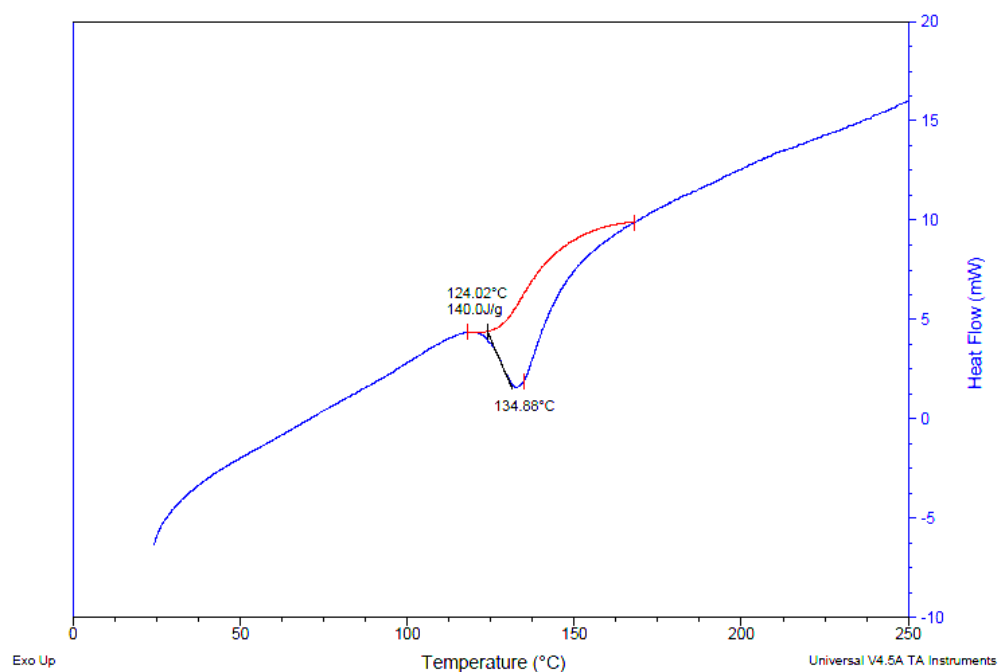


Figure D-1 DSC of polymer obtained from homopolymerization

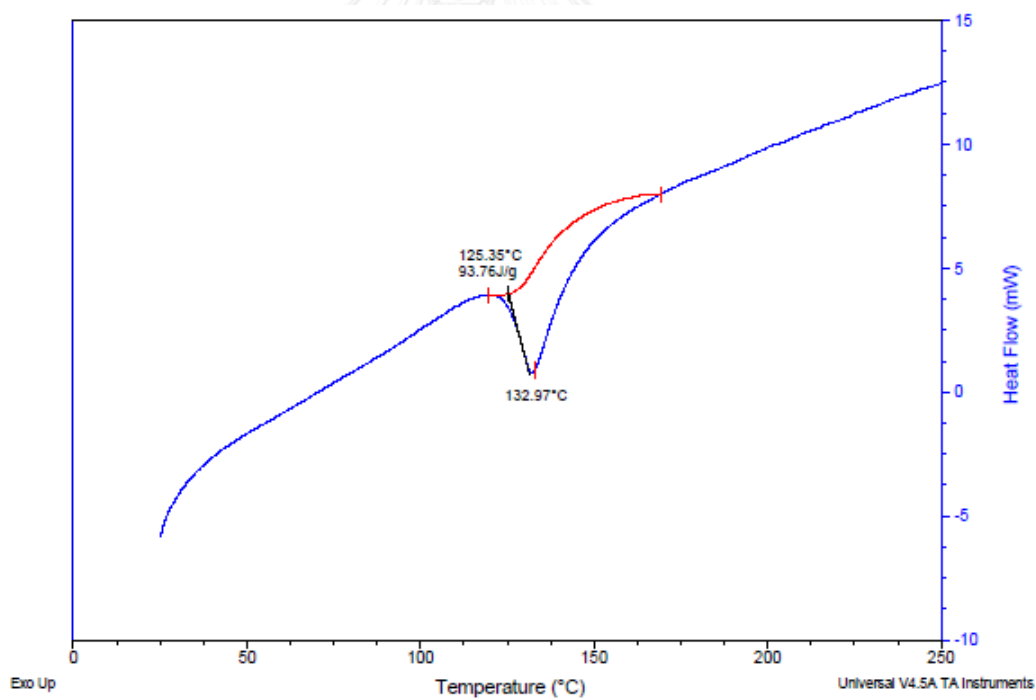


Figure D-2 DSC of of PE-SiO<sub>2</sub>-Com60 obtained from polymerization via *ex situ* immobilization

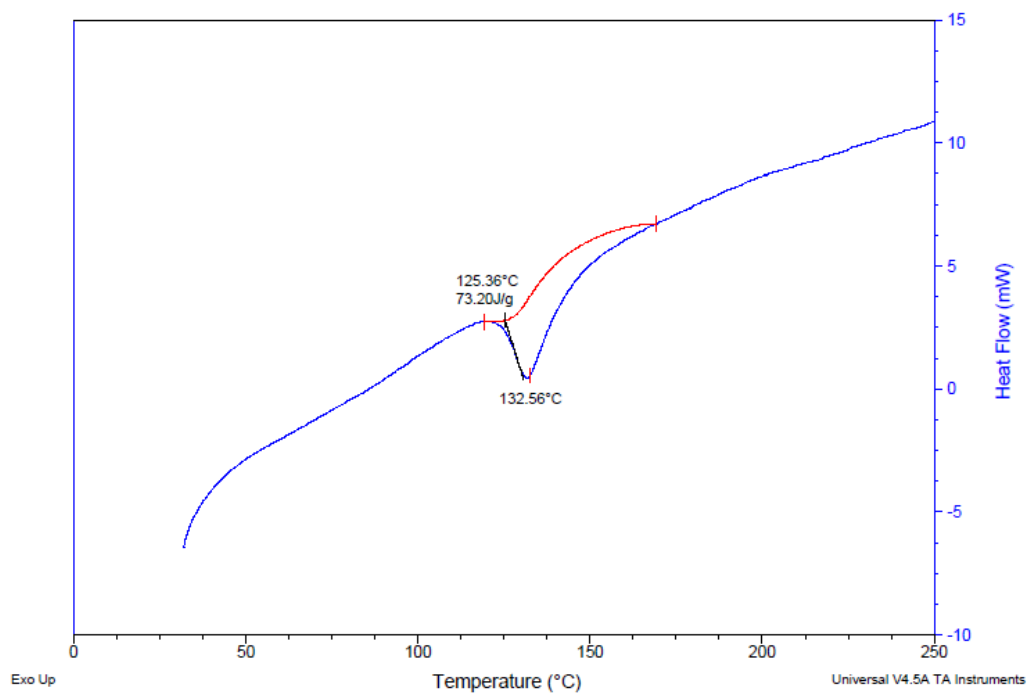


Figure D-3 DSC of of PE-SiO<sub>2</sub>-Com70 obtained from polymerization via *ex situ* immobilization

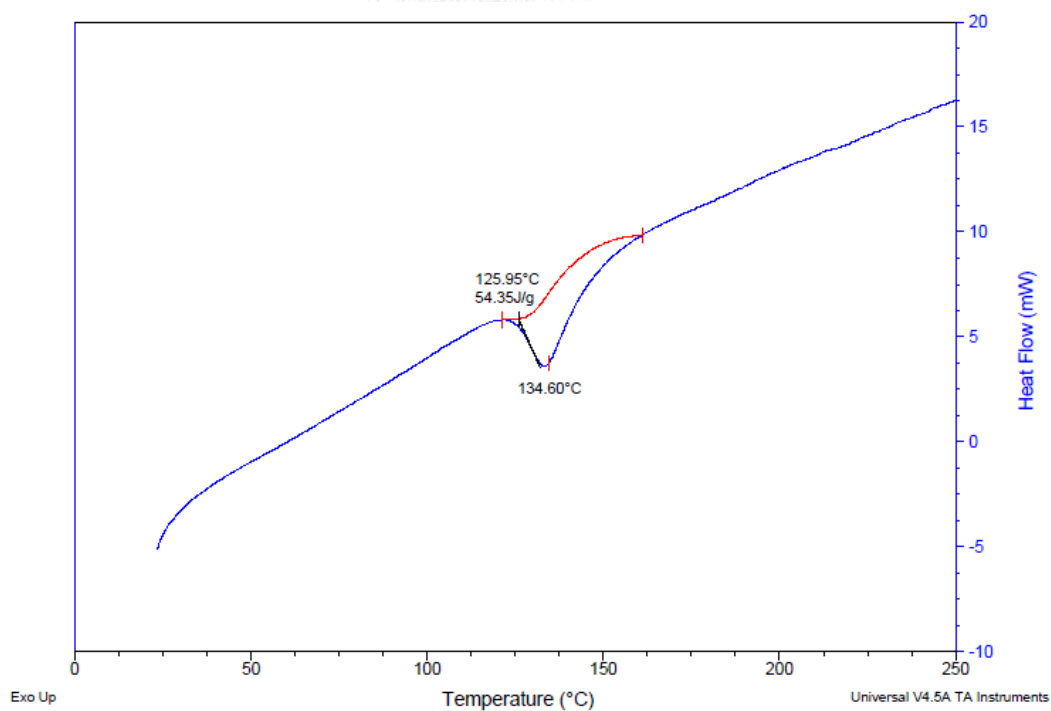


Figure D-4 DSC of of INPE-SiO<sub>2</sub>-RH70 obtained from polymerization via *in situ* immobilization



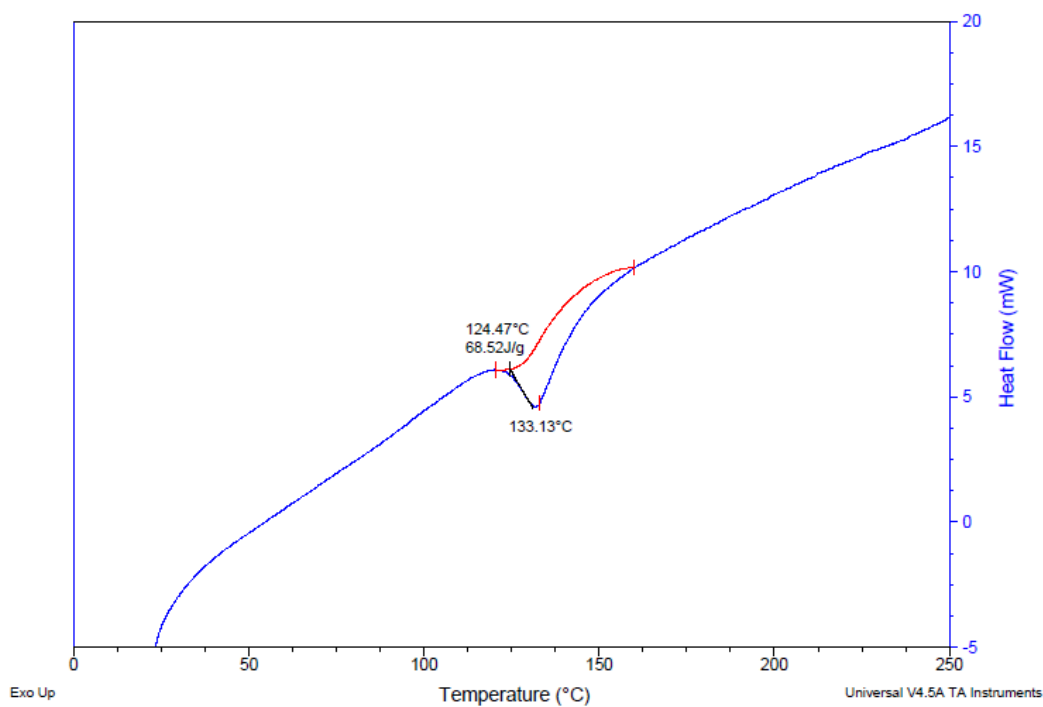


Figure D-5 DSC of of INPE-SiO<sub>2</sub>-Syn70 obtained from polymerization via *in situ* immobilization

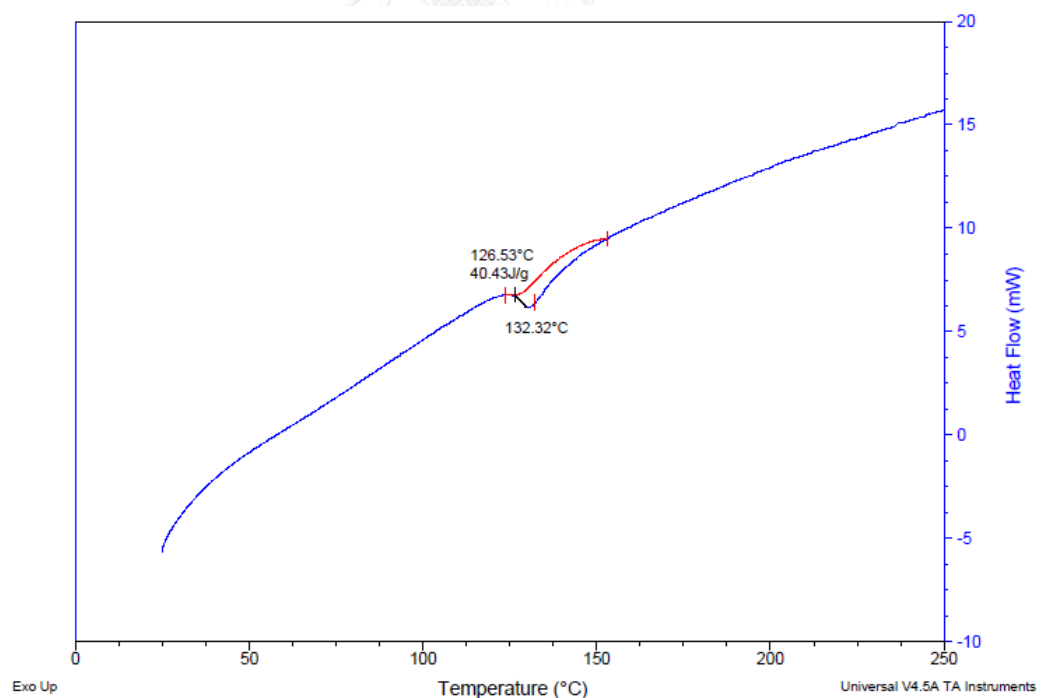


Figure D-6 DSC of of INPE-SiO<sub>2</sub>-Com70 obtained from polymerization via *in situ* immobilization

# APPENDIX E : LIST OF PUBLICATION



Jamnongphol, S.; Jongsomjit, B. “การเตรียมซิลิกาที่เคลือบด้วยพอลิเอทิลีนโดยพอลิเมอร์ไรเซชันแบบอินซิทูด้วยตัวเร่งปฏิกิริยาเมทัลโลซีน” (The Proceeding of 26<sup>th</sup> Innovative Technology Toward Sustainable Development Conference, TIChe 2016, Bangkok, Thailand)



## VITA

Miss Sineenart Jamnongphol was born on December 25, 1992 in Chonburi, Thailand. She earned the Bachelor's Degree of Chemical Engineering from the Department of Chemical Engineering, Faculty of Engineer, King Mongkut's University of Technology Thonburi in April 2015. Thereafter, she continued her Master's study at the Department of Chemical Engineering, Chulalongkorn University in June 2015.

